

Investigating the role of NMDA receptor activity in neural circuit remodeling and gene expression in *Xenopus laevis*

Andrew T. Schultz

Integrated Program in Neuroscience
Department of Neurology and Neurosurgery



McGill

A thesis submitted to McGill University
in partial fulfillment of the requirements
for the degree of Master of Science.

August 14, 2021

TABLE OF CONTENTS

ABSTRACT	4
RÉSUMÉ	5
ACKNOWLEDGEMENTS	7
ABBREVIATIONS	8
PREFACE TO CHAPTER 1: INTRODUCTION	9
CHAPTER 1: INTRODUCTION	9
1.1. OVERVIEW.....	9
1.2. THE <i>XENOPUS LAEVIS</i> RETINOTECTAL SYSTEM AS A MODEL OF CIRCUIT DEVELOPMENT	10
1.3. ANATOMICAL STRUCTURE OF THE <i>XENOPUS</i> RETINOTECTAL SYSTEM	11
1.4. MOLECULAR GUIDANCE CUES INSTRUCT AXONAL PATHFINDING.....	12
1.5. NEURONAL ACTIVITY PATTERNS INSTRUCT THE REFINEMENT OF CIRCUITS.....	15
1.5.1. <i>Hebbian and Stentian plasticity</i>	17
1.6. ACTIVITY-DEPENDENT PLASTICITY IS MEDIATED BY NMDA RECEPTORS.....	20
1.6.1. <i>Biophysics and signal transduction of NMDA receptors</i>	22
1.6.2. <i>NMDA receptor regulation of axonal morphology</i>	24
1.6.3. <i>NMDA receptors, synapse development, and functional composition</i>	26
1.7. D-SERINE AUGMENTS NMDA RECEPTOR ACTIVITY AND CIRCUIT REFINEMENT	30
1.7.1. <i>NMDA receptor co-agonism in synaptic and morphological development</i>	34
1.7.2. <i>The case for retrograde signaling: Does D-serine act on postsynaptic NMDA receptors to mediate the structural stabilization of presynaptic axon arbors?</i>	37
1.8. NEURONAL ACTIVITY-DEPENDENT GENE EXPRESSION	39
1.8.1. <i>Synaptic-nuclear communication</i>	39
1.8.2. <i>NMDA receptor-mediated gene expression</i>	41
1.8.3. <i>Gene expression, translation, and plasticity</i>	43
1.8.4. <i>Drugs and Genes: Can D-serine bridge the gap to activity-dependent transcriptomics?</i>	47
PREFACE TO CHAPTER 2: AIMS & RESULTS	48
CHAPTER 2: AIMS & RESULTS	49
2.1. AIM I: DETERMINATION OF WHETHER D-SERINE ACTIONS ON POSTSYNAPTIC NMDA RECEPTORS MEDIATES RETROGRADE STABILIZATION OF RGC AXON ARBORS	49
2.1.1. <i>Rationale</i>	49
2.1.2. <i>Experimental approach</i>	50
2.1.3. <i>Materials and methods</i>	51
2.1.4. <i>Results</i>	53
2.2. AIM II: CHARACTERIZATION OF BRAIN GENE EXPRESSION IN RESPONSE TO CHRONIC D-SERINE REARING AND NMDA RECEPTOR BLOCKADE	61
2.2.1. <i>Rationale</i>	61
2.2.2. <i>Experimental approach</i>	62
2.2.3. <i>Materials and methods</i>	64
2.2.4. <i>Results</i>	66
PREFACE TO CHAPTER 3: GENERAL DISCUSSION	86
CHAPTER 3: GENERAL DISCUSSION	86
CONCLUSION	95

REFERENCES CITED..... 97
APPENDIX..... 121

Abstract

Functions of the nervous system are predicated on the development of precisely organized neural circuitries that enable the transduction of sensory information into internal representations of the environment. This structure-function relationship is exemplified in topographically organized sensory maps. As sensory maps mature during development, their connectivity becomes dictated by patterns of neuronal activity. Integral to activity-dependent plasticity is the glutamatergic NMDA receptor (NMDAR), the gating of which serves as a detector of coincident pre- and postsynaptic activity to mediate plasticity. To study the role of NMDARs in plasticity, our lab utilizes the pharmacological application of the receptor co-agonist D-serine. D-serine rearing has previously been shown to acutely augment NMDAR conductance, and chronically promote synapse maturation and NMDAR-dependent presynaptic axonal arbor stabilization in the *Xenopus laevis* retinotectal circuit. To strengthen our model, I have sought to clarify the mechanisms by which D-serine drives presynaptic axonal arbor stabilization and gene expression in the *Xenopus* brain. Experimental results suggest that chronic D-serine treatment promotes presynaptic arbor stabilization by acting on postsynaptic NMDARs but may be doing so in parallel with an NMDAR-independent signaling pathway. Additionally, transcriptomic analyses of brain tissue mRNA indicate that chronic D-serine rearing induces broad changes in gene expression, as does chronic NMDAR antagonism, many of which have been implicated in plasticity. To our surprise, chronic D-serine and NMDAR antagonist treatment also converge on a subset of genes, revealing an unexpected degree of coregulation of gene products downstream of both putative NMDAR augmentation and blockade.

Résumé

Les fonctions du system nerveux sont basées sur le développement de circuits neuronaux précisément organisés qui permettent la transduction des informations sensorielles en représentations internes de l'environnement. Cette relation entre structure et fonction est illustrée dans l'organisation topographique des cartes sensorielles. Comme les cartes sensorielles mûrissent durant le développement, leur connectivité est dictée par des motifs d'activité neuronale. Le récepteur pour glutamate N-méthyle-D-aspartate (NMDAR), l'ouverture desquels sert de détecteur de coïncidence entre l'activité pré- et post-synaptique, est essentiel à la plasticité qui dépend de l'activité neuronale. Pour étudier le rôle de NMDARs dans la plasticité, notre laboratoire utilise l'application pharmacologique de co-agoniste au récepteur, D-sérine. Élevage en présence de D-sérine peut augmenter avec acuité la conductance des NMDARs et promouvoir chroniquement la maturation des synapses et la stabilisation des treilles des axones présynaptiques dépendant de l'activité de NMDAR dans le circuit rétino-tectal de *Xenopus laevis*. Pour renforcer notre modèle, j'ai cherché à clarifier les mécanismes par lesquels D-sérine provoque la stabilisation des treilles d'axones présynaptiques et l'expression des gènes dans le cerveau de *Xenopus*. Les résultats expérimentaux suggèrent que l'administration chronique de D-sérine promouvoit la stabilisation des treilles en agissant sur les NMDARs postsynaptiques mais pourraient aussi le faire en parallèle avec un chemin de signallement qui dépend de NMDAR. Aditionnellement, les analyses transcriptomiques de l'ARN messager du tissu de cerveau indiquent que l'élevage en présence de D-sérine, de même que l'antagonisme du signallement NMDAR, induit de vastes changements à l'expression de gènes, un grand nombre desquels sont impliqués en plasticité. Étonnamment, l'application chronique de D-sérine et antagoniste de NMDAR converge aussi à un sous-ensemble

de gènes, dévoilant ainsi un degré inattendu de co-régulation de produits de gènes en aval de l'augmentation et le blocage putatif de NMDAR.

Acknowledgements

What successes I achieve I owe much to the people around me – I would not be able to do it without their support. This lesson has especially resonated with me during my time in the IPN. The past two years have been challenging – in great ways and occasionally in bad. Yet, I have been most fortunate to be surrounded by amazing mentors, friends, and family. I owe my thanks to each of them.

None of this would have been possible without the unwavering support of Ed Ruthazer, my supervisor. He displayed—and I have no doubt will continue to do so—an incredible level of integrity, patience, understanding, and willingness to help. It has become obvious to me why so many students look up to him, as a scientist and as a dependable person. Thank you for this experience, Ed.

I owe a lot to the members of the Ruthazer lab. Each of them, at one point or another, took the time to teach me and, on occasion, hours out of their busy days to help me. You all are the best:

Ed Ruthazer
Anne Schohl
Cynthia Solek
Marion Van Horn

Elena Kutsarova
Stephen Glasgow
Tony Lim
Phil Kesner

Zahraa Chorghay
Nick Benfey
Ryan McPhedrain
Vanessa Li

A special thanks to Marion for mentoring me during the first semester in the lab, and to Cynthia and Anne for helping with numerous experiments.

I would also like to thank my advisory committee, Keith Murai and Don Van Meyel. Both provided honest encouragement and criticism when I most needed it. I will be taking their lessons with me.

I have always envisioned graduate school as an experience that you do not undertake on your own. You do it with peers, and most importantly with friends. I would be remiss without mentioning them. Phil, Nick, and Ryan, you three were very important. You helped me through the tough times more than you will ever know. Thank you.

To my parents, my brother Conner, and my sister Karly, I owe so much to the four of you. Each of you supported me throughout this process in every way and I can't thank you enough.

Finally, my most special thanks go to Kalyn Rivera. Kalyn, you were, and always will be, my most special person. You never failed in sharing with me my successes and raising me up when I felt at my lowest. You willingly undertook this wild adventure with me, packing up and traveling cross-country, then ultimately into a new one (and now back again). For that, I cannot thank you enough. Here's to many more journeys ahead.

Abbreviations

ACh – Acetylcholine
BDNF – Brain-derived neurotrophic factor
CaM - Calmodulin
CaMKII – Calcium/calmodulin-dependent protein kinase II
CREB – cAMP-responsive element binding protein
DAAO – D-amino acid oxidase
DGE – Differential gene expression
EGFP – Enhanced green fluorescent protein
EphA - Erythropoietin-producing human hepatocellular receptor A
EphB - Erythropoietin-producing human hepatocellular receptor B
EPSP – Excitatory postsynaptic potential
EPSC – Excitatory postsynaptic current
GABA – Gamma-aminobutyric acid
GAP – GTPase activating protein
GEF – Guanine nucleotide exchange factor
IEG – Immediate-early gene
LTD – Long-term depression
LTP – Long-term potentiation
L-VSCC – L-type voltage-sensitive calcium channel
MAPK – Mitogen-activated protein kinase
NMDA – N-methyl-D-aspartate
NMDAR- N-methyl-D-aspartate receptor
NMJ – Neuromuscular junction
qPCR – Quantitative reverse-transcription polymerase chain reaction
Rab – Ras-related protein in brain
RGC – Retinal ganglion cell
SC – Superior colliculus
SR – Serine racemase
TBS – Theta burst stimulation
TTX – Tetrodotoxin

Preface to Chapter 1: Introduction

This chapter was written by Andrew Schultz and edited by Ed Ruthazer.

Chapter 1: Introduction

1.1. Overview

Higher-order functions of the nervous system are contingent on the development of precisely organized neural circuitries that enable the transduction of sensory information into internal representations of the environment. Indeed, nervous systems exemplify the intricate relationship between form and function. One such example of this relationship is the *topographic mapping* of higher order sensory regions, known as *topographic* or *sensory maps*. Akin to how a topographic map of a mountain range preserves information about elevation and 3-dimensional structure, topographic maps preserve the spatial organization of receptive cells in sensory organs in their afferent connectivity. In brain systems that are topographically mapped, neighboring postsynaptic sites receive signals from neighboring neurons or ganglion cells positioned upstream in the flow of sensory information. This preservation of topography in sensory maps enables organisms to perform complex and continuous sensorimotor computations as they interact with their surrounding environment (Cang & Feldheim, 2013) and are likely necessary for—or at least highly conducive to—evolutionary fitness and survival in mobile animals.

Sensory maps form initially through the chemotropic navigation of growing axons (and, over shorter ranges, dendrites) that respond directionally to gradients of molecular guidance cues. The spatiotemporal features of guidance cue expression are thought to occur predominantly under the control of genetic regulation. Upon arriving at their approximate termination zones, axonal growth

cones sprout branches and form synapses with dendritic compartments in diffuse arborization fields. As synapses become functional and capable of transmission, patterned sensory exposure and intrinsic spontaneous activity begin to instruct the refinement of circuits into precise topographic connectivity schemata. Considering the relative contributions of genes and experience in guiding brain development may prompt some to simplify this down to a dichotomy of nature versus nurture. Indeed, this notion has captured the minds of many but may very well be inflicting a disservice to our understanding of how organisms develop. It turns out that, based on current research, nature and nurture are beautifully intertwined, co-dependent, and existing ubiquitously in harmony. Indeed, experience affects gene expression and vice versa. Understanding how neural activity contributes to the development of brain regions such as the formation of sensory maps, from genes to synapses and from circuits to behavior, is an extraordinary challenge in neuroscience. However, such discoveries will undoubtedly enable some of the most groundbreaking insights into the developmental biology of higher-order cognitive functions and their associated pathologies, and perhaps more importantly, will continue to refine the framework that supports our understanding of ourselves and each other.

1.2. The *Xenopus laevis* retinotectal system as a model of circuit development

Studying the mechanics of circuit development and remodeling in primates, such as humans, is constrained by numerous anatomical and observational challenges. Anatomically, sensory maps in primate brains are extremely complex, receiving dynamic feedforward, feedback, and modulatory signals from many brain regions. This makes it exceedingly difficult to establish cause-and-effect, or even verifiable correlations, between discrete features of sensory input and measurable physiological changes in individual neurons and circuit motifs. Additionally, the primate skull is a physical hindrance to traditional techniques for studying plasticity and circuit

refinement such as microscopic visualization of neuronal morphology and analysis of neuronal and synaptic excitability through patch-clamp electrophysiology. To circumvent these challenges, I take advantage of the developing albino *Xenopus laevis* tadpole, whose retinotectal circuit serves as an accessible and more easily discernible model of visual system development. Albino *X. laevis* tadpoles develop externally and rely heavily on vision at early stages of development. Indeed, the visual stimuli to which they are exposed and resulting neuronal activity are utilized to instruct the progressive refinement of the retinotectal circuit. In addition, due to the translucence of their skin, the albino tadpole brain is highly accessible to imaging and morphometric analyses at circuit, single-neuron, and even synaptic resolutions, permitting incredible insights into various aspects of circuit development, map formation, and plasticity (O'Rourke et al., 1990; Ruthazer & Cline, 2004; Munz et al., 2014).

1.3. Anatomical structure of the *Xenopus* retinotectal circuit

The *Xenopus laevis* retinotectal system includes retinal ganglion cells (RGCs) in the eye that extend their axons in a bundle—the optic nerve and tract—across the optic chiasm and form synapses with tectal neurons in the contralateral optic tectum (Holt, 1983; Sakaguchi & Murphey, 1985). Tectal lobes are monocular, in that they receive direct input exclusively from a single eye, although ipsilateral miswiring can occur (Munz et al., 2014; Rahman et al., 2021). Like most animals that rely on vision, the spatial arrangement of RGC somata in the retina is topographically preserved in the layout of synaptic connections that form between the branches of their axonal arbors and the dendritic arbors of tectal neurons. Specifically, axonal projections from RGC somata positioned in the most nasal parts of the retina (that is, closest to the nose) form synaptic connections with the most caudal, or posterior, regions of the optic tectum, whereas RGCs positioned oppositely in the most temporal extremes of the retina extend their axons to the most

rostral—anterior—parts of the optic tectum. RGCs occupying intermediate positions along the nasal-temporal axis of the retina project to correspondingly intermediate locations along the caudal-rostral axis of the optic tectum. Likewise, RGC somata positioned orthogonally along the dorsoventral axis of the retina disperse their afferent connections continuously along the lateral-medial axis of the optic tectum (Gaze, 1958; Sperry, 1963; Walter et al., 1987a, 1987b; Feldheim & Leary, 2010; Lemke & Reber, 2005). Because the cellular arrangement of the retina is preserved by the afferent connectivity in the optic tectum, the retinotectal projection is considered *retinotopically* organized.

1.4. Molecular guidance cues instruct axonal pathfinding

The general process of axon guidance is a highly orchestrated and conserved series of molecular interactions that confer the directional growth of axons as they navigate to their approximate termination zones, sometimes meters away, such as the case with motor neurons in the human spinal cord. The leading surface of the extending axon—the growth cone—has embedded in its plasma membrane an organized distribution of guidance receptors that are responsive to diffusible, membrane-, or extracellular matrix-bound guidance ligands. Receptor activation and subsequent signal transduction leads to the polymerization or depolymerization of the growth cone actin cytoskeleton, culminating in either filopodial protrusion and growth cone attraction or collapse and growth cone repulsion, respectively (Dent & Gertler, 2003; Dent et al., 2011). Although the plethora of signaling cascades that regulate actin dynamics in the axonal growth cone exhibit substantial interactive complexity, the simplified notion is that repulsive cues activate RhoA, which facilitates the depolymerization of actin and subsequent growth cone collapse, whereas attractive cues activate both Rac1 and Cdc42, which in turn drive the outward polymerization of actin and resulting filopodial protrusion (Kalil & Dent, 2005; Dent & Gertler,

2003; Dent et al., 2011). The process of molecular guidance occurs in all neurites—axons and dendrites—according to conserved mechanisms.

Molecular determination of axonal termination, specifically, is known as “The Chemoaffinity Hypothesis,” which derives from Roger Sperry’s seminal discovery that when the eye of *Xenopus laevis* is removed and reimplanted at a 180° orientation, the original ordering of RGC axonal terminations in the optic tectum is restored (Sperry, 1943; 1963). This led Sperry to posit that complementary distributions of intrinsically generated molecular cues on RGC axons and in the tectum instruct the mapping of developing retinotectal projections. Holt and Harris (1983) substantiated Sperry’s hypothesis by demonstrating that RGC axons innervate the *Xenopus* optic tectum in an already crudely organized topographic arrangement. Using an *in vitro* stripe assay that just previously served to identify candidate molecular activity in the plasma membranes of posterior tectal neurons (Walter et al., 1987a), the Flanagan and Bonhoeffer labs independently identified the primary molecular signals responsible for the guidance of RGCs in the retinocollicular system of mouse and chick, respectively: the EphA receptors and complement ephrin-A ligands (Cheng et al., 1995; Drescher et al., 1995). Both groups demonstrated that RGCs along the nasal-temporal axis of the retina express an ascending gradient of EphAs—that is, EphAs are most highly expressed in temporal RGCs and lowest in nasal RGCs. Furthermore, a complementary gradient of ephrin-A exists in the superior colliculus (SC) wherein ephrin-A is most highly expressed in the caudal SC and descends rostrally. Because receptor-ligand binding results in growth cone collapse and axonal repulsion (Drescher et al., 1997; Shamah et al., 2001), temporal RGCs, which have high levels of expressed EphA, are unable to penetrate caudal regions of the SC where ephrin-A expression is highest, and thus terminate in the rostral SC. In contrast, nasal RGCs, with low levels of EphA, are permitted by the relative absence of receptor-ligand

interactions to invade the ephrin-A-rich caudal SC. Indeed, disrupting EphA/ephrin-A molecular gradients in mice leads to spatially ectopic RGC termination in the SC (Brown et al., 2000; Feldheim et al., 2000). Thus, the various interactions between complementary and opposing gradients of EphAs and ephrin-As enables the continuous mapping of temporal-nasal RGC axons to the rostral-caudal SC. Similar gradients of EphA-ephrin-A are found in the *Xenopus laevis* retina and optic tectum and direct the initial stages of retinotectal development (Higenell et al., 2012), suggesting that this systematic process is evolutionarily conserved.

The molecular mechanisms that instruct the mapping of the dorsoventral axis of the retina to the lateromedial axis of the tectum/SC are seemingly more complex and incompletely characterized. Although this process appears to be governed by the attractive interaction between EphB and ephrin-B (Hindges et al., 2002), the gradients of EphB and ephrin-B in the frog do not align along the expected anatomical dimensions (Higenell et al., 2012). Eph receptors have a unique property: ephrin ligands are capable of signal transduction when bound by their Eph counterparts (Feldheim & O'Leary, 2010), a process known as *reverse signaling*. Reverse signaling through ephrin-B is proposed to contribute to the retinotopic growth of RGC axons along the dorsoventral dimension of the retina to the lateromedial tectum in *Xenopus* (Mann et al., 2002), yet this theory does not fully reconcile with the distributions of ephrin-B in the tectum, for which any discernible organization appears to be inconsistent with this simple model (Higenell et al., 2012). Additional research is still needed to clarify a more comprehensive understanding of this process, but it remains clear that chemoaffinity maintains a central role in mediating the coarse pathfinding of RGC axons to downstream visual centers of the brain in a variety of animals, including *Xenopus laevis* (Brennan et al., 1997; Monschau et al., 1997; McLaughlin et al., 2003a; Cang & Feldheim, 2013; Lemke & Reber, 2005; Higenell et al., 2012). Interestingly, EphA-ephrin-

A gradients provide the molecular instructions for developmental patterning throughout the brain, including auditory, motor, and somatosensory projections (Cramer & Gabriele, 2014; Kao et al., 2011; Uziel et al., 2006).

1.5. Neuronal activity patterns instruct the refinement of circuits

Upon arriving at their approximate termination zones, RGC growth cones begin to branch, elaborate, and compete for postsynaptic space within dendritic arborization fields (Feldheim et al., 2000; Reber et al., 2004; Schmidt & Easter, 1976) in a manner that is independent of intrinsic neuronal activity (Meyer & Wolcott, 1987). Subsequently, however, as neurons mature and begin to form functional synapses, the connectivity layout of brain circuits, including sensory maps, begins to refine via mechanisms that are governed by neuronal activity, whether this activity is spontaneously generated, such as via retinal waves (Meister et al., 1991; Wong et al., 1993; McLaughlin et al., 2003b; Ackman et al., 2012), or evoked by sensory experience (Gnuegge et al., 2001). In sensory circuits, since neighboring cells in sensory organs exhibit more tightly correlated activity compared to distant cells by nature of their spatial proximity, action potentials convey meaningful information about cellular arrangements that assist in fine-tuning the topography of neural maps to accurately reflect sensory inputs (Kutsarova et al., 2017). Refinement of circuit architecture and connectivity in response to input synchronicity is often referred to as *activity-dependent plasticity*.

Visual systems have long served as informative models for investigating activity-dependent plasticity. In the brains of many species, mainly mammals, visual centers of the brain segregate into ocular dominance columns which receive input from either eye. Hubel and Wiesel were the first to demonstrate that visual experience plays a fundamental role in maintaining the spatial segregation of ocular dominance bands in the kitten visual cortex (Hubel & Wiesel,

1970). Following the surgical closure of one eye, they observed the withdrawal of ocular dominance columns representing that eye into a more limited, compact cortical space, while those representing the non-deprived eye exhibited a corresponding expansion. Since then, many studies have solidified the belief that sensation and accompanying neural activity endow crucial instructions for the refinement of developing sensory maps and neural circuits *in vivo* (Hubel, 1982; Wiesel, 1982; Hensch, 2005; LeBlanc & Fagiolini, 2011). To this day, one of the most convincing demonstrations that activity plays a central role in the development of neural circuits comes from the “three-eyed frog” experiments. Constantine-Paton and Law (1978) showed that the implantation of a supernumerary third eye during embryogenesis in *Rana pipiens* frogs leads to the development of a tectal lobe that is dually innervated by two separate retinal projections. In dually innervated tecta, retinal projections from both eyes segregate into alternating *ocular dominance bands*. Since tectal lobes in frogs--both *Rana pipiens* and *Xenopus laevis*--are normally monocular, this alternating segregation of afferent inputs is likely not the exclusive result of axonal navigation via chemoaffinity cues, as both sets of retinal projections presumably express the analogous repertoires of guidance cue receptors. Moreover, band-like patterns of EphA or ephrin-A have not been observed in the normal or dually innervated optic tectum (Higenell et al., 2012). Instead, dual innervation is likely dictated by activity-dependent mechanisms rooted in the fact that signals coming from two different sources are not temporally synchronized. Indeed, chronic blockade of action potentials in the optic nerve with tetrodotoxin (TTX) results in the desegregation of ocular dominance bands into tectal space that is uniformly innervated (Reh & Constantine-Paton, 1985), suggesting that electrical signals originating in the retina carry with them important instructions for the progression of developmental plasticity.

Broad efforts have been taken to understand the instructive roles of action potentials in coordinating activity-dependent circuit refinement. The use of TTX, which irreversibly prevents the generation of action potentials by blocking voltage-gated sodium channels, has proven to be a useful tool for investigating this phenomenon. In goldfish that have had one of their optic nerves surgically cut, injection of TTX into the corresponding eye prevents the refinement of receptive fields as the regenerating nerves innervate the optic tectum (Schmidt & Edwards, 1993). They observed that the lack of receptive field refinement persists for months following the wash-off of TTX and demonstrated that this outcome is not the result of permanent changes in the retina or optic tectum because re-cutting the optic nerve following TTX wash-off permits the formation of normal receptive fields by the newly extending RGC projections. Gnuegge et al. (2001) substantiated the claim that action potentials instruct the formation of receptive fields by demonstrating that TTX rearing results in enlarged arborization fields in RGC axons. In addition to studying the roles of action potentials in guiding the development of higher-order map motifs such as receptive fields, researchers have also used TTX to investigate how action potentials drive the development and structural plasticity of the axons themselves. For example, Cohen-Cory (1999) showed that acute intraoptic application of TTX in *Xenopus laevis* tadpoles leads to a prompt increase in overall axon arbor branch dynamics, implying that action potentials, or certain patterns thereof, enable the stabilization of branches. Additionally, Cohen-Cory demonstrated that long-term increases in arbor complexity due to action potential blockade are restored by the endogenous upregulation of brain-derived neurotrophic factor (BDNF), implying that axon potentials may engage multiple signaling pathways that dictate axonal morphology.

1.5.1. Hebbian and Stentian plasticity

As circuits develop, it is necessary for the synaptic connections to progressively strengthen or weaken; these processes facilitate the development of circuitry that facilitates the optimal flow of sensorimotor information during behavior. Mechanistically, alterations in the strength of synaptic transmission occur largely in response to patterns of neuronal activity—specifically the temporal characteristics of action potentials as they integrate at defined circuit motifs. Donald Hebb was the first to posit that the temporal correlation of neuronal activities dictates the synaptic strength of connected neurons and underlies associative learning (Hebb, 1949). Carla Shatz described Hebb’s postulate with the now-dogmatic slogan, “cells that fire together wire together.” Specifically, a synapse is strengthened if its transmission contributes to the generation of a postsynaptic action potential. This form of plasticity is referred to as *Hebbian plasticity*. A canonical experimental model of Hebbian plasticity is long-term potentiation (LTP) of synaptic strength. Bliss and Lømo (1973) provided the first experimental characterization of LTP in the rabbit hippocampus, which at the time they termed “long-lasting potentiation” of synaptic transmission. They observed that, immediately following high frequency (100 Hz) tetanic stimulation of nerve fibers in the perforant path, an afferent projection to the dentate gyrus, dentate granule cells exhibited heightened excitatory postsynaptic potentials (EPSPs) in response to subsequent stimulation. Douglas and Goddard (1975) and Andersen et al. (1977) characterized the same phenomenon in the rat and guinea pig hippocampus, respectively, and the former rebranded it as “long-term potentiation”. LTP under conditions of tetanic presynaptic stimulation, such as by theta-burst stimulation (TBS; i.e., four brief, repetitious bursts of high-frequency stimulation; Larson & Lynch, 1986; Larson et al., 1986), have since been rigorously tested in a variety of animals and neural circuits and—although it does not occur at all synapses (Volianskis et al., 2015)—remains to this day one of the most convincing paradigms for the induction of Hebbian strengthening. Wigström and Gustafsson

(1986) demonstrated that LTP is robustly induced when postsynaptic current injection coincides with presynaptic stimulation. This suggests that LTP occurs when the presynaptic release of neurotransmitter is temporally correlated with postsynaptic depolarization. LTP therefore fulfills Hebb's postulate that "cells that fire together wire together" to form the neural assemblies that likely underlie associative learning. In fact, many assert that the fundamental loci of learning and memory are the synapses themselves (Bliss & Collingridge, 1993; Bliss et al., 2014), and that the principal driving mechanism that couples synapses to the dynamic progression of these higher-order cognitive processes is LTP (Albright et al., 2000; Martin et al., 2000).

In physiological conditions, neural activity patterns are often not synchronized. Indeed, the progressive weakening of synaptic connections that exhibit transmission which is uncorrelated with postsynaptic action potentials is a fundamental component of the developmental fine-tuning of neural circuits. Gunther Stent (1973) posited that there must also be a complementary mechanism to Hebbian plasticity that guides circuit remodeling in the inevitable event of unsynchronized activity patterns. Experimental evidence has corroborated the existence of *Stentian plasticity*, or the progressive weakening of neuronal connectivity due to uncorrelated activity (Rahman et al., 2020). An experimental paradigm that manifests the synaptic implications of Stentian plasticity is the long-term depression (LTD) of synaptic strength. LTD has been characterized in a variety of circuits and brain areas, including the hippocampus and cerebellum (Massey & Bashir, 2007). LTD was first observed as a form of *heterosynaptic* depression; that is, LTP at a particular synapse facilitates the depression of neighboring, unstimulated synapses in hippocampal CA1 circuits and in the dentate gyrus (Lynch et al., 1977; Levy & Steward, 1979). Thus, heterosynaptic LTD differs from LTP in that it can be induced in the absence of presynaptic activity, an observation that Hebb may not have anticipated. Subsequently, however, Barrionuevo

et al. (1980) confirmed that LTP induced by tetanic stimulation can be effectively abolished by subsequent low-frequency (1-5 Hz) stimulation. This form of synaptic depression is known also as *depotentiation*. On the other hand, *de novo* homosynaptic LTD has since been observed at CA1-Schaffer collateral synapses (Dudek & Bear, 1992; Mulkey & Malenka, 1992) and in the visual cortex (Kirkwood & Bear, 1994). Homosynaptic depotentiation and *de novo* synaptic depression are thought to endow the developing brain with distinct synapse-specific rewiring capabilities and, together with heterosynaptic LTD, support a diverse repertoire of mechanisms by which activity-dependent plasticity is executed over the course of neurodevelopment (Massey & Bashir, 2007).

1.6. Activity-dependent plasticity is mediated by NMDA receptors

Activity-dependent plasticity derives largely from the collective spatiotemporal characteristics of intrinsic circuit activity. It is thus imperative to consider the mechanisms that mobilize plasticity at this level of extrapolation. Hebbian plasticity mechanisms, which ultimately confer the formation of neural assemblies, bestow unique refinements in functional and structural connectivity and derive largely from the repeated activation of N-methyl-D-aspartate (NMDA) receptors (NMDARs). NMDAR activation requires both the binding of glutamate—released by the apposed presynaptic terminal—and depolarizing membrane potential. Thus, NMDARs function as molecular detectors of coincident pre- and postsynaptic activation and support the necessary conditions for driving Hebbian refinement mechanisms such as LTP. Collingridge et al. (1983a), using NMDAR antagonists first discovered by the McLennan and Watkins laboratories (McLennan & Lodge, 1979; Davies et al., 1981), were the first to demonstrate that NMDARs are necessary for the induction of LTP at CA3 Schaffer collateral-CA1 synapses in the rat hippocampus. Early experiments showed that application of NMDA, an agonist of NMDARs, is insufficient to drive LTP (Collingridge et al., 1983a; 1983b). Subsequent experiments revealed

that receptor activation is highly voltage-dependent; at resting membrane potentials, the NMDAR ion pore remains blocked by a Mg^{2+} ion, but at depolarizing potentials Mg^{2+} is relieved and ionotropic flux is permitted (Coan & Collingridge, 1985; Nowak et al., 1984; Mayer et al., 1984; Herron et al., 1986). Lynch et al. (1983) were the first to demonstrate the requirement of postsynaptic ionotropic Ca^{2+} activity for the induction of LTP. Shortly after, it was discovered that NMDARs are highly permeable to Ca^{2+} (MacDermott et al., 1986), which spurred the notion that LTP is driven primarily by the flux of Ca^{2+} through NMDARs into dendritic compartments (Volianskis et al., 2015). Using confocal microscopy, researchers were able to successfully visualize NMDAR-mediated Ca^{2+} responses in individual postsynaptic neurons during LTP induction (Alford et al., 1993), imparting considerable credence to the notion that postsynaptic NMDARs are the primary molecular initiators of LTP and Hebbian plasticity.

Indeed, great strides have been made in the past four decades in elucidating the functional contribution of NMDARs to retinotectal circuit refinement, many of which derive from experiments in *Xenopus laevis*. For example, chronic slow-release of APV, a competitive NMDAR antagonist, from a synthetic polymer implanted above dually innervated optic tecta of three-eyed frogs incites the desegregation of ocular dominance bands (Cline et al., 1987), suggesting a prominent role of NMDAR activity in mediating input convergence. Additionally, pharmacological NMDAR blockade suppresses the development of normal retinotopy in wild-type animals (Cline & Constantine-Paton, 1989). By exploiting ipsilateral RGC axonal projections in the *Xenopus* optic tectum (see **section 1.5.2**), Munz et al. (2014) demonstrated the necessity of NMDAR activation for axonal remodeling. Neighboring axonal projections that are activated out of synchrony less effectively drive postsynaptic activation and exhibit more exploratory growth. In contrast, neighboring RGC axons that are stimulated synchronously display marked reductions

in overall arbor complexity and branch dynamics. Axonal stabilization in response to correlated neighboring activity is largely eliminated by NMDAR blockade, supporting a role of NMDAR activation in presynaptic Hebbian stabilization and reversal of exploratory growth.

LTD is also thought to be mediated, at least in part, by NMDARs. Evidence suggests that the direction of plasticity (e.g., LTP versus LTD) is primarily dependent on the magnitude and temporal dynamics of postsynaptic Ca^{2+} influx through NMDARs (Berberich et al., 2007; Lüscher & Malenka, 2012; Paoletti et al., 2013). While coincident pre- and postsynaptic activation gates the rapid, high-magnitude influx of Ca^{2+} through NMDARs for the potentiation synaptic strength (Lisman et al., 2002), unsynchronized activity, such as when glutamate binding occurs in the absence of postsynaptic depolarization, facilitates basal-level Ca^{2+} flux that leads to diminished excitatory transmission (i.e., synaptic depression; Mulkey et al. 1993, 1994; Carroll et al. 2001). Thus, in terms of their manifestations on synaptic transmission and dependence on NMDAR activation state, LTD and LTP are often considered functionally inverse. Both mechanisms, differentially galvanized by the precise spatiotemporal characteristics of pre- and postsynaptic activity patterns that determine the ionotropic kinetics of NMDARs, constitute a bidirectional “tug-of-war” between synaptic strengthening and weakening, and shepherd the progressive development of circuit architecture.

1.6.1. Biophysics and signal transduction of NMDA receptors

NMDARs are hetero-tetrameric glutamate receptors comprised of four subunits: two obligatory GluN1 (N1) subunits and typically two GluN2 (N2) subunits: N2A, N2B, N2C, or N2D (Paoletti et al., 2013). Although not as common, GluN3 subunits can take the place of N2 subunits. GluN2 subunits contain glutamate binding sites, whereas the GluN1 subunits have binding sites for the co-agonists glycine or D-serine (Paoletti et al., 2013); binding of both subunits is necessary

for NMDAR current flux (Johnson & Ascher, 1987; Kleckner & Dingledine, 1988). Fully assembled NMDARs contain an ion pore that is permeable to calcium, sodium, and potassium ions. The ion pore is blocked by a magnesium ion at resting membrane potentials. Displacement of Mg^{2+} occurs only when the N2 subunits are bound by glutamate—which is released by the juxtaposed presynaptic terminal—and the adjacent membrane is depolarized (Paoletti et al., 2013). Simultaneous postsynaptic depolarization can occur in several ways, including the activation of an adjacent excitatory synapses, dendritic spike generation (Holthoff et al., 2006), or back-propagating action potentials (Koester & Sakmann, 1998; Nevian & Sakmann, 2004). Thus, binding of glutamate that is released by a presynaptic terminal and postsynaptic depolarization are required for ionotropic receptor activity, effectively rendering the NMDAR a detector of coincident pre- and postsynaptic activity (Nowak et al., 1984). If both conditions are met and the ion channel is gated, the receptor pore permits the efflux of K^+ and the influx of Na^+ and Ca^{2+} . The latter of which, Ca^{2+} , is central to various forms of intracellular signal transduction including those that are necessary for the induction of Hebbian or Stentian plasticity and gene expression. At basal levels of activity, such as during unsynchronized pre- and postsynaptic activity or low frequency stimulation, NMDARs grant basal level entry of Ca^{2+} that can, in turn, induce LTD by engaging calcineurin (CaN) and a host of phosphatases that ultimately lead to the dephosphorylation and internalization of α -amino-3-hydroxy-5-methyl-4-isoxazolepropionic acid type glutamate receptors (AMPA; Mulkey et al., 1993, 1994; Carroll et al., 2001), which are the principal conduits for high-magnitude excitatory transmission. Conversely, in the event of temporally correlated glutamate binding and postsynaptic depolarization, NMDARs permit rapid, strong influxes of Ca^{2+} into the postsynaptic compartment. High concentrations of intracellular Ca^{2+} trigger several effectors, but arguably the most important for the rapid induction of LTP is

calmodulin and Ca²⁺/calmodulin-dependent kinase II (CaMKII). In rat forebrain neurons, CaMKII is directly associated with the GluN1 and GluN2B subunits of NMDARs and this association increases when NMDARs are activated, bringing CaMKII closer to sources of Ca²⁺ influx (Leonard et al., 1999). Activated CaMKII, which has the unique ability to remain persistently active via autophosphorylation, facilitates the incorporation and stabilization of AMPARs at the postsynaptic density (PSD; Herring & Nicoll, 2016). Malinow et al. (1989) demonstrated that the induction of LTP is blocked when postsynaptic CaMKII activation is prevented in CA1 pyramidal neurons.

1.6.2. NMDA receptor regulation of axonal morphology

Cline et al. (1987) were the first to show that NMDARs are necessary for the proper development of alternating ocular dominance bands by demonstrating that NMDAR blockade with APV results in band desegregation. Subsequently, the Cline lab extended their findings to wild-type animals by showing that blockade of NMDAR activation disrupts normal spatial termination and elaboration of RGC axon arbors in the *Xenopus* optic tectum (Cline & Constantine-Paton, 1989). These experiments provided the first evidence that NMDARs play a crucial role in activity-dependent refinement of sensory maps and laid the groundwork for subsequent investigations into the presynaptic structural correlates of activity-dependent developmental plasticity.

A hallmark stage of topographic map development is the initial overlapping innervation of axonal branches in coarse termination zones, followed by the selective pruning of inputs into largely non-overlapping patches via NMDAR-dependent mechanisms that are driven by the spatiotemporal characteristics of input activity. Indeed, the dually innervated tectum of the three-eyed frog has proven to be an indispensable model for studying these processes because it permits *in vivo* morphological visualization of neighboring axonal arbors that originate from different eyes

and thus exhibit fundamentally unsynchronized activity patterns. Ruthazer et al. (2003) demonstrated that NMDARs are necessary for the preferential stabilization of neighboring axonal afferents from the same eye and the destabilization of inputs that converge from different eyes, processes that appear to be dependent on mechanisms comparable to LTP and heterosynaptic LTD, respectively (Van Dongen, 2009). This finding lends substantial credence to the position that NMDARs function as coincidence detectors and are capable of bidirectionally mediating presynaptic branch dynamics. Together with the finding that postsynaptic activity contributes to the reorganization of thalamic axonal projections in the visual cortex following eye-suturing (Hata & Stryker, 1994), these experiments provide seminal evidence for the presence of a retrograde signal that controls axonal arbor stability.

A considerable drawback of the three-eyed frog is that it differs from the natural development of the *Xenopus laevis* retinotectal circuit, which, in wild-type animals, is comprised of tectal lobes that are monocularly innervated by the contralateral retina. However, even under normal conditions, ipsilateral projections do occur, albeit infrequently. By exposing both eyes to synchronous or asynchronous visual stimuli, Munz et al. (2014) sought to exploit this miswiring phenomenon to directly assess the outcomes of NMDAR-dependent Hebbian mechanisms on retinotectal synaptic transmission and RGC axonal arbor dynamics. They observed that, in electrophysiological recordings of tectal neurons that receive input from both contra- and ipsilateral RGC projections, synchronous stimulation of both eyes maintains the synaptic strength of ipsilateral inputs relative to contralateral inputs. Conversely, asynchronous stimulation of both eyes leads to rapid weakening of ipsilateral retinotectal synaptic strength, presumably because ipsilateral projections are unable to sufficiently contribute to the generation of action potentials in tectal neurons. Evidenced by *in vivo* time-lapse imaging of labeled ipsilateral RGCs, the

researchers observed that asynchronous stimulation of both eyes leads to very rapid elongation *and* elimination of branch tips, as well as an increase in arbor size—mirroring the structural effects of NMDAR blockade (Ruthazer et al., 2003) and consistent with the notion that exploratory growth occurs robustly in the absence of synaptic stabilization resulting from correlated activity. In line with this, application of the NMDAR antagonist MK801 does not prevent exploratory growth following asynchronous stimulation. Synchronous stimulation of both eyes, on the other hand, has largely the opposite effects on ipsilateral RGC axonal morphology: namely, a decrease in the rate of branch tip elongation and retraction, an effect that is abolished by NMDAR blockade. Furthermore, branches formed during synchronous stimulation have, on average, longer lifetimes than those formed during asynchronous stimulation, suggesting correlated activity promotes presynaptic structural stability. Taken together, Munz et al. (2014) show that the precise temporal relationship of neighboring input activity supports a divergence of Hebbian stabilization mediated by NMDAR activation and Stentian exploration.

1.6.3. NMDA receptors, synapse development, and functional composition

Brain development is fundamentally contingent on the development of synapses. Mature synapses are either excitatory or inhibitory—meaning their activation produces membrane depolarization or hyperpolarization, respectively. Synaptic excitation and inhibition derive primarily from the ionotropic activity of NMDARs and AMPARs or GABARs, respectively. However, at early stages of development, immature excitatory synapses, termed *nascent* or *silent synapses*, are comprised solely of NMDARs, and GABAergic synapses themselves may mediate excitatory rather than inhibitory transmission due to high intracellular concentrations of Cl⁻ (Akerman & Cline, 2007; Ben-Ari et al., 1997). Experimental evidence from studies in developing hippocampal and retinotectal circuits indicates that GABAergic EPSPs facilitates the voltage-

dependent displacement of Mg^{2+} from NMDARs and subsequent ionotropic activity at adjacent silent synapses (Leinenkugel et al., 1997; Akerman & Cline, 2006; Akerman & Cline, 2007). NMDAR-mediated influx of Ca^{2+} and subsequent activation of CaMKII facilitates the endocytotic insertion and lateral diffusion to the postsynaptic density of hetero-tetrameric AMPARs combinatorially composed of GluA1, GluA2, and GluA3 subunits, which in turn enables the heightening of synaptic excitation and potentiation (Akerman & Cline, 2006; Hayashi et al., 2000; Shi et al., 1999; Malinow & Malenka, 2002).

At more immature glutamatergic synapses, NMDARs are composed primarily of GluN1 and GluN2B (Barria & Malinow, 2002). During postnatal stages of mammalian development, GluN2A expression begins to increase, and by adulthood, GluN2A far exceeds levels of GluN2B at most glutamatergic synapses (Monyer et al., 1994; Barth & Malenka, 2001). GluN2B-containing NMDARs exhibit higher ionotropic conductance than GluN2A-containing NMDARs and thus more robustly permit initial synaptic excitation and plasticity (Hestrin, 1992; Erreger et al., 2005; Shipton & Paulsen, 2013). The trafficking of N2B to immature synapses appears to be independent of neuronal activity, whereas GluN2A trafficking to synapses is largely an activity-dependent process (Barria & Malinow, 2002). Following the initial gating of GluN2B-containing NMDARs via adjacent GABAergic transmission and upregulation of AMPAR excitatory signaling, synaptic NMDAR subunit composition begins to shift more towards GluN2A, and as synaptic activation persists, so does the integration of GluN2A into synaptic NMDARs.

Over the course of brain development, and even at mature central synapses, NMDARs exhibit astonishing compositional and corresponding functional diversity. Notably, receptor subunit composition endows unique permeabilities and conductance for Ca^{2+} , which is of course decisive in dictating the route of plasticity. For example, GluN2A- and GluN2B-containing NMDARs have

high ionotropic conductance, Ca^{2+} permeability, and sensitivity to Mg^{2+} , whereas NMDARs containing GluN2C or GluN2D exhibit properties of lower conductance, Ca^{2+} permeability, and Mg^{2+} sensitivity (Paoletti et al., 2013). GluN3 subunits are even less sensitive to Mg^{2+} blockade than GluN2C and GluN2D subunits and may explain why some NMDARs on oligodendrocyte myelin sheaths can be activated in the absence of any considerable depolarization (Burzomato et al., 2010). Several additional properties of NMDARs are strongly influenced by the interactions between GluN2 and GluN1 subunits, such as gating probability, agonist sensitivity, and deactivation kinetics. For example, GluN1/N2A NMDARs exhibit the highest channel open probability and fastest ESPC decay compared to other subunit combinations that have been studied, however, are also the least sensitive to glutamate and co-agonist binding (Paoletti et al., 2013). Presumably owing to these characteristics, recombinant GluN1/N2A receptors expressed in HEK293 cells display considerably larger charge-transfer and corresponding Ca^{2+} influx during tetanic stimulation protocols used to induce LTP compared to GluN1/N2B receptors, whereas GluN1/N2B NMDARs contribute more to signaling in response to low-frequency stimulation (i.e., an LTD induction protocol; Erreger et al., 2005). In line with this, at hippocampal CA1 synapses, LTP, but not LTD, is abolished in response to selective pharmacological antagonism of GluN2A, whereas the opposite is true under conditions of GluN2B antagonism (Liu et al., 2004). Similar demonstrations have been made in response to pharmacological antagonism at amygdalar (Dalton et al., 2012) and perirhinal cortical synapses (Massey et al., 2004), as well as in response to genetic knockout of GluN2A in the mouse superior colliculus (Zhao & Constantine-Paton, 2007) and at mossy fiber-granule cell synapses (Andreescu et al., 2011). Aligning with their purported effects on LTP and LTD, Kim et al. (2005) demonstrated that activation of GluN2A- and GluN2B-containing NMDARs differentially impact the trafficking of AMPARs. Specifically, they found

that, in mature hippocampal neurons, GluN2A and GluN2B in activated states exert bidirectional effects on Ras-ERK signaling that ultimately stimulates the insertion or removal of surface AMPARs, respectively. Altogether, these observations have led some to posit that GluN2A and GluN2B predominantly contribute to LTP and LTD, respectively. However, ample evidence has exposed that this dichotomy is likely an oversimplification. Paoletti et al. (2013) proposes that LTP might instead rely on the cooperative action of di-heteromeric GluN1/N2A receptors that allow high magnitude Ca^{2+} influx and tri-heteromeric GluN1/N2A/N2B receptors that facilitate the recruitment of molecules necessary for the sustained physiological effects of LTP induction. In support of this assertion, Wang et al. (2011) demonstrated that GluN2B-, but not GluN2A-containing NMDARs in cortical neurons uniquely interact with CaMKII and the mTOR pathway to engage specialized cellular processes. Other studies have demonstrated that the induction of LTP is contingent on the interaction between GluN2B and CaMKII (Barria & Malinow, 2005; Zhou et al., 2007), which facilitates the tethering of activated CaMKII to the PSD (Leonard et al., 1999; Bayer et al., 2001), thereby coupling it to Ca^{2+} influx and AMPAR substrates for sustained phosphorylation (Shipton & Paulsen, 2014). Interestingly, GluN2 subunits also show specificity for different exchange factors that target Ras, a family of small GTPases that have been widely implicated in AMPAR trafficking and synaptic plasticity (Zhu et al., 2002; Gu & Stornetta, 2007; Stornetta & Zhu, 2011). During LTP at CA1 hippocampal synapses, GluN2A interacts with Ras-GRF2, which in turn facilitates signaling via the Erk1/2-MAPK pathway, whereas LTD induces the association of N2B and Ras-GRF1 and the subsequent activation of p38 MAPK (Jin & Feig, 2010; Li et al., 2006). Indeed, it appears that the functional endowment of NMDARs is fundamentally dictated by the integrative roles of different subunits and how these subunits interact, and most certainly the dynamic physiological contexts of the synapses they occupy.

The subunit composition of NMDARs endows special functional roles that, unsurprisingly, have extrapolated effects on neuronal morphology, and thus on circuit architecture. For example, overexpression of the carboxy terminus of GluN2B in CA1 pyramidal neurons promotes an increase in the total arbor path (which is total arbor length multiplied by a measure of arbor curvature, i.e., tortuosity) of dendritic arbors, revealing that subunit-specific signaling through the carboxy terminus may contribute more to the morphological development of arbors than ionotropic activity (Keith et al., 2019). Likewise, pharmacological antagonism of GluN2B with ifenprodil, but not GluN2A, suppresses basal dendritic growth of organotypic pyramidal neurons explanted from rat visual cortex (Gonda et al., 2020). In the *Xenopus* optic tectum, GluN2A and GluN2B possess both shared and unique roles in regulating dendritic morphology of tectal neurons. Overexpression of either GluN2A or GluN2B suppresses visual experience-dependent increases in the growth rate of dendritic arbors normally seen in control neurons, and impairs the development of localized branch clusters, which are thought to be important structural correlates of typical input segregation during topographic map refinement. Knockdown of GluN2A also suppresses branch clustering, an outcome that is absent in response to GluN2B knockdown. Furthermore, the dendritic arbors of neurons overexpressing GluN2B are considerably more dynamic than control or GluN2A-overexpressing neurons (Ewald et al., 2008). Taken together, these observations emphasize the astonishing functional diversity of NMDARs at levels beyond the synapse. Certainly, there is still much to be discovered, but it remains abundantly clear that the molecular composition of NMDARs constitutes a sophisticated avenue through which activity-dependent plasticity can be regulated and, like topographic maps, serves yet another elegant example of the intricate relationship between form and function.

1.7. D-serine augments NMDA receptor activity and circuit refinement

Characterizing the various roles of NMDARs in plasticity and circuit refinement has largely occurred via loss-of-function experiments such as pharmacological blockade of receptor activity or genetic knock-out of receptor subunits. This is ultimately problematic because NMDARs contribute substantially to normal excitatory transmission and patterned activity during development (Miller et al., 1989; Feldman et al., 1996; Ruthazer et al., 2003). Researchers have recently sought to circumvent this issue by exploiting another important biophysical feature of the NMDAR: the co-agonist binding site on the GluN1 subunit (Van Horn et al., 2017). First identified as the “glycine site” due to its measured affinity for the amino acid glycine and tissue colocalization with NMDA binding (Johnson & Ascher, 1987; Bristow et al., 1986), the NMDAR co-agonist binding site has since emerged as a decisive regulator of receptor activation (Wolosker, 2007; Van Horn et al., 2013). Indeed, it was discovered early on that exogenous glycine potentiates NMDAR currents in mouse neurons and is, in fact, required for the activation of NMDARs expressed in *Xenopus* oocytes (Johnson & Ascher, 1987; Kleckner & Dingledine, 1988). Glycine, however, acts also as an inhibitory neurotransmitter, and thus is not straightforward to probe the effects of NMDAR gain-of-function on circuit development.

More recently, it was discovered that the distribution of the amino acid D-serine roughly matches that of NMDARs in the vertebrate brain (Hashimoto et al., 1993) and is released from cultured astrocytes upon exposure to non-NMDA glutamate receptor agonists (Schell et al., 1995), spurring the intriguing possibility that NMDAR activity and receptor-mediated plasticity are modulated by gliotransmission of D-serine. Yang et al. (2003) demonstrated that LTP is promptly induced by correlated activation in hippocampal neurons cultured in medium that contains astrocytes. In contrast, LTP expression does not occur in the absence of astrocytes in culture but can be induced by the additional exogenous application of D-serine. Moreover, LTP is abolished

in neurons cultured with astrocytes and in hippocampal slices following NMDAR antagonism, co-agonist site antagonism, and degradation of endogenous D-serine, altogether substantiating the importance of astrocytic D-serine in synaptic potentiation. Subsequent studies have also revealed the necessity of bioavailable D-serine for the induction of NMDAR-dependent LTP at Schaffer collateral-CA1 synapses (Papouin et al., 2012; Le Bail et al., 2015) and at synapses in the amygdala (Li et al., 2013). Together, these studies illustrate that astroglial modulation of D-serine likely constitutes a fundamental mechanism by which synaptic plasticity is selectively and specifically regulated.

The metabolic pathway that channels the distribution, kinetics, and bioavailability of D-serine is known as *The Serine Shuttle* (Wolosker, 2011; Wolosker & Radzishevsky) and has emerged as a pivotal regulator of neuronal development and survival (Furuya et al., 2000; Hirabayashi & Furuya, 2008; de Koning et al., 2003). In the mammalian brain, glucose is taken up from capillaries and synthesized into L-serine. L-serine is then transported to neurons where it is converted to D-serine by serine racemase (SR). D-serine can then be released from neurons to perform autocrine signaling at synaptic NMDARs, or it can be transported back to astrocytes and released at glutamatergic synapses (Van Horn et al., 2013). Recent evidence suggests that the former constitutes the predominant mechanism of D-serine signaling at mammalian central synapses (Wolosker et al., 2016), but studies in other organisms have indicated that D-serine resides extensively in astroglia (Sild & Van Horn, 2013). More than likely, D-serine signaling and the mechanics of the serine shuttle differ to some degree between organisms, but it remains abundantly clear that the potentiation of NMDARs by D-serine and the role of glia in controlling D-serine bioavailability are evolutionarily conserved.

To better understand the role of D-serine in NMDAR-mediated synaptic development and activity-dependent circuit refinement, Van Horn et al. (2017) used immunohistochemistry (IHC) to first show that D-serine is indeed present in radial glial cells in the *Xenopus* optic tectum, and that acute elevation of extracellular D-serine increases the amplitude of evoked NMDAR-EPSCs in tectal neurons. Although AMPAR-EPSCs are largely unaffected by acute D-serine exposure, pharmacological activation of AMPARs produces elevated levels of extracellular D-serine, suggesting that D-serine availability at synapses is modulated by glutamatergic transmission and itself may contribute to modulating characteristics of synaptic excitation over longer periods of time. Indeed, chronic (48hr) bath exposure to D-serine provokes higher frequency AMPAR-mediated EPSCs in tectal neurons. Likewise, chronic D-serine rearing generates an increase in AMPA/NMDA ratio and a reduction in paired-pulse ratio, consistent with the notions that signaling downstream of repeated NMDAR activation confers synaptic unsilencing and maturation by upregulating AMPAR surface expression (Wu et al., 1996) and facilitating the probability of presynaptic release of glutamate (Aizenman & Cline, 2007), consecutively. In line with this, degradation of extracellular D-serine using D-amino acid oxidase (DAAO) inhibits synaptic maturation as demonstrated by a reduction in AMPAR-EPSC amplitude and frequency in tectal neurons.

After having established that D-serine contributes to normal excitatory synaptic transmission and maturation, Van Horn et al. (2017) sought to probe the role of D-serine at the cellular and circuit levels. By performing time-lapse two-photon imaging on EGFP-labeled RGCs innervating the optic tectum, they discovered that D-serine promotes a striking reduction in axon arbor complexity beginning just 24 hours following the onset of rearing, observed as significantly fewer branch tips and decreased total arbor lengths compared to control RGCs. This effect is largely

abolished by concurrent application of MK801, confirming that the effects of D-serine indeed are mediated by its action on NMDARs. Lending credence to this notion, time-lapse imaging of axon arbor dynamics reveals a striking reduction in both branches added and lost over a period of one hour in animals chronically reared in D-serine. Finally, the researchers found that D-serine elicits the enlargement of ON receptive fields in tectal neurons, suggesting a potentially behaviorally relevant impact on retinotectal circuit development.

Taken together, there are a variety of implications of this study, as well as new and exciting experimental opportunities that derive from their findings. By increasing NMDAR ionotropic conductance, D-serine promotes both the maturation of retinotectal synapses and the stabilization of RGC axon arbors. These outcomes are strikingly analogous to those of LTP (Wu et al., 1996) and the structural changes following correlated activity (Munz et al., 2014; Kutsarova et al., 2017), respectively. Bearing this in mind, it appears that chronic D-serine exposure primes the visual circuit towards activity-dependent stabilization while preserving the temporal characteristics of intrinsic neural activity patterns. It is surprising that D-serine promotes the enlargement of ON receptive fields, though this could simply be the result of D-serine indiscriminately enhancing NMDAR activity and preventing the normal specificity of synaptic pruning and input convergence (Van Horn et al., 2017). Nevertheless, these findings lay the foundation for a novel method that can be applied to investigate the molecular mediators of activity-dependent circuit refinement and gene expression—endeavors that previously have proved cumbersome and difficult, due largely to the fact that, in physiological conditions, Hebbian and Stentian mechanisms are likely synapse-specific, which hinders the pursuit to extract downstream effects at the level of cells and circuits.

1.7.1. NMDA receptor co-agonism in synaptic and morphological development

The molecular makeup of NMDARs is a tightly controlled process throughout the course of development (see **section 1.6.4**). As neural maps establish, synaptic NMDARs progress from being primarily composed of GluN1 and GluN2B to predominantly containing GluN1 and GluN2A by adulthood (Monyer et al., 1994; Barth & Malenka, 2001). This compositional progression endows NMDARs with biophysical and resulting functional properties that permit neural circuits to appropriately respond to the changing conditions that ultimately compel development. In addition to their subunit composition, NMDARs can also be categorized based on their spatial arrangements: synaptic or extrasynaptic NMDARs. Synaptic NMDARs have been implicated time and again in the generation of activity-dependent LTP and LTD (Liu et al., 2004; Massey et al., 2004; Berberich et al., 2005). Interestingly, it has been demonstrated that extrasynaptic NMDAR activation by glutamate release from astrocytes contributes to neuronal synchrony (Fellin et al., 2004) and, in the case of aberrant function (e.g., by facilitating excitotoxicity, modifying protein recruitment, or altering gene expression), the onset of various neurodegenerative disorders (Bordji et al., 2010; Milnerwood et al., 2010). Although functional differences are presumably due, at least in part, to differences in molecular composition, recent studies have shown that activation of spatially segregated synaptic and extrasynaptic NMDARs are differentially controlled by distinct pools of endogenous co-agonists, D-serine and glycine, respectively, for which they have opposing preferences (Papouin et al., 2012). At least two mechanisms converge to confer these selective preferences: GluN1 subunits of NMDARs display a higher affinity for D-serine through the molecular interaction with GluN2A subunits compared to GluN2B subunits (whereas the association of GluN1 and GluN2B results in an affinity for glycine that exceeds that of D-serine), and the availability of glycine at the synaptic cleft is actively curtailed by localized glial glycine transporters. Moreover, Papouin et al. (2012) observed that

synaptic NMDARs are composed primarily of GluN1/N2A, in contrast to extrasynaptic receptors that exhibit a compositional propensity for GluN1/N2B, which is consistent with previous studies (Steigerwald et al., 2000; Groc et al., 2006). The spatial partitioning of NMDAR subtypes may, in fact, be dependent on the co-agonists themselves, as D-serine and glycine selectively impede the membrane diffusion of GluN2B and GluN2A subunits to the PSD, respectively. Although an enticing explanation of why synaptic and extrasynaptic NMDARs tend to exhibit different subunit compositions, based on their results, the researchers could not strictly conclude if co-agonist distribution exerts control over the spatial localization of NMDAR subtypes, or vice versa. Advancing this stream of inquiry, Ferreira et al (2017) sought to probe this question and uncover the molecular mediators that influence D-serine's ability to selectively instruct the trafficking of GluN2B at postsynaptic compartments. Importantly, the researchers found that there is little to no difference in the *intrinsic* affinity of D-serine and glycine for GluN2A and GluN2B subunits; what ultimately matters are the relative concentrations of each at the synaptic cleft. In conditions where D-serine is at higher relative concentrations than glycine, GluN2B-containing NMDARs are rapidly bound by D-serine and undergo a conformational change that prevents the NMDAR C-terminus from associating with PDZ-scaffold proteins (e.g., PSD-95), thereby reducing the rate at which GluN2B subunits are incorporated into synaptic NMDARs and promoting the retention of GluN2B at extrasynaptic locations. In contrast, when glycine is more abundant than D-serine, glycine stimulates an alternative conformational change in the C-terminus of GluN2B-containing NMDARs that accelerates the tethering of these receptors to the PSD. The authors propose a model wherein the retention of GluN2B at extrasynaptic sites in response to D-serine-dominated conditions prompts the signal unmasking and subsequent endocytotic internalization of GluN2B-containing NMDARs, in line with studies that have examined the roles of subunit-specific and co-

agonist-induced NMDAR internalization (Roche et al., 2001; Nong et al., 2003). On the other hand, glycine increases the synaptic composition of GluN2B by promoting its molecular adherence to postsynaptic scaffolding proteins, altogether synthesizing a parsimonious model claiming that the balance of co-agonist availability at the synaptic cleft fundamentally determines the rate at which GluN2B-containing NMDARs are successfully integrated at synaptic or retained at extrasynaptic locations.

1.7.2. The case for retrograde signaling: Does D-serine act on postsynaptic NMDA receptors to mediate the structural stabilization of presynaptic axon arbors?

An abundance of evidence indicates that, during activity-dependent refinement of the *Xenopus* retinotectal circuit, repeated activation of postsynaptic NMDARs mediates the release of a retrograde signal that acts on and promotes the structural stabilization of presynaptic axonal arbors. Ruthazer et al. (2003) demonstrated that, in dually innervated tectal lobes of the three-eyed frog, axonal branches in regions of the neuropil occupied by projections from the same eye exhibit preferential stabilization compared to regions occupied by afferents originating in the other eye, an outcome that is curtailed by NMDAR blockade. This morphological behavior of presynaptic arbors is presumably only possible through the correlation detection capabilities of postsynaptic NMDARs in tectal neurons, and similarly, nor would the NMDAR-dependent effects of synchronized presentation of ocular stimuli to both eyes on ipsilateral RGC axonal stabilization observed by Munz et al. (2014). Furthermore, expression of a constitutively active form of CaMKII that does not contain the autoinhibitory regulatory domain, which functionally mirrors the activation of CaMKII during the induction of LTP, in *Xenopus* tectal neurons promotes the structural refinement of RGC axonal arbors *in vivo* by enhancing the rate of branch retraction (Zou

& Cline, 1996). This observation strongly suggests the presence of a retrograde signal that is acted on by active CaMKII that somehow functions to stabilize presynaptic branches, suppress axonal arbor elaboration, and promote retinotectal synapse maturation (Zou & Cline, 1996; Kutsarova et al., 2017). Finally, in an elaborate series of experiments similar in execution to Zou & Cline (1996), Cantalops et al. (2000) demonstrated that postsynaptic expression of CPG15, an activity-dependent gene with documented functional roles in plasticity, in *Xenopus* tectal neurons promotes presynaptic arbor elaboration. In this case, the complexity of presynaptic arbor branching induced by CPG15 is increased, which may suggest that CPG15 downregulates the expression of an existing retrograde stabilizing signal or upregulates a retrograde signal that engages exploratory growth. In either case, a retrograde signal is a necessary condition for the structural outcomes observed.

In our system, D-serine promotes retinotectal synapse maturation and presynaptic RGC axonal arbor stabilization, and experimental observations demonstrate that D-serine acts on NMDARs on tectal neurons. Van Horn et al. (2017) demonstrated that chronic D-serine rearing reduces short-term branch dynamics and promotes the structural hyper-stabilization of presynaptic RGC axonal arbors via a NMDAR-dependent mechanism; concurrent blockade of NMDAR ionotropic activity with MK801 prevents the stabilizing effects of D-serine. As expected, acute D-serine exposure promotes an increase in tectal neuron NMDAR amplitude, but no change in presynaptic release properties. Yet chronic D-serine rearing results in a profound increase in vesicular release probability in addition to structural stabilization, suggesting the presence of a retrograde stabilizing signal if this population of receptors is, in fact, responsible for the structural effects of D-serine on RGC axonal morphology. This begs the question: do postsynaptic NMDARs on tectal neurons mediate the release of a retrograde signal in response to chronically elevated levels of D-serine?

Aim I of my projects seeks to reconcile this uncertainty, the resolution of which fundamentally steers our understanding of the cellular and molecular mechanisms that enable activity- and NMDAR-dependent circuit development.

1.8. Neuronal activity-dependent gene expression

It has been known for decades that sensory experience fundamentally sculpts the architecture of higher-order brain regions (Hubel & Wiesel, 1970) and the organization of their constituent synapses (Hubel, 1982; Wiesel, 1982). Sensation is manifested in neurons as patterns of electrical activity, so somehow patterns of neuronal activity must translate to changes in gene expression. It has been extensively demonstrated that Ca^{2+} performs integrative signaling to the nucleus to activate gene expression programs (Sheng & Greenberg, 1990; Lanahan & Worley, 1998; Zhang et al., 2007). In the case of glutamatergic transmission and plasticity, NMDARs are the primary source of Ca^{2+} , whereas L-type voltage-sensitive calcium channels (L-VSCCs) are the primary contributors to the influx of Ca^{2+} in response to evoked neuronal activity. Investigations into how different patterns of neural activity, or the induction, expression, or maintenance of plasticity impact gene expression have generated voluminous catalogues of *activity-regulated genes*. Given that neural activity patterns are highly heterogeneous, driven by diverse sensory experiences, and mediate the activity of a variety of receptors and signaling pathways, the study of activity-dependent gene expression has proved challenging, but has undoubtedly led to some of the most impressive discoveries in neuroscience.

1.8.1. Synaptic-nuclear communication

Perhaps the most extensively studied activity-dependent gene is the *immediate-early gene* (IEG) c-Fos, whose expression is rapidly induced by growth factor stimulation (Greenberg & Ziff,

1984; Greenberg et al., 1985) and membrane depolarization via cholinergic receptor and L-VSCC activation (Greenberg et al., 1986; Morgan & Curran, 1986). The expression of c-Fos has also been demonstrated to be induced by various forms of neural activity including seizures and electrical stimulation of neurons in the rat spinal cord, sensorimotor cortex, and dentate gyrus (Morgan et al., 1987; Saffen et al., 1988; Hunt et al., 1987; Sagar et al., 1988; Dragunow & Robertson, 1987; Douglas et al., 1988). Ghosh & Greenberg (1995) subsequently demonstrated that Ca^{2+} signaling constitutes the primary link between synaptic activity and nuclear gene expression in neurons. Indeed, it turns out that the source of intracellular Ca^{2+} (e.g., NMDARs or L-VSCCs) is a major determinant of the expression programs that are engaged (Lerea & McNamara, 1993; Bading et al., 1993; Deisseroth et al., 1996; Bito et al., 1996; Dolmetch et al., 2001; Hardingham et al., 2001; Hardingham et al., 2002; Karpova et al., 2013).

Investigations into the functional consequences of synaptic or evoked neuronal activation on transcriptional regulation have led to the identification of effectors that are acted on dynamically by intracellular Ca^{2+} and in turn signal to the nucleus to regulate the expression of activity-dependent genes. The most well-characterized is the transcription factor cAMP-responsive element binding protein (CREB). CREB resides in the nucleus, adhered to DNA regulatory motifs in either phosphorylated or dephosphorylated states and coupled to its co-activator CREB binding protein (CBP). When phosphorylated, CREB drives the expression of a variety of genes associated with cell survival, neuroprotection, synaptic plasticity, and learning and memory (Silva et al., 1998; Bonni et al., 1999; Ahn et al., 2000; Mayr & Montminy, 2001; Lonze et al., 2002; Mantamadiotis et al., 2002). The signals that determine the phosphorylation state of CREB are multitudinous but derive principally from synaptic and dendritic Ca^{2+} transients, such as those that occur through L-VSCCs or NMDARs at activated synapses. Importantly, Ca^{2+} transients at

synapses are often enhanced by the subsequent release of Ca^{2+} from internal stores such as the dendritic endoplasmic reticulum network (Hardingham et al., 2001). Ca^{2+} released intracellularly can then diffuse to the nucleus where it acts as a robust mediator of gene expression by acting directly on fast-acting regulatory kinases such as CaMKIV (Wu et al., 2001). Activated nuclear CaMKIV then exerts control over the phosphorylation state of CREB via interactions with CBP (Impey et al., 2002). Synaptic and dendritic Ca^{2+} can also regulate the activity of CREB through the slower-acting Ras-ERK1/2 signaling pathway (Bading & Greenberg, 1991; Ginty et al., 1994; Xing et al., 1996), however, CaMKIV activation by nuclear Ca^{2+} still appears to maintain a necessary role in this process (Chawla et al., 1998; Hu et al., 1999).

1.8.2. NMDA receptor-dependent gene expression

Given their high permeability for Ca^{2+} and role in coincident activity detection, NMDARs have been distinguished as important regulators of activity-dependent gene expression. Cole et al. (1989), motivated by the observations that IEGs are expressed in response to various forms of neural activity, surmised that NMDAR activation serves as a robust mediator for the expression of activity-dependent genes, such as IEGs. Indeed, following induction of LTP through high frequency stimulation of the perforant path in the hippocampus *in vivo*, they observed marked increases in the levels of mRNA corresponding to the IEG *zif268* in afferent granule cells. Moreover, concurrent pharmacological NMDAR antagonism abolishes the increases in *zif268* transcript abundance, highlighting the necessity of NMDAR activation for LTP-induced IEG upregulation. Subsequently, Bading et al. (1995) corroborated the proposed contribution of NMDARs in gene expression by demonstrating that, in cultured hippocampal neurons, glutamate treatment results in substantial increases in the abundance of transcripts for six IEGs: *c-Fos*, *FosB*, *c-Jun*, *JunB*, *Zif268*, and *Nur77*. Utilizing various selective antagonists for NMDARs and non-

NMDA type glutamate receptors in conjunction with calcium imaging, the researchers verified that NMDARs are the primary source of Ca^{2+} that is required for IEG expression in these neurons. Altogether these results establish a causal, activity-dependent role of NMDARs in coupling glutamatergic transmission to gene transcription.

Reflective of their functionally distinct contributions to plasticity, synaptic and extrasynaptic NMDARs exert largely opposing effects on gene expression (Hardingham & Bading, 2010). It is now known that activation of synaptic NMDARs generates Ca^{2+} transients that promote CREB phosphorylation and the regulation of genes involved in cell survival and plasticity. In contrast, extrasynaptic NMDARs are primarily responsible for the expression genes that contribute to the onset of neurotoxicity. Indeed, it has been demonstrated that CREB shut-off via excessive agonism of extrasynaptic NMDARs leads to mitochondrial dysfunction and cell death (Hardingham & Bading, 2002). Both receptor pools achieve these effects on gene expression by converging on and exerting opposing effects on the activation state of CREB through the regulation of ERK1/2. For example, while Ca^{2+} transients through synaptic NMDARs typically result in the activation of ERK1/2 signaling and subsequent phosphorylation of CREB, extrasynaptic NMDAR activation suppresses ERK1/2 (Ivanov et al., 2006), which in turn mediates CREB dephosphorylation (Hardingham et al., 2002; Hardingham & Bading, 2002). Extrasynaptic NMDARs can also impact the phosphorylation state of CREB through Jacob, which is localized to the nucleus in its activated state via its Ca^{2+} -sensitive binding partner Calcineurin where it promotes the dephosphorylation of CREB (Dieterich et al., 2008; Karpova et al., 2013).

A potentially important factor in the functional delineation of synaptic and extrasynaptic NMDARs in the regulation of gene expression is subunit composition. Studies have demonstrated that, in the mature brain, GluN2A is more abundant in synaptic NMDARs, while GluN2B is more

abundant in extrasynaptic NMDARs (Steigerwald et al., 2000; Groc et al., 2006; Martel et al., 2009; Papouin et al., 2012). Therefore, the subunits themselves may endow synaptic and extrasynaptic NMDARs with their functionally distinct abilities to bidirectionally control gene expression. However, many of the findings related to this have been controversial. For example, Lui et al. (2007) demonstrated that pharmacological agonism of GluN2A or GluN2B promotes cell survival or death, respectively, whereas other studies have shown that these outcomes occur in different contexts by the activation of either subunit (von Engelhardt et al., 2007; Papadia et al., 2008; Martel et al., 2009). Creating additional challenges is the fact that NMDARs can also exist as tri-heteromeric receptors composed of combinations of GluN2A and GluN2B, and even GluN2C and GluN2D (Hatton & Paoletti, 2005). It is not strictly known how manipulating one of these subunits, whether through pharmacological means or genetic knockout, affects the function of the others in an assembled NMDAR. Of potential significance here is the observation that GluN2A and GluN2B have differing roles in ERK1/2 signaling (Jin & Feig, 2010; Li et al., 2006). Because ERK1/2 is an important modulator of CREB, this signaling pathway may prove to shed light on the functional differences of GluN2A and GluN2B on gene expression. Indeed, additional research is required to come to a more comprehensive understanding of how NMDAR subunit composition effects receptor-mediated gene expression.

1.8.3. Gene expression, translation, and plasticity

Immediate stages of plasticity are thought to rely principally on pools of proteins and other biomolecules that latently reside within or near synaptic compartments. The structural and functional persistence of plastic modifications over the course of hours, days or longer, however, are thought to require gene expression and the synthesis of *de novo* proteins. In support of this, the induction of LTP in rat hippocampal neurons is followed by detectable changes in gene

expression (Qian et al., 1993), and late phase LTP is prevented in these neurons when transcription is pharmacologically inhibited (Nguyen et al., 1994). Not surprisingly, NMDARs appear to be important mediators of this process; NMDAR antagonism prevents CREB phosphorylation and subsequent activity-dependent gene expression that otherwise would have been engaged by LTP-inducing protocols (Gandolfi et al., 2017). The pursuit to characterize the crosstalk between plasticity and gene expression has uncovered an abundance of expression pathways that materialize the emergent features of structural and functional plasticity.

One of the most well-studied activity-dependent genes that has been implicated in plasticity is BDNF. Several studies have demonstrated that BDNF transcription is induced by Ca^{2+} entry through L-VSCCs and NMDARs and the subsequent phosphorylation of CREB in hippocampal neurons (Zafra et al., 1990; Zafra et al., 1991; Ghosh et al., 1994; Tao et al., 1998). BDNF is also transcribed following the induction of LTP at various synaptic populations in the hippocampus (Patterson et al., 19992; Castrén et al., 1993; Dragunow et al., 1993). Expressed BDNF itself provides feedback augmentation of synaptic transmission and plasticity. Lohof et al. (1993) demonstrated that BDNF application facilitates an increase in the rate of spontaneous release of acetylcholine (ACh) from presynaptic terminals of the neuromuscular junction (NMJ) in *Xenopus laevis*. Furthermore, elevated BDNF levels lead to the potentiation of Schaffer collateral-CA1 synapses in hippocampal slices (Kang & Schuman, 1995), and facilitate increased sensitivity to LTP induction and sustained LTP expression (Figurov et al., 1996). Conversely, LTP is suppressed in hippocampal neurons in BDNF knockout mice (Korte et al., 1995; Patterson et al., 1996). The activity-dependent regulation of BDNF and its active feedback on pre- and postsynaptic physiology (Lessmann et al., 1994; Levine et al., 1995) thus enables it to exert striking control over circuit development, including activity-dependent development of dendritic arbors

(McAllister et al., 1995; McAllister et al., 1996), the maintenance of ocular dominance bands in visual cortex (Cabelli et al., 1995) and presynaptic RGC axonal remodeling in *Xenopus* (Cohen-Cory & Fraser, 1995).

Of relevance to retinotectal plasticity in *Xenopus* is Neuritin/candidate plasticity gene 15 (CPG15). CPG15 has been found to be upregulated by synaptic plasticity (Nedivi et al., 1993) and glutamatergic transmission in rats (Nedivi et al., 1996). In *Xenopus*, CPG15 expression in tectal neurons is induced by kainic acid, a glutamatergic agonist, and promotes retinotectal synapse maturation and the elaboration of dendritic and axonal arbors *in vivo* (Cantalalops et al., 2000). These observations demonstrate the bidirectional relationship of plasticity and gene expression: while gene expression is induced by and required for the maintenance of plasticity, gene expression can also facilitate the generation of both structural and functional plasticity in neurons. Indeed, CPG15 presents a causal link between activity-dependent gene expression and plasticity.

The characteristics of transcriptional regulation are determined by transcription factors, which themselves are common effectors downstream of plasticity. One such transcription factor expressed in neurons is Nuclear Factor in Activated T-cells (NFAT). Translocation of NFAT to the nucleus is stimulated by CaN-mediated dephosphorylation (Graef et al., 1999). Once in the nucleus, NFAT contributes to the transcriptional underpinnings of axonal outgrowth in response to neurotrophic stimulation (Graef et al., 2003; Growth & Mermelstein, 2003), suggesting that NFAT may be important during developmental plasticity. Indeed, Schwartz et al. (2009) demonstrated that, in the *Xenopus* retinotectal system, visually evoked activity facilitates CaN/NFAT activation in tectal neurons, and preventing this interaction drastically alters dendritic morphology, arbor dynamics, and AMPAR-mediated transmission. NFAT likely regulates gene expression by directing interacting with CBP and altering the phosphorylation state of CREB

(Garcia-Rodriguez & Rao, 1998; Yang et al., 2001). Taken together, these findings demonstrate the central importance of dynamic interactions between transcription factors and synaptic activity-dependent molecules in the regulation of genes during developmental plasticity.

Of course, transcription alone is typically insufficient to appreciably impinge on plasticity and neuronal physiology. Transcripts must be translated into proteins, either in the nucleus or locally at or near synapses. Protein synthesis under the control of synaptic activity has emerged as a crucial conglomerate of mechanisms that define the progression of later stages of functional and structural plasticity. A master regulator of protein synthesis in neurons is the protein kinase mechanistic target of rapamycin (mTOR), which, depending on cellular conditions, can form complexes known as TORC1 and TORC2. Activated TORC1, with its adapter protein Raptor, phosphorylates downstream targets involved in translation initiation (Hay & Sonenberg, 2004) and is itself regulated by the Ras-family small GTPase Rheb (Saxton & Sabatini, 2017). In the *Xenopus* retinotectal system, Gobert et al. (2020) demonstrated that dendritic growth and branching are highly influenced by mTOR-TORC1 activity. Specifically, inhibition of TORC1 via Raptor knockdown in tectal neurons leads to significant reductions in dendritic arbor length and the number of dendritic branch tips. Moreover, analogous TORC1 inhibition leads to a decrease in the amplitude and frequency of AMPA-mediated mEPSPs at retinotectal synapses, indicating that TORC1 activity—and presumably downstream translation—is necessary for dendritic and glutamatergic synapse development. Indeed, by enhancing TORC1 activation through the overexpression of Rheb, the researchers observed largely the opposite effects: enhanced synaptic maturation and dendritic elaboration. Together, these demonstrations reveal a central role of the mTOR pathway in regulating retinotectal circuit development and underscore the likely necessity of *de novo* translation for the maintenance of developmental plasticity in the *Xenopus* optic tectum.

1.8.4. Drugs & Genes: Can D-serine bridge the gap to activity-dependent transcriptomics?

Modes of NMDAR activity are highly context-dependent, making it challenging to assess the various roles of this receptor in terms as broad as gene expression. It is likely that which genes and gene programs are engaged by NMDARs is dependent on a wide variety of converging factors, such as spatiotemporal characteristics of input signaling and summation, predominant NMDAR subunit composition and subtype (e.g., GluN2A- versus GluN2B-containing NMDARs, or synaptic versus extrasynaptic receptor pools), and experimental protocols used to drive NMDAR activation (e.g., LTP induction through TBS, glutamate application, pharmacological blockade with APV or MK801, etc.). The use of D-serine rearing as a pharmacological modulator of NMDAR activity offers numerous benefits for the study of activity-dependent gene expression. Most importantly, application of D-serine maintains the spatiotemporal characteristics of neural activity because alone, D-serine availability is insufficient to drive NMDAR gating. Indeed, NMDAR activation is contingent on the binding of glutamate released from presynaptic terminals and membrane depolarization. This characteristic function of D-serine in glutamatergic transmission is incredibly important to consider in the context of activity-dependent gene expression. After all, divergence from ordinary patterns of neuronal activity will yield artifactual experimental results that are not reflective of physiological activity. Furthermore, it has been well-demonstrated by numerous labs that D-serine is the primary *endogenous* co-agonist of *synaptic* NMDARs (Papouin et al., 2012; Ferreira et al., 2017) and that synaptic NMDARs contribute substantially to Ca²⁺ transients that are often required for IEG expression (Bading et al., 1995). This enables researchers to begin to parse out the specific contributions of synaptic activity, as opposed to extrasynaptic activity or both, to various downstream processes. However, there are

two potential caveats worth considering. Namely, whether the specificity of D-serine to synaptic NMDARs generalizes to *Xenopus* retinotectal synapses is less certain, nor are the effects of supraphysiological levels of D-serine on different pools of NMDARs. It remains a possibility that, at levels that exceed physiological conditions, D-serine stimulates both synaptic and extrasynaptic NMDAR pools. Nevertheless, it has been demonstrated that supraphysiological D-serine levels induce a variety of outcomes—structural and functional refinement and synaptic potentiation, for example—that align with the observed outcomes of LTP, which is likely mediated primarily by synaptic NMDARs (Van Horn et al., 2017; Erreger et al., 2005; Kamenetz et al., 2003). Finally, D-serine has only been shown to have a significant impact on ionotropic NMDAR signaling and raises the possibility of coming to more valid conclusions about the contributions of NMDAR-mediated Ca^{2+} signaling in downstream regulatory processes. This is critically important in the study of activity-dependent gene expression because synaptic-nuclear signaling is mediated primarily by intracellular calcium (Lerea & McNamara, 1993; Bading et al., 1993; Deisseroth et al., 1996; Bito et al., 1996; Dolmetch et al., 2001; Hardingham et al., 2001; Hardingham et al., 2002; Karpova et al., 2013). Therefore, the use of D-serine as a pharmacological modulator of NMDAR activity presents unique possibilities for investigating synaptic plasticity- and activity-dependent gene expression.

Preface to Chapter 2: Aims & Results

Training of methodological skillsets required for **Aim I** were provided by Marion Van Horn, Phil Kesner, and Ed Ruthazer. All data pertaining to **Aim I** was collected and analyzed by Andrew Schultz. Training of wet-lab methodological skillsets required for **Aim II** were provided by Anne Schohl and Cynthia Solek. Brain and mRNA extractions for RNA-seq and qRT-PCR were

performed by Anne Schohl and Marion Van Horn. RNA-seq assaying was performed by G enome Qu ebec. qRT-PCR was performed by Cynthia Solek with help from Andrew Schultz. All RNA-seq data analyses were performed by Andrew Schultz. Analysis tools and programs required for RNA-seq were supplied by the Galaxy Project (Jalili et al., 2020), a publicly available online hub for the analysis of next-generation sequencing data. This chapter was written by Andrew Schultz and edited by Ed Ruthazer.

Chapter 2: Aims & Results

2.1. Aim I: Determination of whether D-serine actions on postsynaptic NMDA receptors mediates retrograde stabilization of RGC axon arbors

2.1.1. Rationale

Activity-dependent plasticity is a central driving force behind the refinement of sensory maps and is engaged in large part through the gating of NMDARs in response to coincident activity patterns. The presence of a co-agonist binding site suggests that NMDAR activation kinetics can be modulated by the bioavailability of synaptic co-agonists. Following the discoveries that D-serine is actively shuttled by astrocytes and the induction of LTP is contingent on astrocytic D-serine at (Yang et al., 2003; Le Bail et al., 2015), it is now widely accepted that endogenous D-serine functions as a gliotransmitter that targets and modulates the activity of synaptic NMDARs *in vivo*. Importantly, altered D-serine levels have been reported in cases of neurological disorders, notably those with pathological aberrances in synaptic plasticity such as Alzheimer’s disease, Schizophrenia, Epilepsy, and models of Amyotrophic lateral sclerosis (Madeira et al., 2015; Sasabe et al., 2007; MacKay et al., 2019), underscoring the diagnostic and potentially therapeutic significance of this signaling molecule. To address how the interaction between D-serine and

NMDARs contributes to the refinement of neural circuits, Van Horn et al. (2017) demonstrated that acutely administered D-serine acts on and augments NMDAR activity and, under conditions of chronic rearing, drives the retinotectal circuit towards synaptic maturation and structural refinement. Indeed, these observed outcomes are strikingly akin to alterations induced by temporally correlated activity patterns (Munz et al., 2014; Kutsarova et al., 2017), raising the possibility that D-serine can be broadly applicable to the study of activity-dependent plasticity. However, of importance in the attempt to understand this from a mechanistic standpoint, it is ultimately necessary to determine if D-serine drives presynaptic stabilization by acting specifically on pre- or postsynaptic NMDARs, or both. The widely accepted notion is that Hebbian plasticity, which facilitates structural stabilization, derives from the repeated activation of postsynaptic NMDARs, given their unique spatial positioning to detect coincident pre- and postsynaptic activity in the form of vesicular release of glutamate and membrane depolarization, respectively. Here, I have sought the answer to whether D-serine engages tectal NMDARs to drive retrograde presynaptic RGC axonal arbor stabilization.

2.1.2. Experimental approach

To determine if D-serine promotes the retrograde structural stabilization of presynaptic RGC axons by acting on and potentiating postsynaptic NMDARs, I have used an innovative new system developed in the lab to generate animals harboring postsynaptic-specific knockdown of GluN1 (Kesner et al., 2020), the obligatory NMDAR subunit that contains the co-agonist binding site. Injection of an oligonucleotide morpholino (MO) against GluN1 (GluN1-MO), which disrupts its translation, or a non-targeting control sequence (Ctrl-MO), into one cell at the two-cell stage of development yields hemimorphant animals with NMDAR knockdown (NMDAR-KD) in one half of the body, and thus one half of the brain (Kesner et al., 2020). Because the RGCs extend their

axons to the contralateral hemisphere, this results in an animal that lacks postsynaptic NMDARs in the retinotectal system on one side and presynaptic NMDARs in the opposite hemisphere. Subsequently, at developmental stages 43-45, the retina contralateral to MO expression was electroporated with GFP plasmid to yield sparsely labeled wild-type RGC axons that innervate optic tectum containing GluN1-MO or Ctrl-MO. 48 hours following electroporation at roughly developmental stage 47, two-photon imaging of labeled RGC axon arbors commences. Animals receiving chronic D-serine rearing (100 μ M) begin treatment immediately after the first imaging session; those not receiving D-serine remain in 0.1x MBSH. Images of the same labeled axons are subsequently acquired 48 hours later, thus generating day 0 and day 2 images to be used for morphometric analyses. Thus, the four experimental conditions include: (1) tectal Ctrl-MO, (2) tectal Ctrl-MO + bath D-serine, (3) tectal GluN1-MO, and (4) tectal GluN1-MO + bath D-serine. Using time-lapse two-photon images, labeled RGC axon arbors are digitally reconstructed in Imaris and the following morphological features are quantified: total arbor length and the number of branch tips. Both metrics are plotted for each sample as repeated measures over the 48-hour period and experimental conditions are compared using one-way or two-way ANOVA and a Tukey post-hoc correction for multiple comparisons depending on data structure (see **Fig. 2 & 3** captions). My original hypothesis was that, if D-serine acts principally via postsynaptic NMDARs to mediate retrograde presynaptic axon stabilization, the presence of postsynaptic GluN1-MO will rescue the effects of D-serine on branch tip number and arbor length (i.e., in RGCs from the GluN1-MO + D-serine condition), restoring them to control values.

2.1.3. Materials and methods

Oligonucleotide morpholino microinjection. Antisense morpholino oligonucleotide against GluN1 5' UTR sequence (CTGTGCCAAGCGGAGCCAATGTCCT) or a control non-targeting

sequence (CCTCTTACCTCAGTTACAATTTATA) is reconstituted in autoclaved water and 10ng is microinjected into one cell at the two-cell stage of development of in vitro fertilized *Xenopus laevis* embryos. Developed by PK and replicated from Kesner et al. (2020).

Retinal EGFP electroporation. EGFP plasmid is mixed with autoclaved water and a miniscule amount of fast green dye for a working concentration of 1.5 μ g/ μ l. Stage 43-45 tadpoles were anesthetized in 0.02% MS-222 (in 0.1% MBSH solution) and was injected into the vitreous humor of the non-MO-containing eye situated contralateral to MO expression. Positive and negative electrodes connected to a stimulator with a 3 μ F capacitor inserted in parallel were positioned to straddle the eye and remained in contact with the lens, followed by the administration of 3-6 electrical pulses (30V intensity, 1.6ms duration). Developed by ER and replicated from Van Horn et al. (2017).

***In vivo* time-lapse imaging.** In vivo time-lapse imaging was performed using a confocal microscope customized for multiphoton imaging with an Olympus 60x (1.0 NA) water immersion objective. At 48 h post-electroporation, animals with sparse GFP-labeled RGC axons (containing 25 or fewer branches) innervating the optic tectum were anesthetized in 0.02% MS-222 and positioned under the objective. Z-stack images were acquired using Fluoview software. Immediately following acquisition of day 0 images, animals receiving D-serine treatment began rearing in 100 μ M D-serine solution (in 0.1% MBSH). Images of the same axonal arbors were subsequently acquired 48 h later. Developed by ER.

Axon reconstruction and morphometry. Z-stack image files (Olympus Multitiff format) were first denoised using CANDLE program in MATLAB (Coupé et al., 2012). Denoised images were then digitally reconstructed using auto-depth manual process tracing in Imaris (Bitplane).

Quantifications for total arbor length and the number of branch tips were extracted using Imaris, which performed these calculations automatically, and values were inputted into GraphPad Prism 9 for statistical analysis and graphical visualization. Morphometric time-lapse analyses are performed using repeated measures one-way or two-way ANOVA (depending on the format of the dataset) followed by Tukey post-hoc test for multiple comparisons. Developed by ER.

2.1.4. Results

Representative images of RGC axons are displayed in **Figure 1**. Group sample sizes were as follows: Ctrl-MO n=8, Ctrl-MO + D-serine n=9, GluN1-MO n=7, GluN1-MO + D-serine n=8.

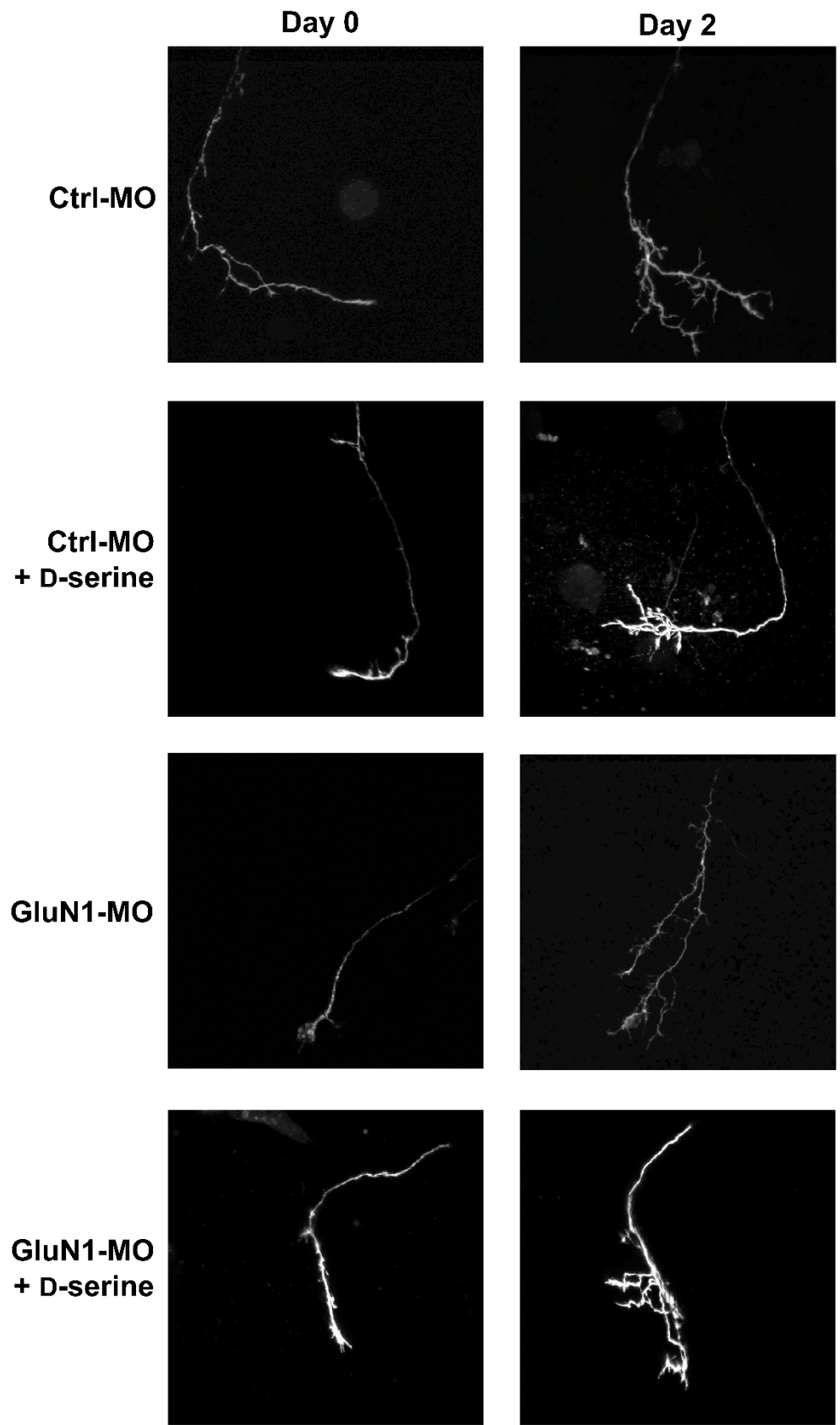
Time-lapse data corroborate the effects on RGC axon arbor branch tips of D-serine observed by Van Horn et al. (2017) and of tectal GluN1-MO by Kesner et al. (2020). In support of Van Horn et al. (2017), chronic D-serine rearing promoted a significant reduction in the number of branch tips in Ctrl-MO hemimorphant animals (**Fig. 2A**), suggesting that chronic D-serine rearing worked as expected. However, no significant effect of D-serine or postsynaptic GluN1-MO was observed on total arbor length (**Fig. 3A**). This is in stark contrast to Van Horn et al. (2017) and Kesner et al. (2020), who observed a striking reduction in arbor length under conditions of chronic D-serine and a moderate, but non-significant, increase in RGC arbor length in the presence of tectal GluN1-MO, respectively. However, the presence of GluN1-MO in tectal neurons did promote the development of RGC axon arbors that exhibited greater number of branch tips compared to Ctrl-MO (**Fig. 2A**), which aligns with the findings of Kesner et al. (2020); however, unlike in Kesner et al. (2020), the increase observed in this study was statistically significant. Because day 0 values are not identical, we chose to examine normalized measurements. Normalizing to day 0 values accounted for initial differences and provided insight into the rate at

which branch tips and arbor length were added to RGCs over the course of the two-day period. In normalized datasets, the presence of the GluN1-MO did significantly increase the rate at which new branches and arbor lengths were added (**Fig. 2B & 3B**, respectively), as was expected based on the findings of Kesner et al. (2020). Because there were no significant differences in day 0 values for the number of branch tips or total arbor length, we chose to examine the number of added branch tips and the change in arbor length between day 0 and day 2 (**Fig. 2C & 3C**, respectively). Doing so provided insight into how D-serine and the presence of GluN1-MO impacted the rates of these morphological changes. Here, D-serine resulted in a significant decrease in the number of branches added to RGCs in Ctrl-MO tectum (**Fig. 2C**). Additionally, the presence of the GluN1-MO resulted in significant increases in the number of RGC branch tips added (**Fig. 2C**) and arbor length added between day 0 and 2 (**Fig. 3C**). Together, these demonstrations substantiate the well-established notion that postsynaptic NMDARs mediate the structural stabilization of presynaptic branches through the action of a retrograde signal and indicate that D-serine and tectal GluN1-MO exerted effects on the number of RGC axon arbor branch tips like those previously reported (Van Horn et al., 2017; Kesner et al., 2020). Why neither manipulation replicated earlier findings on total arbor length—except GluN1-MO on normalized arbor length relative to Ctrl-MO (**Fig. 3B**)—is perplexing but may be explained by the relatively small sample sizes. Alternatively, the lack of an effect of D-serine on total arbor length may be explained by three samples that exhibited low day 0 arbor lengths, meaning that normalized values were thus relatively high and may not be representative of the condition or effect of D-serine in physiological conditions. According to **Figure 3A**, there were slight trends manifesting an effect on arbor length, and perhaps with the addition of more samples both D-serine and GluN1-MO might exert previously reported effects on arbor length akin to those observed on branch tip number (**Fig. 2A**).

Tectal GluN1-MO does not fully abrogate effects of D-serine on presynaptic morphology, but results suggest that D-serine might be functioning through multiple pathways. Most strikingly, though GluN1-MO did rescue the effects of D-serine rearing on axonal branch number to Ctrl-MO values (**Fig. 2A & 2B**, though the latter revealed no effect of D-serine under Ctrl-MO conditions), D-serine appeared to still promote a reduction in the number of RGC branch tips in the case of postsynaptic NMDAR knockdown via GluN1-MO compared to GluN1-MO without D-serine treatment (**Fig. 2A**). Additionally, the presence of tectal GluN1-MO completely restored the effect of D-serine in reducing branch tip addition to Ctrl-MO values, but not to GluN1-MO values (**Fig. 2C & 3C**), suggesting that D-serine still exerted stabilizing effects on branch tips via a postsynaptic NMDAR-independent mechanism. Likewise, tectal GluN1-MO restored arbor length addition (**Fig. 3C**), but because no effect of D-serine on reducing arbor length, normalized length, or length addition was observed in Ctrl-MO conditions (**Fig. 3A-C**), the latter finding is challenging to interpret. Together, these results demonstrate that, while D-serine did mediate presynaptic RGC axonal arbor stabilization by acting on postsynaptic NMDARs, it likely also functioned in tandem with another pathway to the same end. However, it should be noted that five of the seven samples in the GluN1-MO condition originate from animals of the same cohort, and these five cells display the largest arbors in the condition. Therefore, these samples may not be truly representative, and the addition of more samples in this condition may bring the mean value closer to the values exhibited in the GluN1-MO + D-serine condition.

The results of this experiment are both encouraging and perplexing. Several of the measures corroborate Van Horn et al. (2017) and Kesner et al. (2020) by indicating that D-serine promoted a reduction in the number of branch tips on RGCs and that postsynaptic NMDARs contributed to the structural stabilization of presynaptic branches, respectively. These results also seem to imply

that D-serine promoted presynaptic stabilization of RGCs through two different mechanisms: one through postsynaptic NMDARs and another through a mechanism that has yet to be elucidated. Possible explanations for this are discussed in detail in **Chapter 3: General Discussion**. However, it should again be stressed that some RGCs observed may not be fully representative of their conditions. A few more cells will likely have to be added to the Ctrl-MO + D-serine and GluN1-MO conditions to come to concrete conclusions regarding the precise contribution of postsynaptic NMDARs to D-serine-mediated stabilization of presynaptic RGC axon arbors.



↑ **Figure 1. Representative time-lapse images of RGC axonal arbors over a two-day period.** Experimental conditions include Ctrl-MO, Ctrl-MO + D-serine, GluN1-MO, and GluN1-MO + D-serine. RGCs were electroporated with EGFP approximately 48 h prior to day 0 imaging sessions. *In vivo* time-lapse imaging was performed using a confocal microscope customized for multiphoton imaging with an Olympus 60x (1.0 NA) water immersion objective. Immediately following the acquisition of day 0 images, animals that received D-serine treatment were placed in bath D-serine (100 μ M D-serine in 0.1x MBSH solution). Animals not receiving D-serine remained in 0.1x MBSH solution. 48 h after the first imaging session, day 2 images were acquired for the same EGFP-labeled RGCs. Following the completion of imaging sessions, Z-stack images were denoised, imported into Imaris (Bitplane), and digitally reconstructed using auto-depth (or manual when required) process tracing.

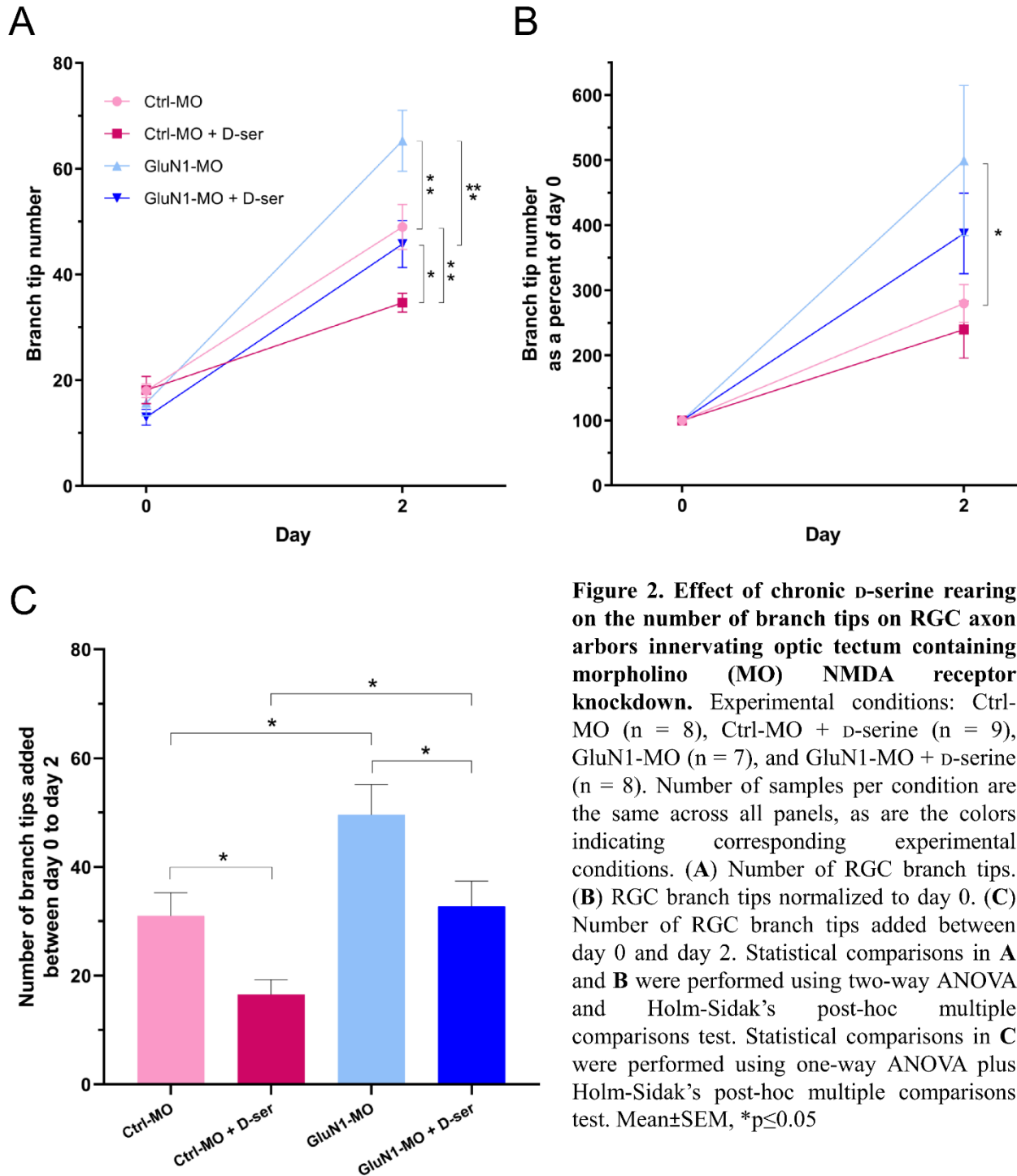


Figure 2. Effect of chronic D-serine rearing on the number of branch tips on RGC axon arbors innervating optic tectum containing morpholino (MO) NMDA receptor knockdown. Experimental conditions: Ctrl-MO (n = 8), Ctrl-MO + D-serine (n = 9), GluN1-MO (n = 7), and GluN1-MO + D-serine (n = 8). Number of samples per condition are the same across all panels, as are the colors indicating corresponding experimental conditions. **(A)** Number of RGC branch tips. **(B)** RGC branch tips normalized to day 0. **(C)** Number of RGC branch tips added between day 0 and day 2. Statistical comparisons in **A** and **B** were performed using two-way ANOVA and Holm-Sidak's post-hoc multiple comparisons test. Statistical comparisons in **C** were performed using one-way ANOVA plus Holm-Sidak's post-hoc multiple comparisons test. Mean±SEM, *p≤0.05

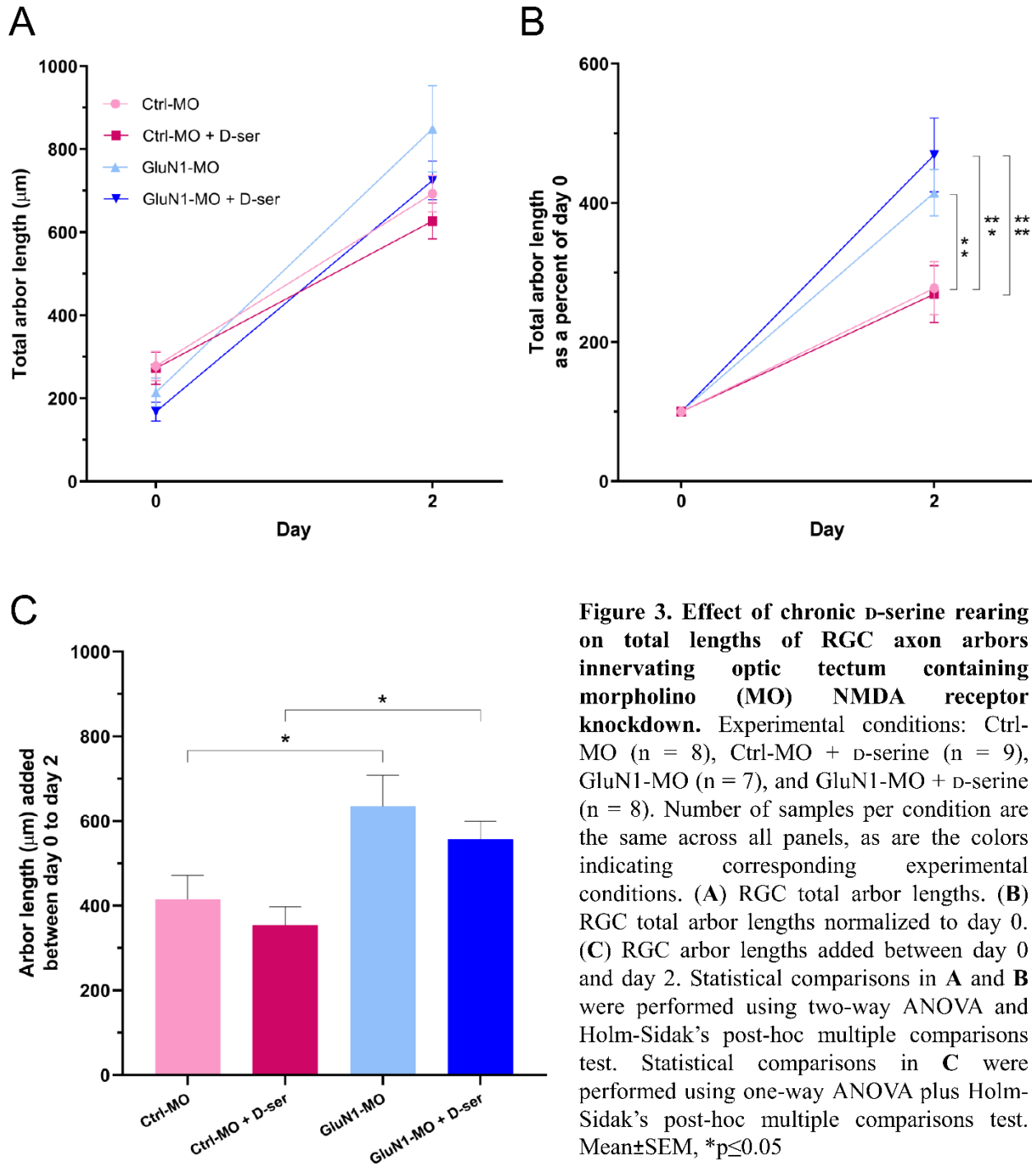


Figure 3. Effect of chronic D-serine rearing on total lengths of RGC axon arbors innervating optic tectum containing morpholino (MO) NMDA receptor knockdown. Experimental conditions: Ctrl-MO (n = 8), Ctrl-MO + D-serine (n = 9), GluN1-MO (n = 7), and GluN1-MO + D-serine (n = 8). Number of samples per condition are the same across all panels, as are the colors indicating corresponding experimental conditions. (A) RGC total arbor lengths. (B) RGC total arbor lengths normalized to day 0. (C) RGC arbor lengths added between day 0 and day 2. Statistical comparisons in A and B were performed using two-way ANOVA and Holm-Sidak's post-hoc multiple comparisons test. Statistical comparisons in C were performed using one-way ANOVA plus Holm-Sidak's post-hoc multiple comparisons test. Mean±SEM, *p≤0.05

2.2. Aim II: Characterization of brain gene expression in response to chronic D-serine rearing and NMDA receptor blockade.

2.2.1. Rationale

An enduring challenge in cellular neuroscience is deciphering the crosstalk between neuronal and synaptic activity, plasticity, and gene expression. Although this task is certainly broad in scope, owing primarily to the fact that many candidates have likely yet to be identified, it remains clear that NMDARs are central conduits that gate the downstream outcomes of activity-dependent plasticity, such as gene expression (Qian et al., 1993; Nguyen et al., 1994). Hence, **Aim II** leverages the robust effects of D-serine on NMDAR activation, retinotectal circuit refinement, and the induction of LTP at central synapses, while maintaining intrinsic patterns of neural activity, to generate a pool of candidate transcriptional effectors of synaptic activation and activity-dependent plasticity.

Aim II arose from a defining question that succeeds my first hypothesis but has since evolved into an inquiry much broader in scope. Initially, I was curious about if D-serine does, in fact, act on postsynaptic NMDARs to mediate presynaptic stabilization, what signaling mechanisms mediate this process? The most plausible explanation is through the release of a diffusible, or activation of a transmembrane retrograde signal. The results of **Aim I** corroborate the notion of a retrograde signal that is mediated by postsynaptic tectal NMDARs, but also highlight additional complexities that are likely embedded in D-serine-NMDAR signaling during circuit refinement. Nevertheless, emerging evidence is beginning to underscore the continuum between plasticity and activity-dependent gene expression (West et al., 2001; Tabuchi, 2008). Given the robustness of D-serine's effects on circuit stabilization over days, it stands to reason that a retrograde signal, if it is present, might be differentially expressed in tectal neurons and detectable in transcriptomic assays

such as RNA-seq. More broadly, we believe that chronic D-serine rearing presents an exquisite opportunity to probe the plethora of genes and gene programs that are engaged by NMDAR activation and the induction of activity-dependent plasticity. Because D-serine profoundly augments glutamatergic transmission by acutely enhancing NMDAR currents, and chronically promotes glutamatergic retinotectal synapse maturation and limits NMDAR-dependent presynaptic remodeling, D-serine rearing can be exploited to investigate the outcomes of synaptic activation on gene expression. Thus, I believe that D-serine induces the expression of unique genes and gene programs, and that many D-serine-regulated genes have implicated roles in plasticity or have been demonstrated by others to be regulated by synaptic or neuronal activity. Likewise, pharmacological NMDAR blockade should induce distinct genes and gene programs that are putatively regulated by NMDAR activity and, by cross-referencing with D-serine-regulated genes, will begin to reveal which D-serine-regulated genes are likely to be NMDAR-dependent. **Aim II** provides a novel, unbiased characterization of D-serine- and NMDAR blockade-regulated genes in the *Xenopus laevis* brain and explores how both sets of induced gene programs are related and may be contributing to neural plasticity.

2.2.2. Experimental approach

To investigate genes that are regulated by D-serine and NMDAR activity in the *Xenopus laevis* brain, RNA-sequencing was performed on whole brain tissue RNA extracts from three rearing conditions: Control, 100 μ M bath D-serine, and 20 μ M bath (R)-CPP, a competitive antagonist of the NMDAR glutamate binding site (Lehmann et al., 1987). Since D-serine exerts optimal effects on structural stabilization and synaptic maturation about 48 h after bath application (Van Horn et al., 2017) and transcription and translation are believed to take time to achieve considerable functional significance, we chose to perform brain RNA extractions 24 h following drug rearing

onset. In each batch, there were three biological replicates per condition, and each replicate consisted of ten brains. Two separate batches of RNA-seq were performed to increase the number of biological replicates per condition to a maximum of 6 and to assess batch effects. RNA-seq assaying was performed by Génome Québec in Montreal, QC.

Brain tissue transcriptomes from animals reared in D-serine revealed genes that were regulated by chronic D-serine exposure. In contrast, genes that are putatively expressed in an NMDAR activity-dependent manner are those whose expression changes in CPP reared samples. To gather quantitative information on the effects of chronic D-serine and CPP treatment on brain gene expression, differential gene expression (DGE) analyses using DESeq2 (Love et al., 2014) on RNA-seq read counts were performed for samples from either rearing condition against control samples. A detailed layout of the data analysis pipeline executed via Galaxy Project (Jalili et al., 2020) can be found in **section 2.2.3**. Several of the RNA-seq results were then validated using qRT-PCR.

Two distinct datasets were separately analyzed: the first with all 49,109 genes included in the current *Xenopus laevis* v9.2 reference genome (**Fig. 4-7**) and the second that was removed of all genes that displayed batch-dependent effects on expression (**Fig. 8-12**; *how batch dependencies on gene expression were determined will be explained in section 2.2.4.*); these two datasets are henceforth referred to as “primary dataset” and “batch-effects-removed dataset,” respectively. Control samples and samples composed of brain tissue from animals reared in D-serine or CPP are denoted by “Ctrl,” “Dser,” and “CPP,” respectively. Additionally, “_#” indicates which replicate the sample is. Importantly, from this point on, the terms “replicate” and “sample” are typically used interchangeably. Three samples were removed from analysis because they did not pass initial controls for mRNA quality: Ctrl_4, CPP_1, and CPP_4. Therefore, the number of samples in Ctrl,

D-ser, and CPP conditions came to 5, 6, and 4, respectively. “D-serine-regulated genes” refers to genes that exhibited statistically significant differences in transcript abundance according to DGE analysis of D-serine versus Control samples (e.g., Dser vs. Ctrl), whereas “CPP-regulated genes” refers to genes that exhibited statistically significant differences in transcript abundance according to DGE analysis of CPP versus Control samples (e.g., CPP vs. Ctrl). Finally, “coregulated genes” often refers to genes that were co- or anti-regulated by D-serine and CPP rearing, unless explicitly stated otherwise, whereas “non-coregulated genes” refers to *all other* genes that were significantly differentially expressed by D-serine or CPP relative to Control.

2.2.3. Materials and methods

Brain extractions for RNA-seq and qRT-PCR. Prior to brain extractions, animals were reared for 24 hours in 0.1x MSBH (Control), 100µM bath D-serine (CAS No. 312-84-5), or 20µM bath (R)-CPP (CAS No. 126453-07-4) made up in 0.1x MBSH to indicated concentrations. For brain extractions, animals were anesthetized in 0.1% MS-222 and positioned under a microscope. Following cutting the optic nerves and removal of hindbrain sections, the brains were removed and placed in chilled ddH₂O. For RNA-seq, each replicate consisted of 10 brains, and for qRT-PCR, each replicate consisted of 25 brains. In total 18 replicates were extracted for RNA-seq, and three for qRT-PCR. mRNA was extracted from brains immediately after completing all extractions for a single replicate. Following tissue homogenization, RNA was purified using spin column Qiagen RNeasy Mini Kit according to factory specifications.

RNA-seq data analysis pipeline. RNA-seq assaying was performed by Génome Québec Inc. in Montreal, QC. Raw read counts in the form of FASTQ files were acquired from Génome Québec’s online client portal. FASTQ files were then extracted and uploaded to the *Galaxy Project*

(Jalili et al., 2020) EU cloud server. FASTQ files were trimmed of adapter sequences using *Trim Galore!*, followed by quality control checks using *FastQC*. Trimmed read files were subsequently aligned to the *Xenopus laevis* v9.2 reference genome using the *STAR* (Dobin et al., 2013). An annotation file containing exon-intron boundaries and v9.2 gene names was acquired from Xenbase to aid in this alignment. Aligned BAM files were then inputted into *featureCounts* (Liao et al., 2014), along with the previously used gene annotation file, to yield transcript read counts. Tabular count files were inputted into *DESeq2* (Love et al., 2014) for differential expression analyses. Volcano plots and relative expression heatmaps were constructed in GraphPad Prism 8. Significance thresholding in volcano plots was set to an adjusted p-value ≤ 0.05 . Read count values used in the relative expression heatmaps, which were outputted as tabular files by the DESeq2 module, were automatically normalized to sample-specific sequencing depth.

qRT-PCR assay. According to manufacturer specifications, 1 mg of total RNA was used for reverse-transcription with Superscript II or Superscript IV (Invitrogen). TaqMan qRT-PCR (Invitrogen) was performed using custom probes designed against *Xenopus laevis* ube2m.S, rasgrp3.S, and pkn3.S. No amplification was measured in -RT and -template controls. Data were normalized to the reference gene ube2m.S. Relative gene expression was calculated according to Livak and Schmittgen (2001).

qRT-PCR primer design. Primers were designed using Primer3 (<https://primer3.ut.ee/>).

Primer sequences are listed below:

Gene ID	Left/Forward primer	Right/Reverse primer
ube2m.S	AGAGAGGACTGGAAGCCTGT	CGGGTCTTCAGGATTTGGCT
rasgrp3.S	AGAGACCAGCATGGATTTGA	TTAGGATTCCGTGGCTCAAG

pkn3.S	GGCAGGGAAGAGCATGAAG	TCTTCCACCTGTAGAGTTGTTC
--------	---------------------	------------------------

2.2.4. Results

Chronic D-serine and CPP treatment induced the expression of distinct gene programs, but batch-dependent effects were prevalent. In total, 49,109 genes were analyzed in the primary dataset. Transcript read counts were first used in principal component analysis (PCA; **Fig. 4A**) and sample-to-sample distance analysis (i.e., the correlation between samples based on transcript read counts; **Fig. 4B**) to assess dimensionality of the data. Samples cluster almost solely based on batch (**Fig. 4A**) and samples of the same batch were tightly correlated compared to samples of differing batches (**Fig. 4B**), which indicate the strong presence of batch effects in the primary dataset. This will be addressed shortly. **Figure 5** displays a relative expression heatmap of selected genes that exhibited high variability across *all* samples; how relative expression based on read counts was calculated is explained in detail in the figure caption. These data indicate that D-serine and CPP rearing induced gene expression programs that were distinct from each other and distinct from Control samples. DGE analysis was performed using DESeq2 (Love et al., 2014) via Galaxy Project (Jalili et al., 2020; **Fig. 6**); **Figure 6A** displays DGE in response to D-serine rearing and **Fig. 6B** displays DGE in response to CPP rearing. There were 349 D-serine-regulated genes (i.e., that were significantly differentially expressed) and 283 CPP-regulated genes in the primary dataset. Relative expression heatmaps of 95 highly differentially expressed candidate genes based on adjusted p-value in response to D-serine (**Fig. 7A**) or CPP (**Fig. 7B**) indicate that each rearing condition induced gene expression programs that were distinct from control conditions. Of all D-serine- and CPP-regulated genes (**Fig. 6A** & **6B**, respectively), 83 were common and thus constitute the coreregulated dataset. When plotted based on their corresponding log₂fold-changes

from D-serine versus Control and CPP versus Control DGE analyses, coregulated genes display a striking positive linear relationship, indicating that the expression of genes that were coregulated by D-serine and CPP rearing were predominantly regulated in the same direction (i.e., up- or down-regulated; **Supplementary Fig. 1B**; $R^2 = 0.91$). However, the possibility remains that this may have been an artifact of batch effects.

Removal of batch effects corroborated and strengthened previous results. A lingering constraint to making concrete conclusions about the effects of D-serine and CPP rearing on gene expression was the indication of strong batch effects on gene expression. To acquire putative batch effects, DGE analysis was performed on all batch 1 samples (Ctrl_1, Ctrl_2, Ctrl_3, Dser_1, Dser_2, Dser_3, CPP_2, and CPP_3) versus all batch 2 samples (Ctrl_5, Ctrl_6, Dser_4, Dser_5, Dser_6, CPP_5, CPP_6). It is implied that genes that displayed significant differential expression were dependent on batch. Read counts for these genes were then retroactively removed from tabular read count files and DGE analyses were performed again in a manner analogous to previous comparisons. Strikingly, in the batch-effects-removed dataset, samples clustered in PCA based on the condition to which they belong (**Fig. 8A**) and samples in the same condition tended to exhibit more correlation than samples of different conditions (**Fig. 8B**), though the latter is qualitatively less apparent, likely owing to the sheer size and complexity of the read count data. Using the batch-effects-removed dataset, **Fig. 9A** displays DGE in response to D-serine rearing and **Fig. 9B** displays DGE in response to CPP rearing. There were 698 D-serine-regulated genes and 558 CPP-regulated genes in this dataset, each roughly doubling in quantity compared to the primary dataset. These data suggest that DESeq2 was able to extract statistically significant differences in transcript abundance and condition-specific expression profiles more effectively when variance due to batch effects had been reduced. More importantly, however, and addressing one of our primary

hypotheses, these data demonstrate that D-serine and CPP treatment broadly induced the expression of unique gene programs. Many of the regulated genes within these programs have implicated roles in plasticity; **Figure 5** highlights a number of these genes but select candidate genes will be discussed in greater detail in **Chapter 3: General Discussion**.

Of all D-serine- and CPP-regulated genes in the batch-effects-removed dataset, 182 were common and thus coregulated based on expression fold-changes (**Fig. 10B**). As before, coregulated genes displayed a striking positive linear relationship in their fold-changes in response to both rearing conditions ($R^2 = 0.90$). To determine if the occurrence of gene coregulation was simply the result of intrinsic variance within control sample read counts rather than real effects of drug rearing, coefficients of variance of control sample read counts were calculated for coregulated genes versus non-coregulated genes (**Fig. 11A**). Additionally, read counts for control samples of coregulated and non-coregulated genes were normalized to the read count population mean (i.e., the mean of control sample read counts for all coregulated *and* non-coregulated genes) and compared (**Fig. 11B**). Neither comparison was significant, demonstrating that variance in control sample read counts did not account for observed gene coregulation. Thus, coregulation was a real effect of chronic D-serine and CPP rearing.

Together, these findings are quite striking. We originally expected to see an abundance of genes that were anti-regulated because D-serine and CPP have largely inverse effects on NMDAR activation: enhancement versus blockade, respectively. However, this was not the case. The overwhelming propensity for coregulation rather than anti-regulation by both treatments suggests that, where both pathways overlap, they impinge upon signaling to or inside the nucleus in roughly analogous manners. How this functional convergence on transcription may have manifested will be discussed in the following chapter. More broadly, these results demonstrate that chronic D-

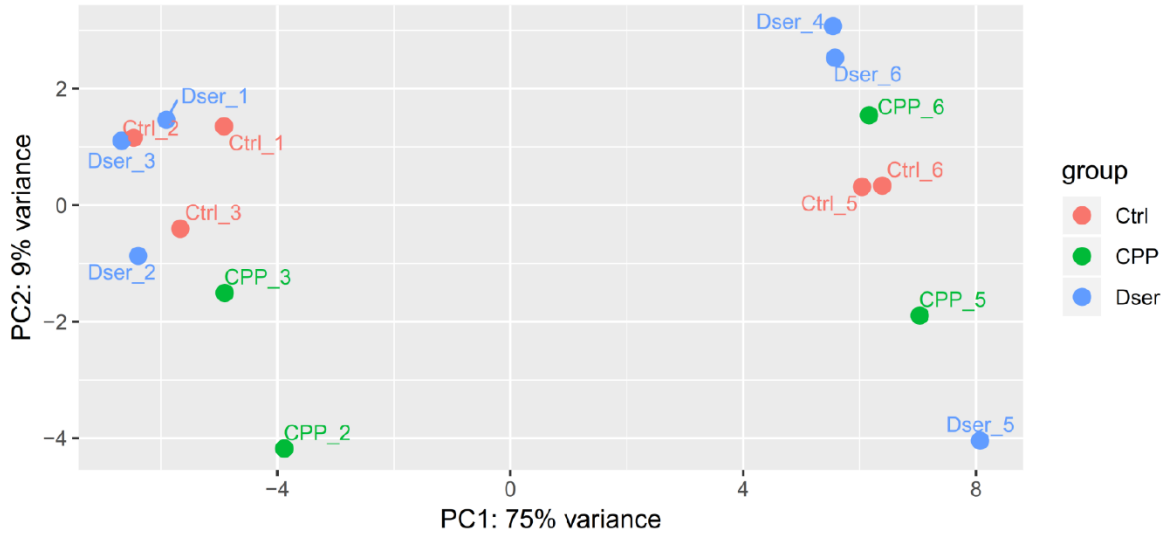
serine and CPP rearing induced the expression of both unique and common gene expression programs.

RNA-seq datasets reveal D-serine-regulated genes that were putatively dependent on NMDAR activity. Using the batch-effects-removed dataset, DGE analysis between D-serine and CPP provided insight into what other genes may have been anti-regulated by the two rearing conditions (**Fig. 10A**). This analysis is not perfect because it did not capture the true effects of each rearing condition on gene expression relative to Control, but when used in conjunction with D-serine versus Control DGE permitted the parsing out of what D-serine-regulated genes were likely to be NMDAR-dependent (**Fig. 12A & 12B**). First, a list of genes that were significantly differentially expressed by D-serine relative to CPP was generated. It is implied that these genes were oppositely affected by D-serine and NMDAR blockade. Subsequently, these genes were selectively filtered through DGE for D-serine vs. Control to yield their true expression effects in response to D-serine rearing. Of the 412 genes that were significantly differentially expressed in D-serine versus CPP, 102 of them were also significantly differentially expressed in D-serine versus Control (**Fig. 12B**). This illustrated what D-serine-regulated genes might have been NMDAR-dependent. However, it did not indicate, strictly, whether the expression of any of these genes were also regulated by CPP. Of the 102 *potentially* NMDAR-dependent genes, 10 of them were also significantly differentially expressed under conditions of chronic CPP rearing relative to control, indicating an effect of NMDAR blockade on their expression. Expression metrics for these ten putative NMDAR-dependent D-serine-regulated genes were displayed via D-serine versus Control DGE volcano plot (**Fig. 12B**) to capture their expression patterns in response to chronic D-serine rearing. The genes are: *abat.S*, *mgea5.S*, *ralb*, *tmem163.L*, *rrp12.S*, *LOC108709985*, *utp4.L*, *slc6a17.S*, *fam163b.L*, and *ankrd9.L*.

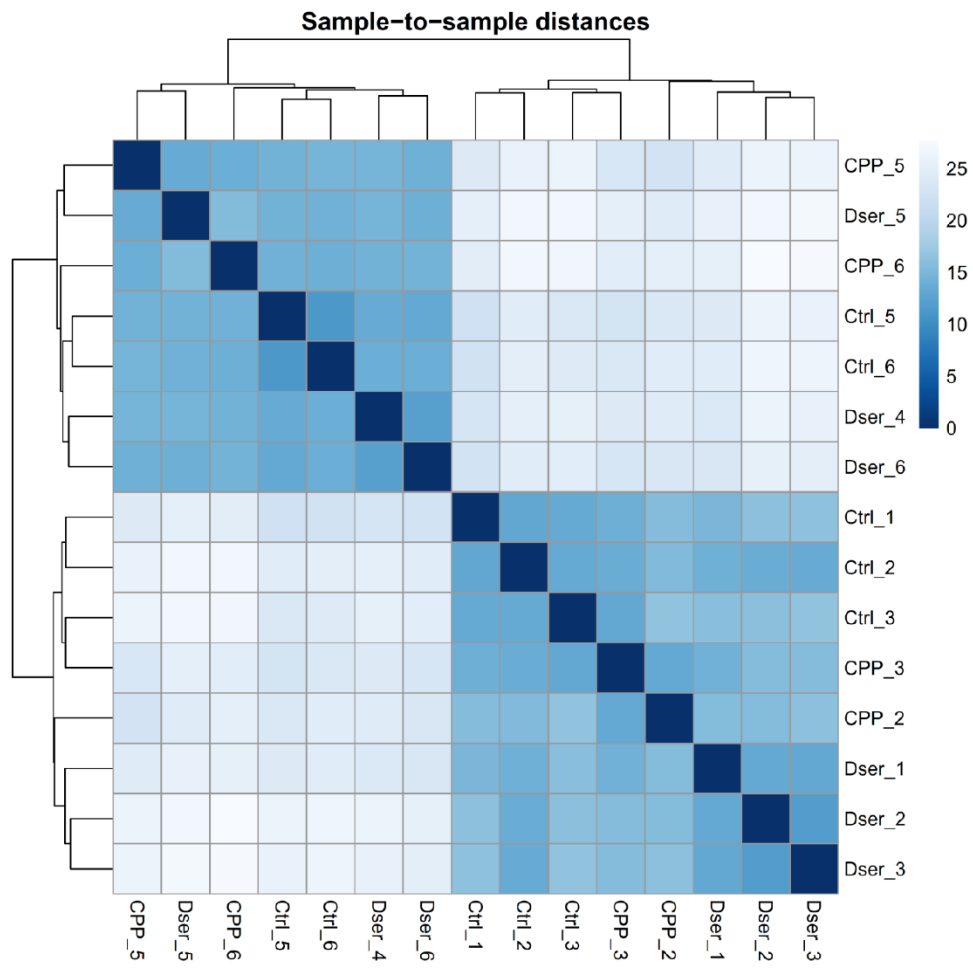
qRT-PCR validates the results of RNA-seq for one of two candidate genes. To validate the results of RNA-seq, qRT-PCR was performed on transcripts corresponding to the genes *rasgrp3.S* and *pkn3.S* (**Fig. 13**). Three biological replicates, each composed of 25 brains from animals reared for 24 h in drug solution, were prepared and then analyzed. The *ube2m.S* gene was used as a reference to calculate mRNA abundance of corresponding target genes (Mughal et al., 2018). In RNA-seq datasets, *rasgrp3.S* was upregulated in response to D-serine rearing (expression fold-change = 2.0) and *pkn3.S* was co-upregulated by D-serine and CPP rearing conditions (expression fold-changes = 1.30 and 1.32, respectively). qRT-PCR confirmed that *rasgrp3.S* transcripts were significantly more abundant in D-serine reared samples compared to controls, with no differences observed in CPP reared samples, both of which were expected based on RNA-seq results (**Fig. 13A**). There were no differences in the abundance of *pkn3.S* transcripts between experimental conditions (**Fig. 13B**). Transcript abundances were subsequently used to calculate expression fold-changes in response to D-serine and CPP rearing. Using all three biological replicates for analysis, no significant changes were measured in expression fold-change of *rasgrp3.S* or *pkn3.S* in D-serine or CPP samples (**Fig. 13C**). Internal controls for the first replicate round of qRT-PCR were suspected of contamination. Thus, when this sample was removed from analysis, *rasgrp3.S* in D-serine treated samples displayed a significant 1.73x fold-change relative to control samples (**Fig. 13D**), consistent with the 2.0x fold-change yielded via RNA-seq datasets. However, *pkn3.S* exhibited no significant fold-changes in expression in D-serine or CPP conditions relative to control. This may ultimately have been due to intrinsic biological variability, or the small number of replicates used for qPCR compared to RNA-seq. It may also have been because the fold-change of *pkn3.S* was relatively low in RNA-seq datasets and thus potentially undetectable by qPCR,

although this explanation is unlikely given the sensitivity of qPCR and the fact that RT-PCR is analogously performed in RNA-seq for the generation of cDNA libraries.

A

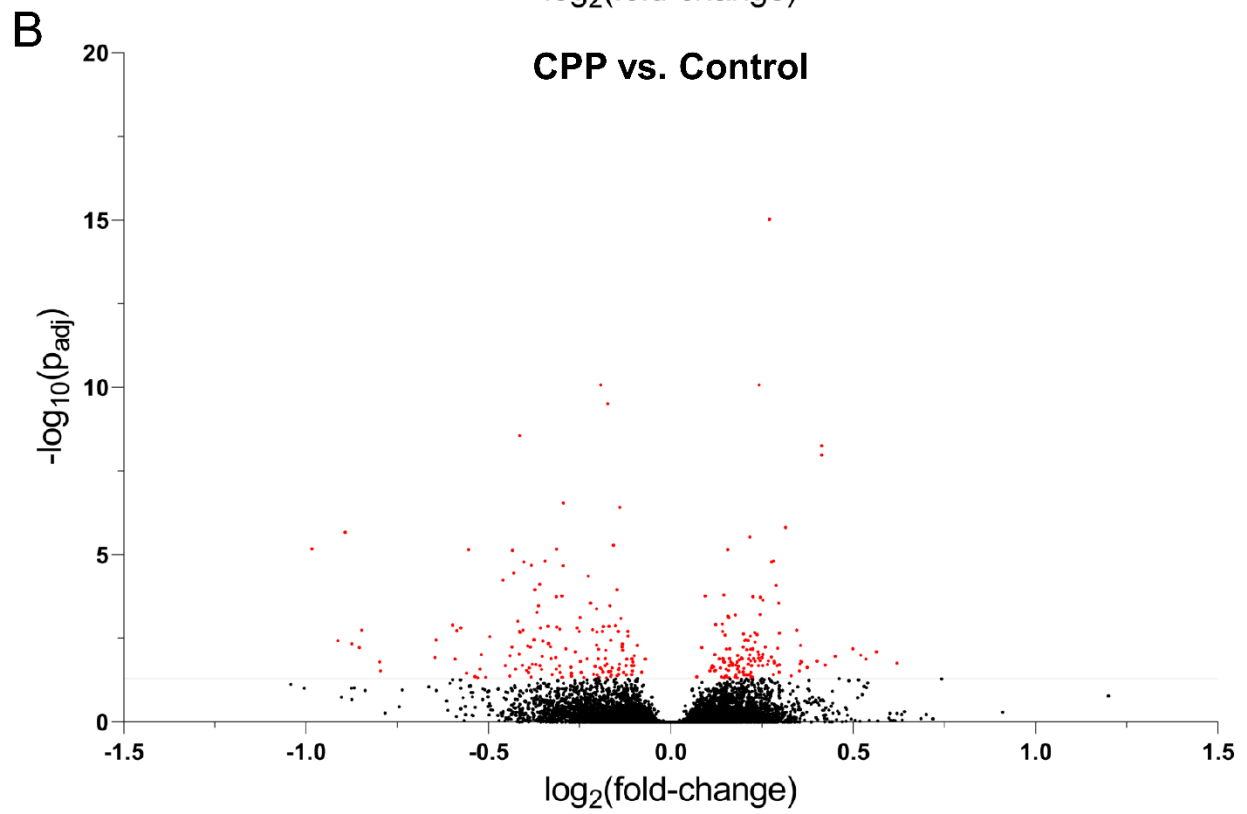
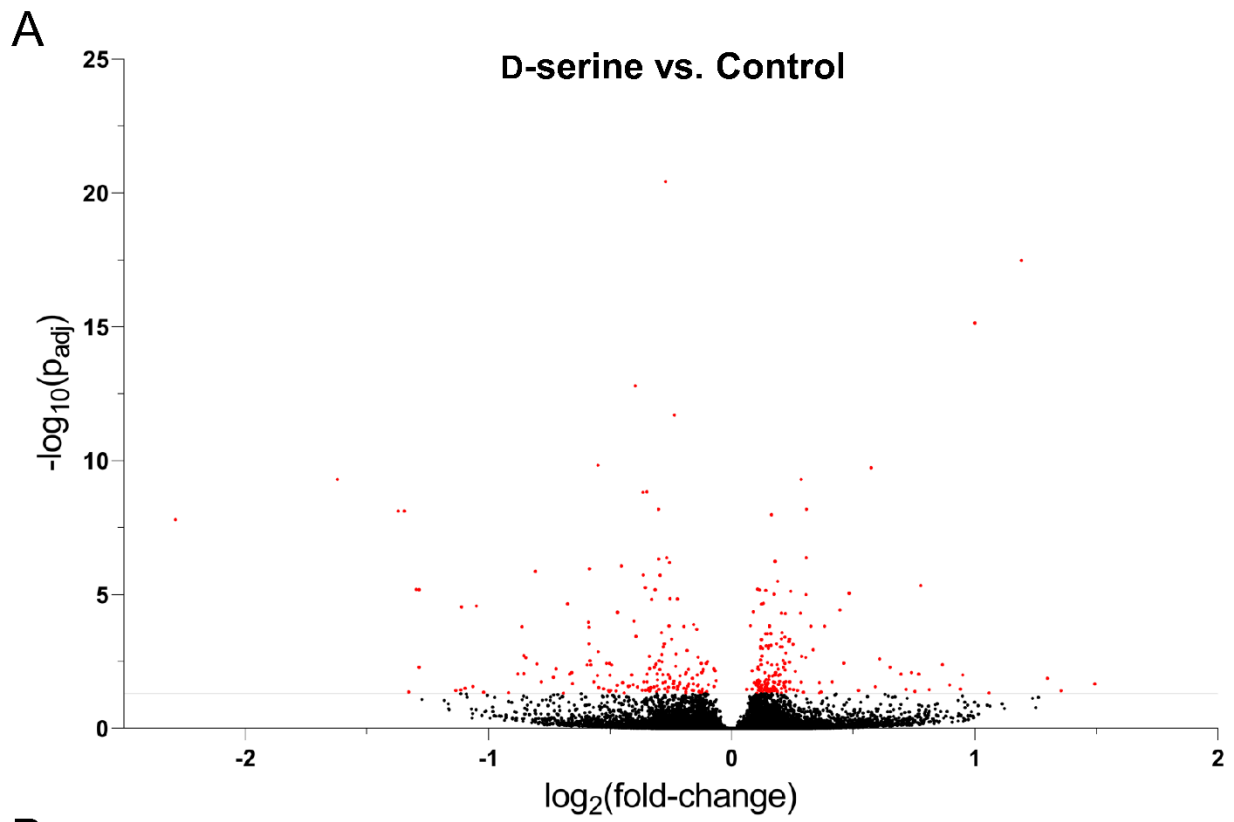


B



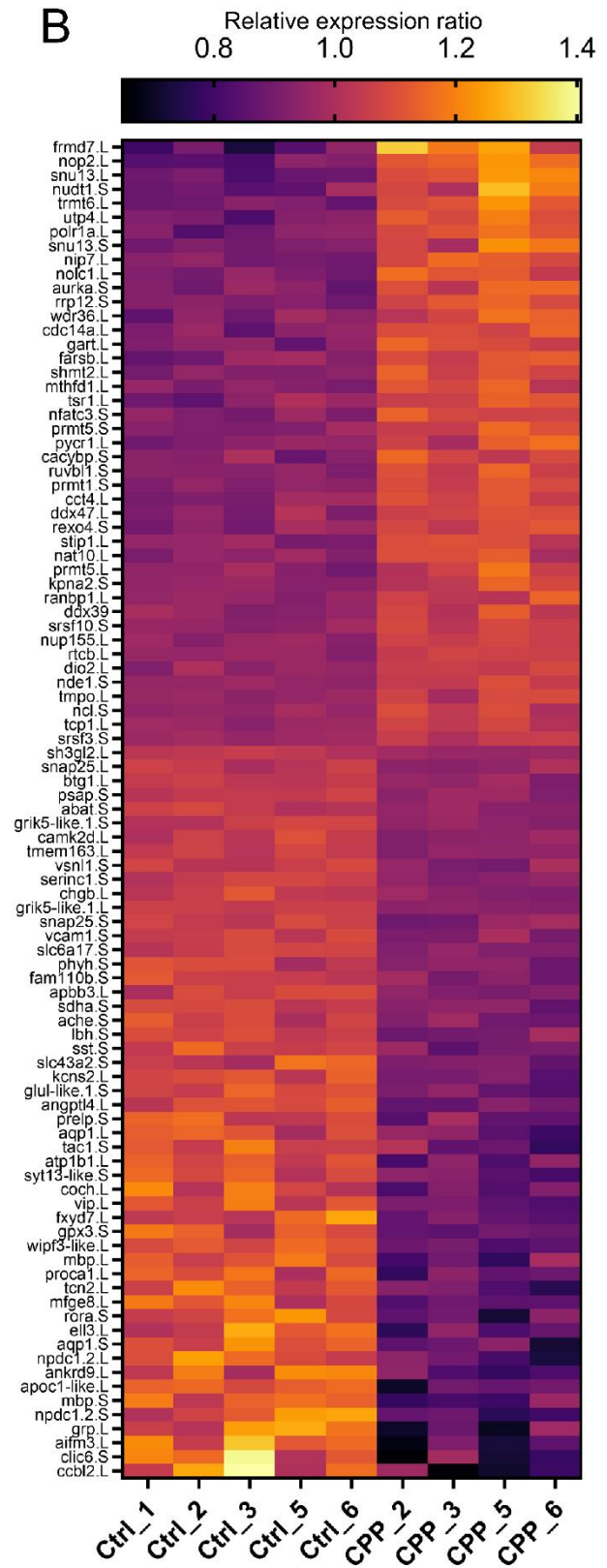
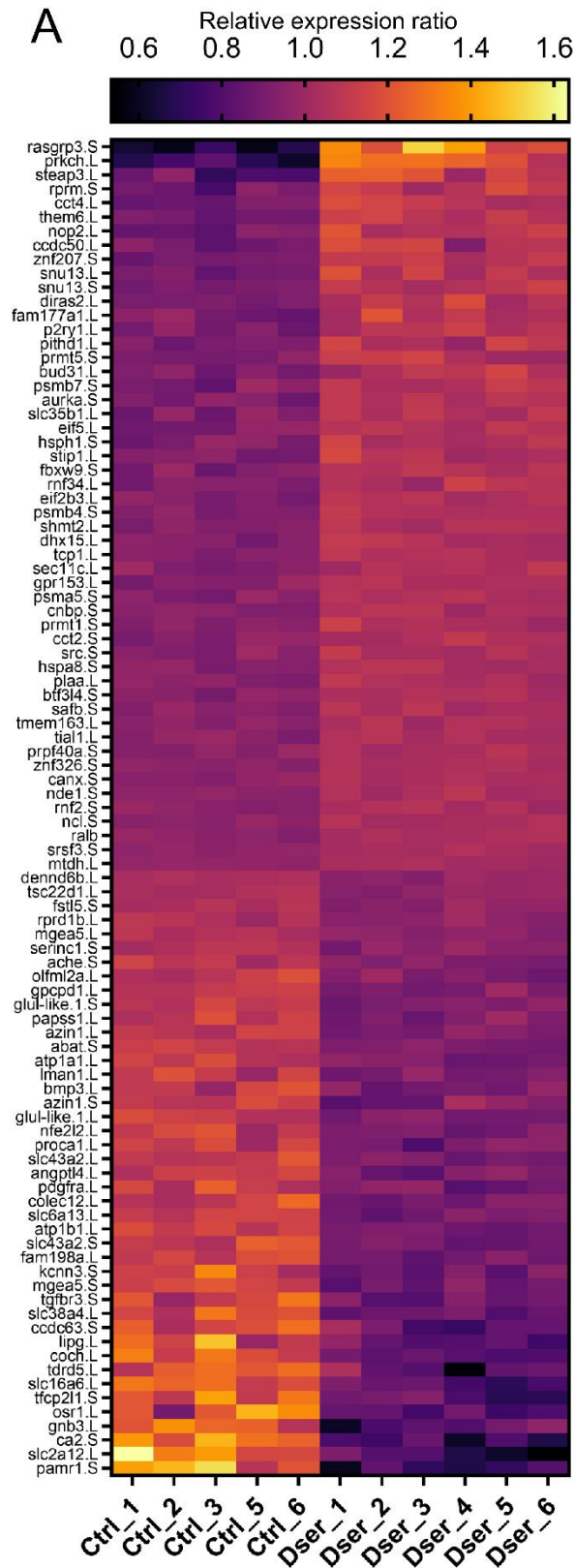
↑ **Figure 4. Dimensionality of primary RNA-seq dataset indicates the presence of batch effects.** (A) Principal component analysis (PCA) and (B) sample-to-sample distances (i.e., correlation between samples based on transcript read counts). “Dser” indicates biological replicates from brain tissue extracted from animals chronically reared D-serine (24 hrs). “CPP” indicates biological replicates from animals chronically reared in the competitive NMDAR glutamate site antagonist CPP, and “Ctrl” indicates control replicates. PCA analysis in (A) indicates samples are markedly clustered based on the batch to which they belong; replicates 1-3 and 4-6 (three samples in total were removed prior to analysis due to unsuccessfully passing mRNA QC tests) were processed and sequenced at different times, and thus each constitute a separate batch. Sample-to-sample distances in (B) indicate that samples of the same batch are more tightly correlated than samples from different batches.

↓ **Figure 5. Expression heatmap displaying the relative abundance of gene transcripts in each sample indicates that chronic D-serine and CPP rearing induce distinct gene programs.** Selected genes were the 75 most variably expressed (e.g., lowest p-values) across all samples according to a likelihood ratio test (LRT) auxiliary tabular output integrated into DESeq2 executed using RStudio. Unannotated genes (e.g., those with “LOC,” “Xelaev,” or “MGC” in the name) were excluded. Transcript read counts used to calculate relative expression were corrected for sample-specific sequencing depth and quantitated as the ratio to the average across *all* samples for a given gene. For example, the value corresponding to the number of corrected read counts for *rasgrp3.S* in the Ctrl_1 replicate was divided by the average number of corrected read counts for *rasgrp3.S* for all 15 samples; this ratio is displayed as a corresponding color. A relative ratio value of 1.0 is equal to the group mean. Chronic rearing in D-serine or CPP occurred for a duration of 24 h prior to brain mRNA extraction, followed by RNA-sequencing. “L” or “S” at the end of each gene name indicates the chromosome on which they are located.

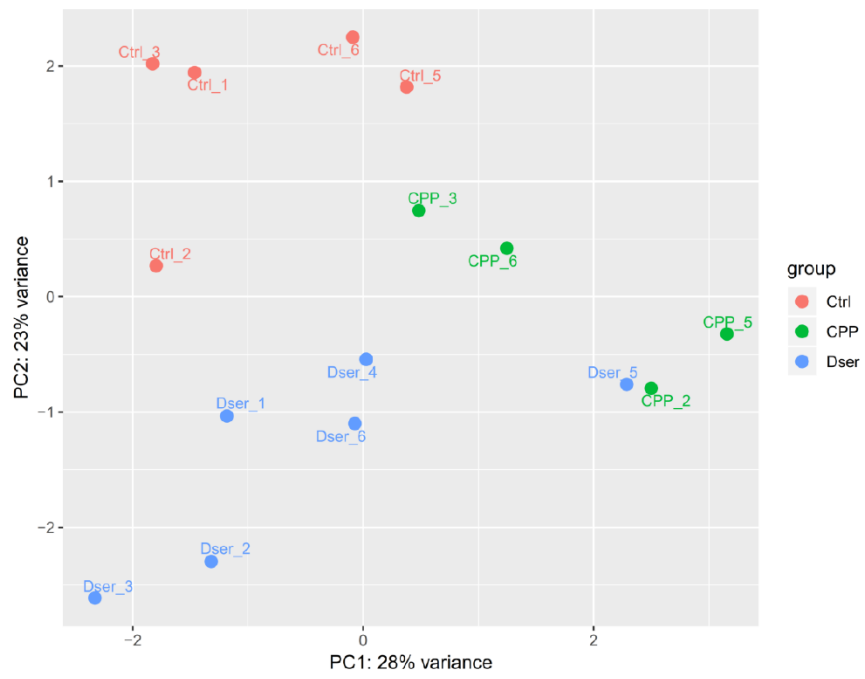


↑ **Figure 6. Differential gene expression under conditions of chronic D-serine or CPP rearing relative to control in primary dataset.** (A) Differential gene expression analysis of D-serine samples (n = 6) vs. Control samples (n = 5). (B) Differential gene expression analysis of CPP samples (n = 4) vs. Control samples. Drug rearing occurred for a duration of 24 h prior to brain mRNA extraction, followed by RNA-sequencing. 49,109 genes were analyzed; each dot corresponds to a single gene. Genes were plotted according to log₂fold-change and adjusted p-value. For example, genes with positive log₂fold-change values reflect transcripts that were more abundant in the treatment condition than in the control condition. Red indicates an adjusted p-value ≤ 0.05 (i.e., positioned above the faint grey line), meaning that gene was significantly differentially expressed in response to rearing; 349 genes were significantly differentially expressed in response to chronic D-serine rearing, whereas 283 were significantly differentially expressed in response to chronic CPP rearing. Differential expression was performed using the DESeq2 program (Love et al., 2014) via the Galaxy Project (Jalili et al., 2020) using mean fit, Cook's outlier filtering, and independent filtering.

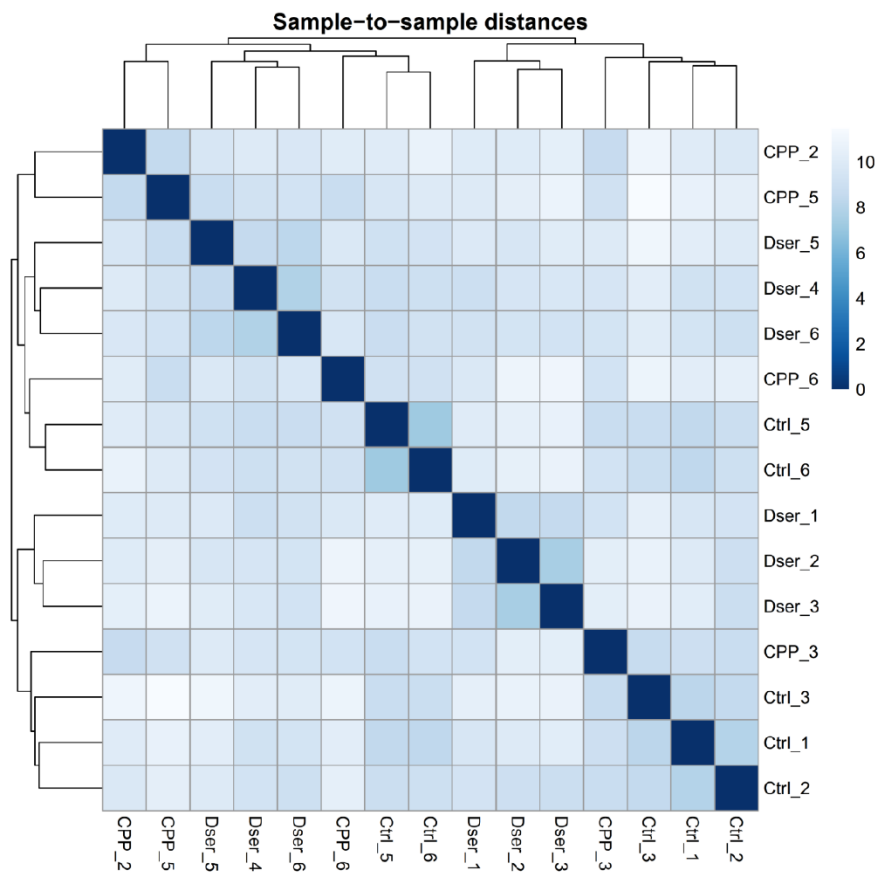
↓ **Figure 7. Relative expression of transcripts that were differentially expressed in response to chronic D-serine or CPP rearing.** (A) Expression heatmap indicates relative abundance of transcripts for D-serine-regulated genes. (B) Expression heatmap indicates relative abundance of transcripts for CPP-regulated genes. Each heatmap displays 95 genes that had the highest adjusted p-values in differential expression analyses (see *Figure 6 and Supplementary Figure 2*), excluding unannotated genes, e.g., those with “LOC,” “Xelaev,” or “MGC” in the name. Read counts used to calculate relative expression were corrected for sample-specific sequencing depths and quantified as a ratio to the average across all samples for a given gene. For example, in (A), the value corresponding to the number of corrected read counts for rasgrp3.S in Ctrl_1 is divided by the average number of corrected read counts for rasgrp3.S for all samples; this ratio is displayed as a color (see *legend above each heatmap*) and thus indicates relative transcript abundance. A ratio value of 1.0 is equal to the group mean. Chronic rearing in D-serine or CPP occurred for a duration of 24 hours prior to brain mRNA extraction, followed by RNA-sequencing. “L” or “S” indicate different chromosomes.



A

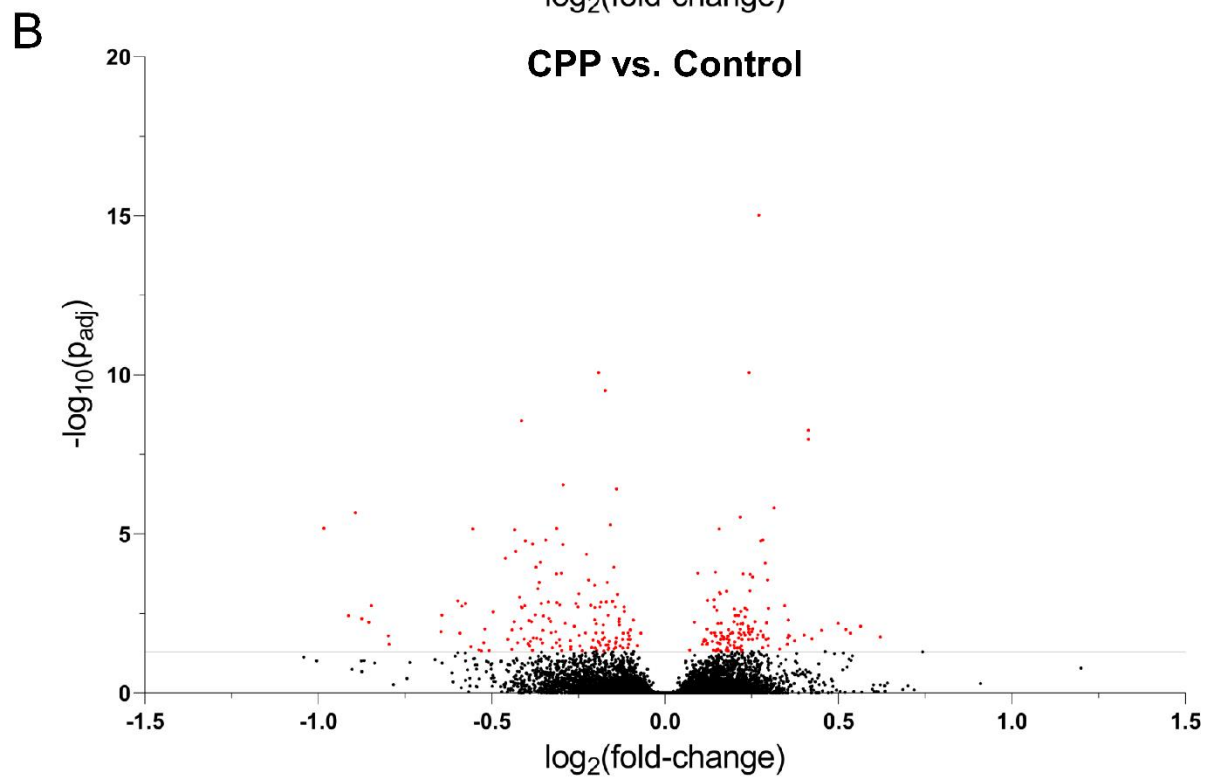
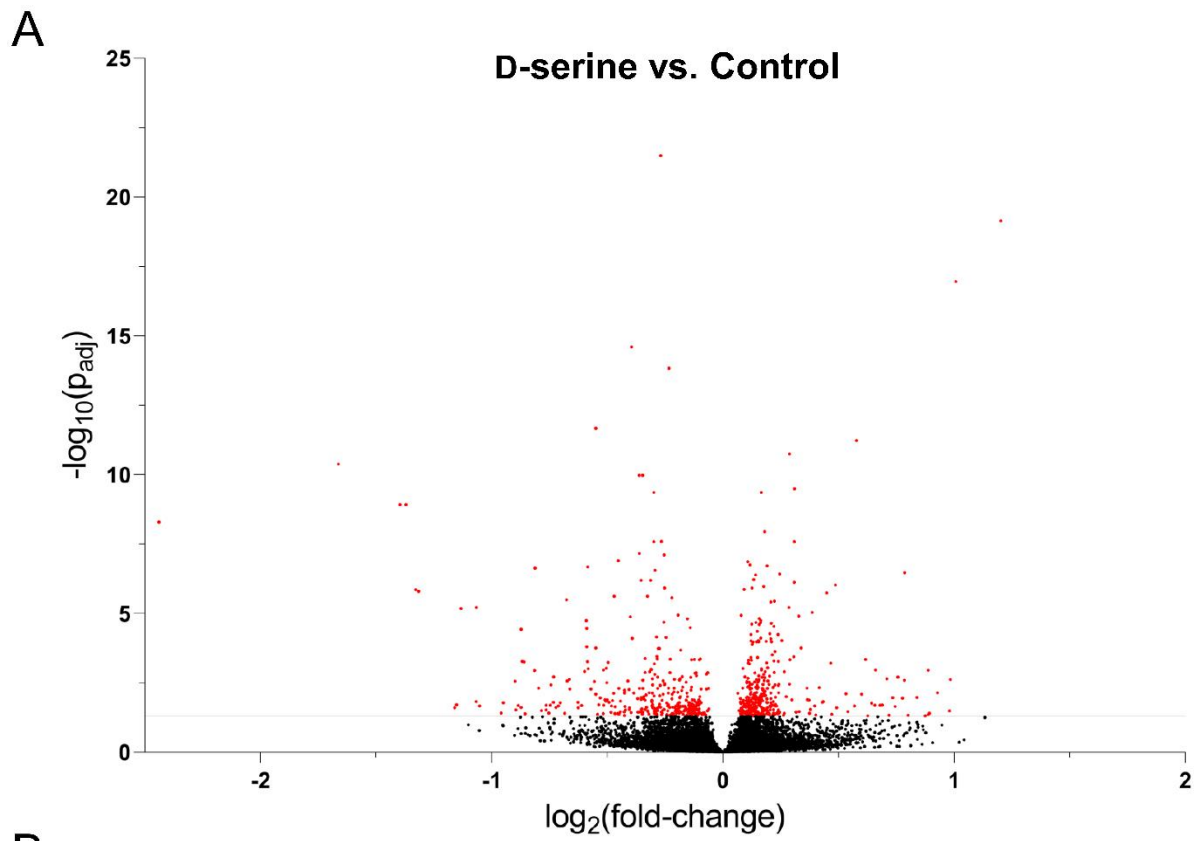


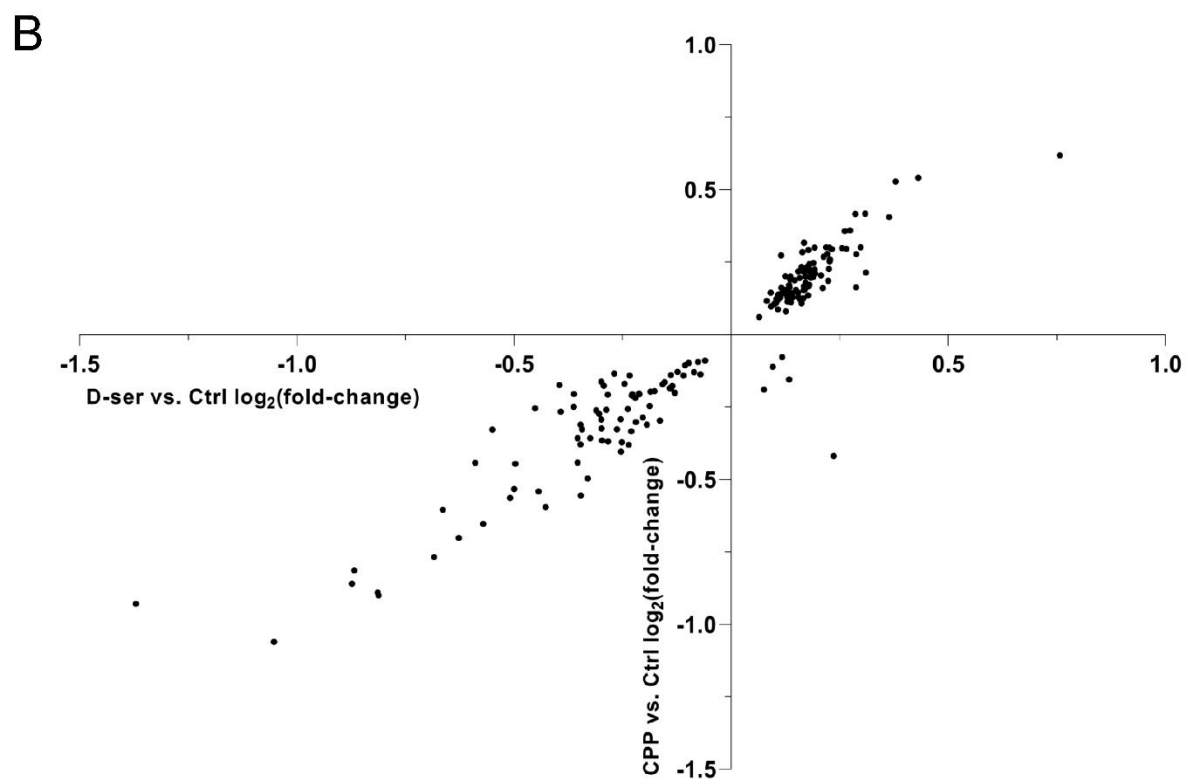
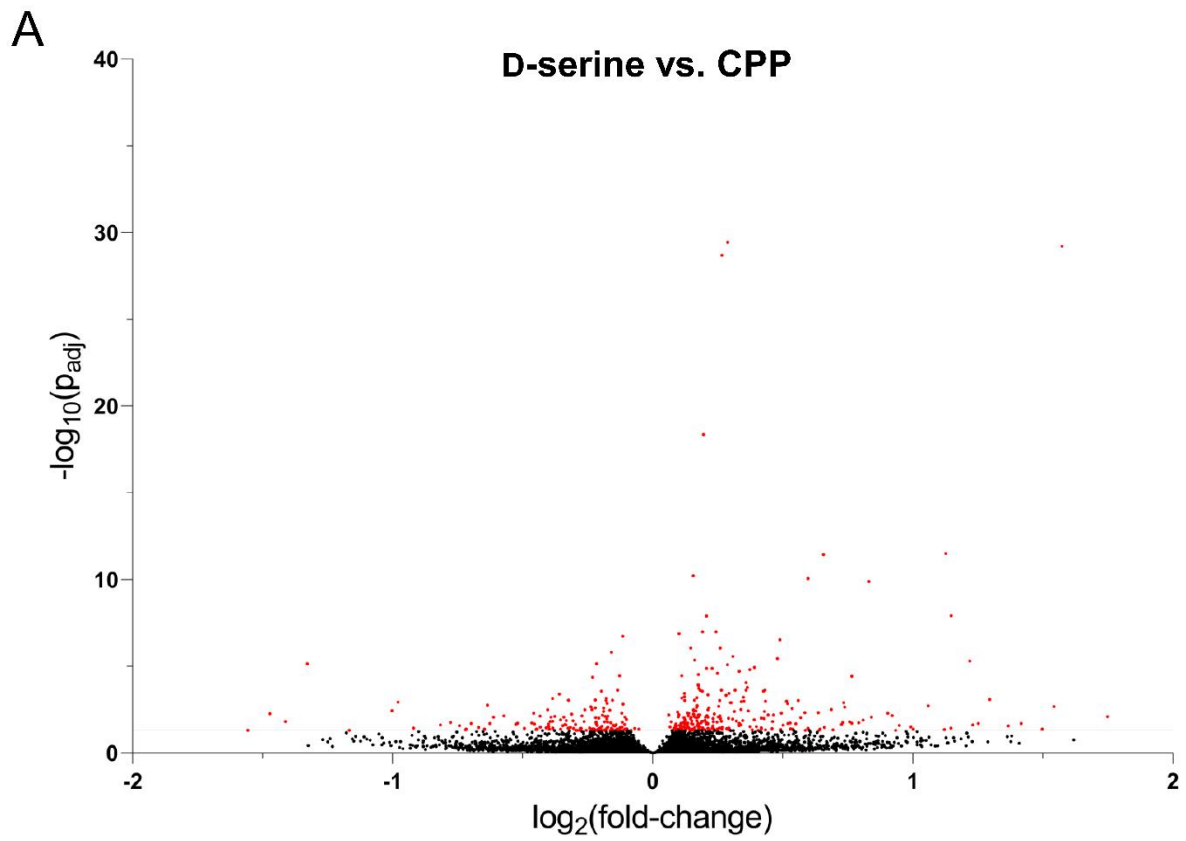
B



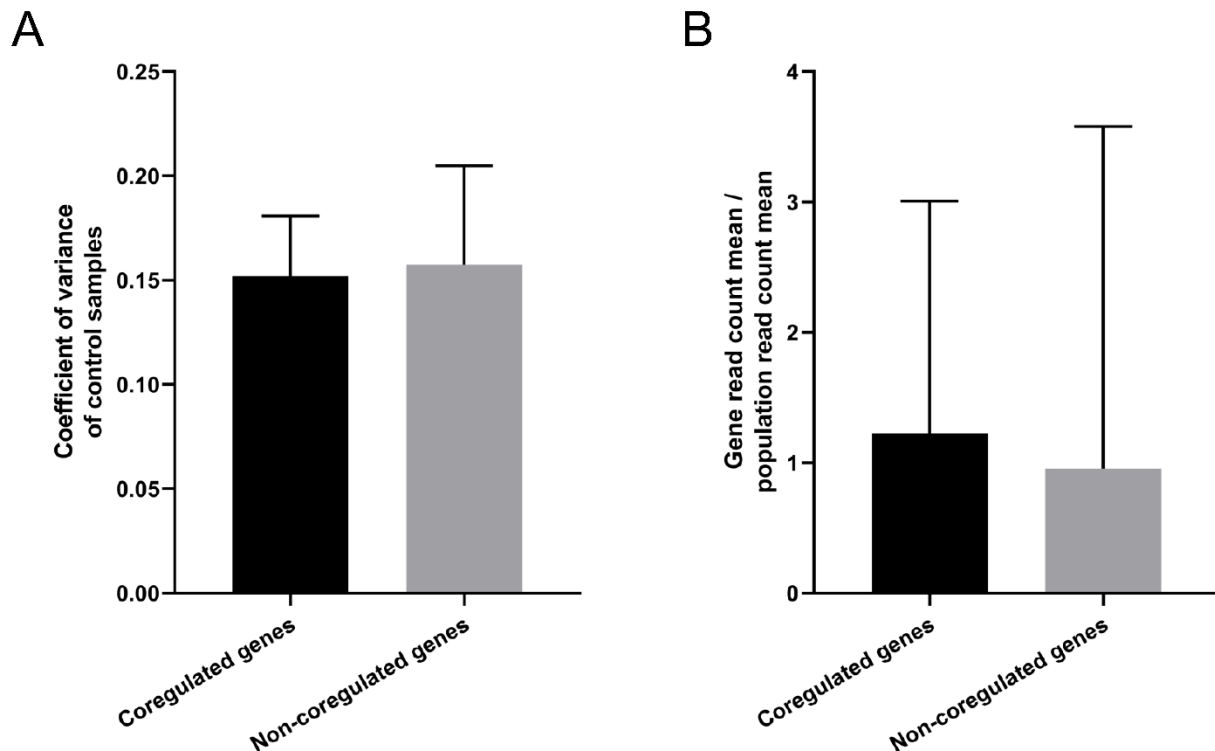
↑ **Figure 8. Removal of batch effects reduces the variance and dimensionality of RNA-seq datasets.** “Dser” indicates biological replicates from brain tissue extracted from animals chronically reared D-serine (24 h). “CPP” indicates biological replicates from animals chronically reared in the competitive NMDAR glutamate site antagonist CPP, and “Ctrl” indicates control replicates. Replicates 1-3 and 4-6 (three samples in total were removed prior to analysis due to unsuccessfully passing mRNA QC tests) were processed and sequenced at different times, and thus each constitute separate batches. To acquire putative batch effects, DGE analysis was performed on all batch 1 samples (Ctrl_1, Ctrl_2, Ctrl_3, Dser_1, Dser_2, Dser_3, CPP_2, and CPP_3) versus all batch 2 samples (Ctrl_5, Ctrl_6, Dser_4, Dser_5, Dser_6, CPP_5, CPP_6). It is implied that genes that displayed significant differential expression are dependent on batch. Read counts for these genes were then retroactively removed. **(A)** PCA analysis indicates that samples from each condition segregated into their own distinct, mostly non-overlapping clusters. Sample-to-sample distances **(B)** indicate that samples of the same condition tended to be more tightly correlated compared to samples from different conditions. These findings suggest that the removal of batch-affected genes reduced the amount of variance between batches and within conditions and permitted the extraction of more meaningful differences in transcript read counts based on experimental condition.

↓ **Figure 9. Differential gene expression under conditions of chronic D-serine or CPP rearing relative to control following the removal of batch-affected genes.** **(A)** Differential gene expression analysis of D-serine samples (n = 6) vs. Control samples (n = 5). **(B)** Differential gene expression analysis of CPP samples (n = 4) vs. Control samples. Drug rearing occurred for a duration of 24 h prior to brain mRNA extraction, followed by RNA-sequencing. 34,961 genes were analyzed (14,148 genes were removed due their batch-dependence); each dot corresponds to a single gene. Genes were plotted according to log₂fold-change and adjusted p-value. For example, genes with positive log₂fold-change values reflect transcripts that were more abundant in the treatment condition than in the control condition. Red indicates an adjusted p-value ≤ 0.05 (i.e., positioned above the faint grey line), meaning that gene was significantly differentially expressed; 698 genes were significantly differentially expressed in response to chronic D-serine rearing, whereas 558 were significantly differentially expressed in response to chronic CPP rearing. The number of differentially expressed genes when batch effects were removed roughly doubles that of the original dataset, but scaled structures of the volcano plots are, for the most part, maintained. Differential expression was performed using the DESeq2 program (Love et al., 2014) via the Galaxy Project (Jalali et al., 2020) using mean fit, Cook’s outlier filtering, and independent filtering.



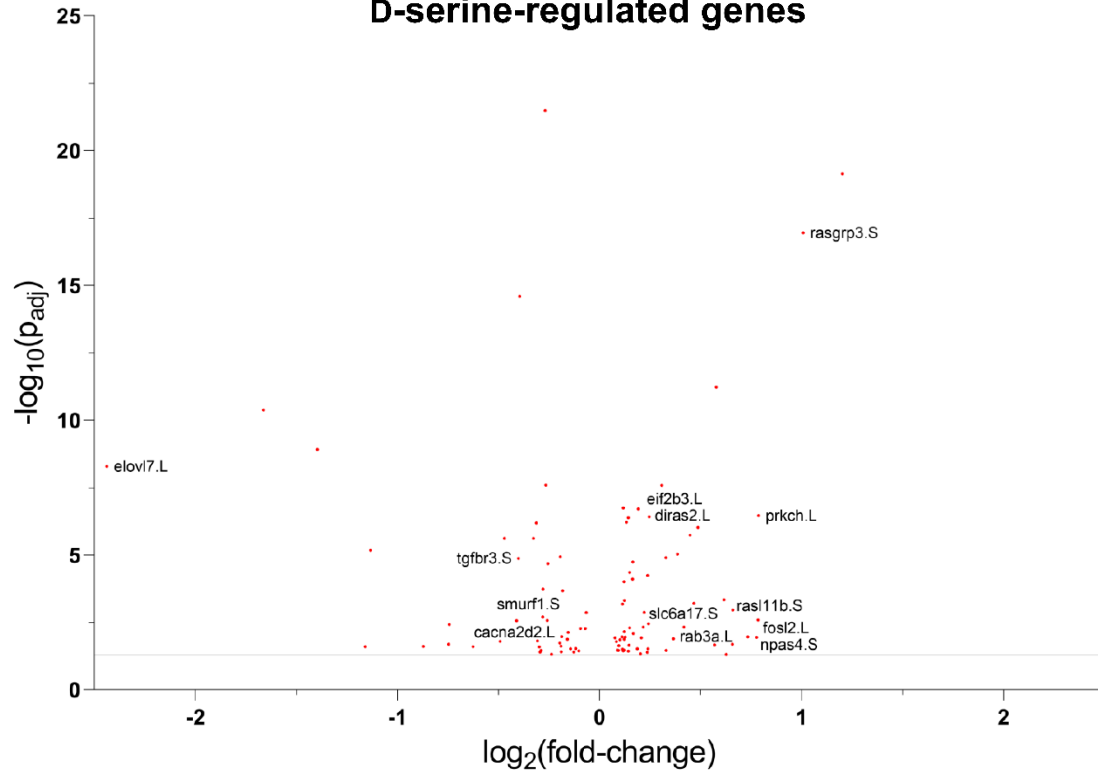
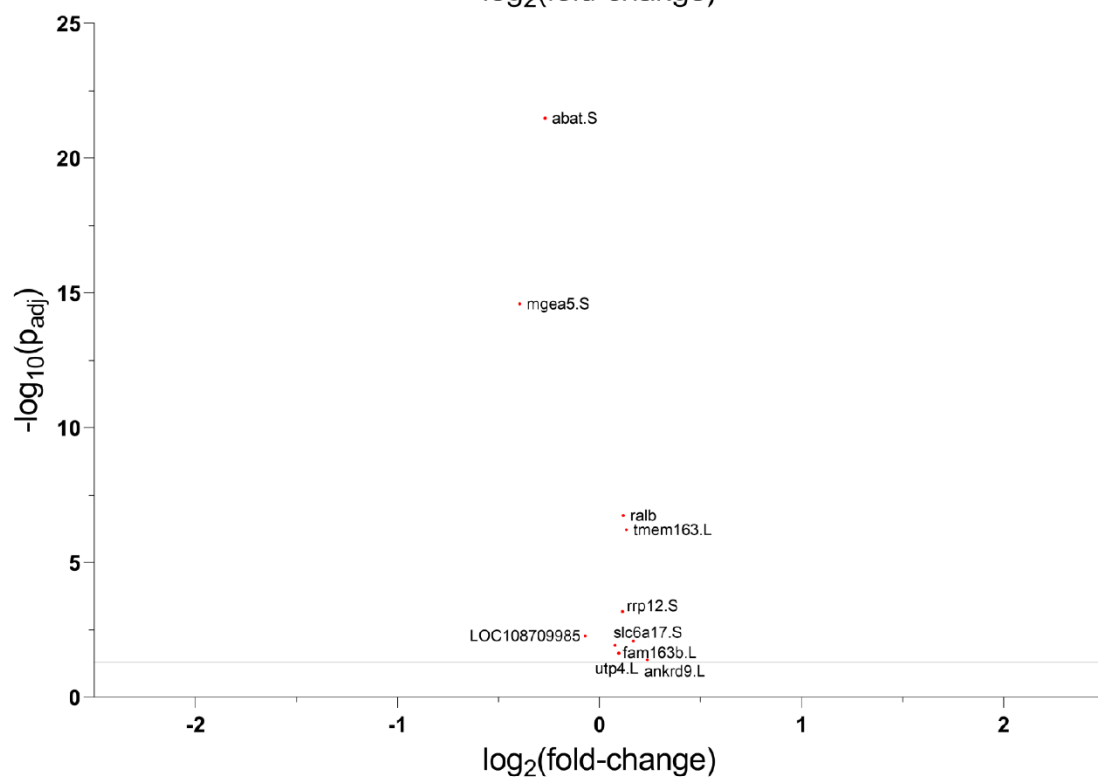


↑ **Figure 10. Relationships between treatment-induced gene expression in batch-effects-removed dataset.** (A) DGE analysis of D-serine vs. CPP rearing conditions. Each point corresponds to a gene. 412 genes in red were significantly more or less abundant in one treatment condition compared to the other and were thus differentially expressed. For example, genes with a positive \log_2 fold-change reflect a transcript that was more abundant in the D-serine condition than in the CPP condition. (B) Genes that were coregulated in response to D-serine and CPP treatment ($n = 182$ genes) displayed a striking positive linear relationship when plotted according to their corresponding \log_2 fold-changes ($R^2 = 0.90$). Genes residing in quadrants 1 or 3 were coregulated by D-serine and CPP, and genes positioned in quadrant 2 were anti-regulated by D-serine and CPP. These data reveal an unexpected degree of coregulation of gene products downstream of both putative NMDAR augmentation and blockade and suggest the convergence onto a subset of effectors, whether in signaling pathways or directly in the nucleus, that control the expression of one or multiple gene programs. Notably, however, coregulated genes did not constitute majorities of the genes that were regulated in response to either rearing condition on their own, but the percentages are nonetheless striking: 26.1% and 32.6% of D-serine regulated genes and CPP-regulated genes, respectively, were coregulated by both treatments.



↑ **Figure 11. Variance among control sample read counts does not explain the occurrence of coregulated genes in the batch-effects-removed RNA-seq dataset.** *Coregulated genes* refers to all genes that are co- or anti-regulated by chronic D-serine and CPP rearing. *Non-coregulated genes* refers to all other genes that are significantly differentially expressed in response to chronic D-serine or CPP rearing. (A) Average coefficients of variance (CV) for control sample read counts. (B) The ratio of gene read count means to the population read count mean (i.e., the mean of all read counts from control samples of all differentially expressed genes) in control samples. Neither comparison was significant, indicating that variance in control samples did not account for gene coregulation and that coregulation was a true effect of treatments. Statistical comparisons performed using unpaired T-tests. Mean±SEM, *p<0.05.

↓ **Figure 12. Differential expression of D-serine mediated genes that are putatively dependent on NMDAR activity.** Genes in the batch-effects-removed dataset that appear differentially expressed in D-serine vs. CPP (see Fig. 10A) were potentially anti-regulated by NMDAR coagonism and blockade, respectively, and thus may have been NMDAR-dependent. Any of these genes that were also significantly differentially expressed by D-serine vs. Control are displayed as such in (A). Some genes have been arbitrarily labeled. Of these 102 genes, 10 of them were also regulated by CPP (vs. Control), indicating that their expression by D-serine was likely NMDAR-dependent. These 10 putative NMDAR-dependent D-serine-regulated genes are displayed in (B) based on their metrics in D-serine vs. Control DGE analysis.

A**NMDAR-dependent
D-serine-regulated genes****B**

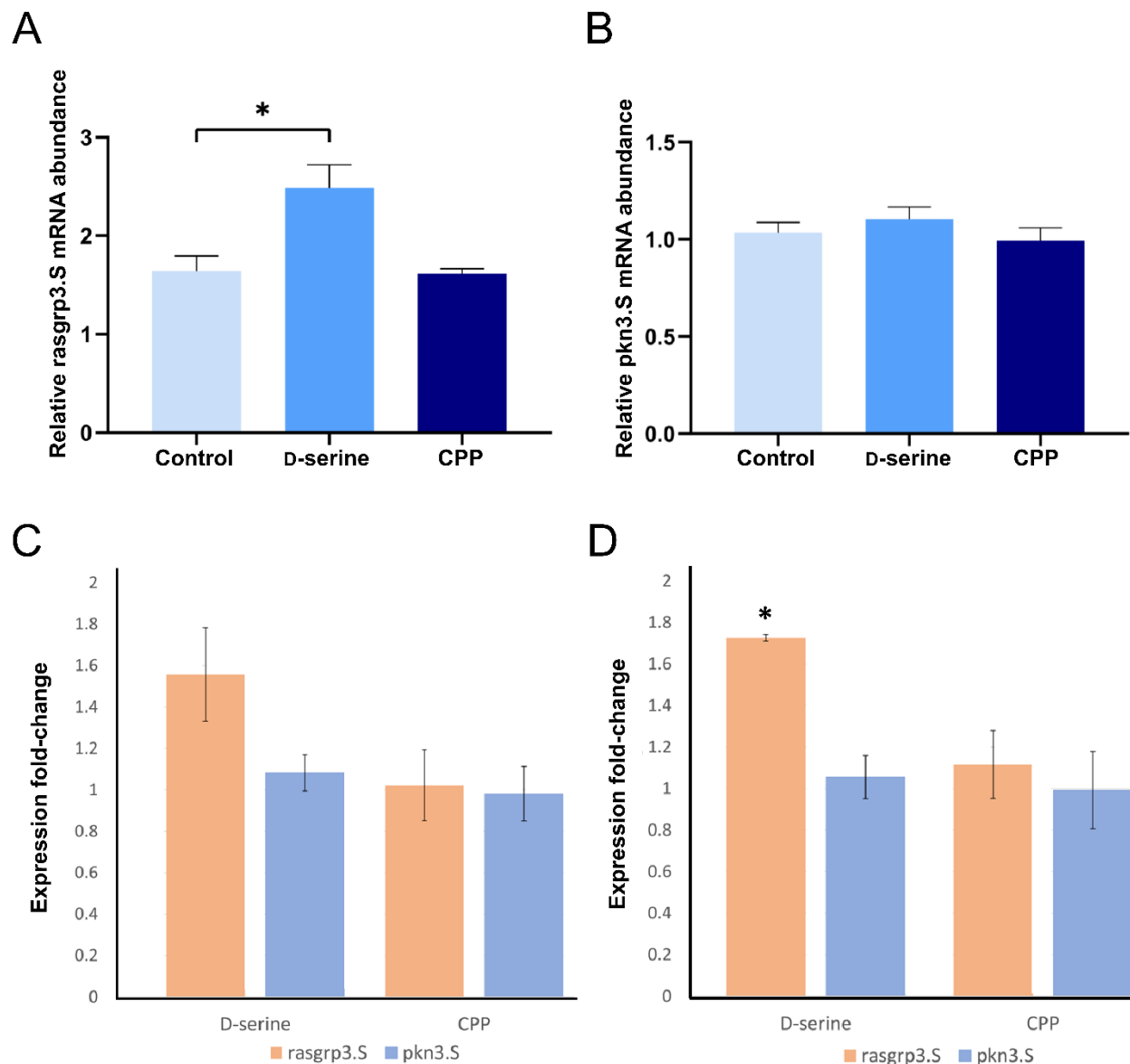


Figure 13. qRT-PCR validation of RNA-seq results for rasgrp3.S and pkn3.S gene transcripts. (A) and (B) display abundance of rasgrp3.S and pkn3.S gene transcripts, respectively, in Control-, D-serine-reared, and CPP-reared samples relative to reference gene transcript abundance. Rasgrp3.S was more abundant in D-serine-reared samples compared to Control and CPP-reared samples, which was consistent with RNA-seq datasets. No differences were measured in pkn3.S abundance among the three conditions, which did not reflect RNA-seq datasets. RNA-seq datasets indicated that pkn3.S was upregulated by both chronic D-serine and CPP relative to Control. (C) Fold-change in expression of rasgrp3.S and pkn3.S genes in all three D-serine and CPP reared samples relative to Control samples. No significant differences were measured. The first sample was suspected of contamination and was thus removed in (D). When the first sample was removed, rasgrp3.S displayed an increased fold-change in D-serine-reared samples relative to Control, which was consistent with RNA-seq datasets. Statistical comparisons were performed using unpaired T-tests. Mean±SEM, * $p \leq 0.05$.

Preface to Chapter 3: General Discussion

This chapter was written by Andrew Schultz and edited by Ed Ruthazer.

Chapter 3: General Discussion

Our lab seeks to understand how neural circuit formation and plasticity is driven by experience and activity patterns. Of central interest is the NMDAR, the principal detector of coincident neural activity. To investigate NMDAR gain-of-function, we have utilized the NMDAR co-agonist D-serine, which drives retinotectal synapse maturation and RGC axonal remodeling, yet it was previously unknown if postsynaptic tectal NMDARs are responsible for the release of a retrograde signal in response to stimulation by D-serine that stabilizes RGC axonal arbors. In support of our hypothesis, I have demonstrated that postsynaptic knockdown of NMDARs mitigates the stabilizing effect of D-serine, restoring RGC arbor morphological features to those of control, untreated cells. Yet, D-serine still promoted a decrease in the RGC branch tip number in postsynaptic tectal NMDAR knockdown compared to tectal NMDAR knockdown without D-serine treatment. Together, these demonstrations reveal that D-serine exerts presynaptic stabilization via two parallel mechanisms: one that is dependent on postsynaptic NMDARs, and another that has not been identified, but may be entirely NMDAR-independent. The aim to strengthen this model thus requires an explanation to this additional layer of complexity to provide a foundation for further experiments.

Indeed, a requisite for the maintenance of activity-dependent circuit refinement over the course of brain development is the regulated expression of genes. Newly expressed transcripts and their protein products are the brick and mortar that permit functional and structural plastic alterations to persist throughout an organism's lifespan. Our lab has demonstrated that, based on morphological

and electrophysiological studies, D-serine effectively mobilizes the retinotectal circuit in *Xenopus* to expedited maturation and NMDAR-dependent structural refinement (Van Horn et al., 2017). To better understand the molecular framework that underlies these outcomes, it is essential that we characterize the transcriptional landscape of D-serine rearing. I have done just that using RNA-seq datasets and have additionally teased apart the gene expression that occurs downstream of NMDAR blockade by CPP. Together, these datasets provide novel insights into the molecular differences, similarities, and crosstalk between D-serine and NMDARs. Notably, chronic D-serine and CPP rearing induce the expression of gene programs that are mostly unique and non-overlapping, but where they do overlap, genes are predominantly co-regulated and expressed at comparable magnitudes—an observation that has been both perplexing and exciting to strive to explain. These results reveal a potential novel convergence of NMDAR augmentation and blockade, and, by bringing to light a plethora of genes implicated in plasticity, bolster our pursuit to use D-serine as an effective tool to interrogate the many hidden facets of neural circuit development.

D-serine may be functioning in parallel through an additional signaling pathway to mediate RGC axonal arbor stabilization. The goal of **Aim I** was to determine if D-serine action on postsynaptic NMDARs was responsible for the presynaptic stabilization of RGC axonal arbors observed by Van Horn et al. (2017) in response to chronic D-serine rearing. Our new results indicate that they were to a large degree because the introduction of postsynaptic GluN1-MO restored branch tip number to Ctrl-MO alone values. However, the demonstration that D-serine still promoted a significant reduction in branch tip number in the presence of tectal GluN1-MO suggests that other NMDAR-dependent mechanisms are at play. First, because GluN1 knockdown via MO was not complete (about a 50% reduction in GluN1 fluorescence; Kesner et al., 2020), the remaining intact NMDARs may have been sufficient to drive presynaptic axonal arbor

stabilization when their ionotropic conductance has been augmented by supraphysiological levels of D-serine. However, this explanation is probably incomplete given the magnitude at which D-serine promoted the reduction of RGC axonal arbor branch tip number in tectal GluN1-MO animals. The second NMDAR-dependent mechanism that could be at play is that D-serine acts on NMDARs in RGC dendritic arbors in the retina. Stabilization of RGC dendritic arbors in response to chronic D-serine rearing may induce a cell-wide response that facilitates the induction of stabilization mechanisms in RGC axonal arbors. Interestingly, Du et al. (2009) demonstrated *in vivo* that the induction of LTP and LTD at *Xenopus* retinotectal synapses spreads retrogradely to RGC dendrites and facilitates the potentiation and depression, respectively, of RGC-bipolar cell synapses. This indicates that the induction of plasticity is capable of ramifying over long distances and exposes the prospect of anterograde spread of plasticity. This hypothesis would be relatively simple to investigate in our model. We could perform retinal electroporation of EFGP followed by time-lapse imaging of sparsely labeled RGCs that have received an intraocular injection (or periodic injections to maintain elevated concentrations) of D-serine or saline into the vitreous humor of the same eye. If augmentation by D-serine of dendritic NMDARs in RGCs facilitates the anterograde spread of plasticity, the observed outcome should be a reduction in the number of branch tips and total arbor length of labeled, tectal-innervating RGCs in animals that have received intraocular D-serine compared to those that received saline.

D-serine may also act on presynaptic NMDARs. While this is likely true, the documented roles of presynaptic NMDARs in axonal development are inconsistent with a role in mediating structural stabilization. Namely, Kesner et al. (2020), using the same hemimorphant GluN1-MO half-animal model except in the opposite tectal lobe (i.e., wild-type optic tectum and GluN1-MO RGCs), demonstrated that knockdown of presynaptic GluN1 results in a marked reduction in overall axonal

arbor complexity, including total arbor length and the number of branch tips. This suggests that presynaptic NMDAR activation is primarily responsible for driving exploratory branching and arbor growth, not arbor stabilization.

The remaining and final possibility is that D-serine promotes presynaptic RGC stabilization through an additional NMDAR-independent pathway. For example, it remains to be studied how elevated levels of D-serine impact the dynamics of the serine shuttle. Because neurons uptake D-serine (Wolosker & Balu, 2020), D-serine rearing may lead to elevated levels of intracellular D-serine. If this were to occur in RGCs, it is plausible that D-serine exerts direct impacts on intracellular signaling or metabolism in axonal arbors that leads to branch stabilization. However, no evidence exists that suggests this could be the case. Indeed, the serine shuttle, including its cellular and molecular components, are central to gliotransmission of D-serine and are likely susceptible to forms of regulation.

D-serine and CPP rearing generate unique, non-opposing gene expression profiles. An important and unexpected finding that came out of Aim II was that D-serine and CPP individually had distinct profound effects on gene expression and did not have appreciably opposing effects on genes that were regulated by both. Our expectation regarding the latter observation was instead that genes would exhibit more opposition in their regulation by chronic D-serine and CPP treatment; D-serine has been shown to augment NMDAR conductance, while CPP blocks receptor activation (Van Horn et al., 2017; Lehmann et al., 1987). However, it should be noted that D-serine and CPP likely do not have strictly opposing effects on NMDAR activation and signaling. Namely, while co-agonism, in this case by D-serine, has been demonstrated to enhance ionotropic signaling (Johnson & Ascher, 1987; Van Horn et al., 2017), CPP prevents both ionotropic and metabotropic signaling by competitively blocking the glutamate binding site (Lehmann et al., 1987). Therefore,

because LTD is thought to be dependent on NMDAR metabotropic signaling (Nabavi et al., 2013), CPP should effectively impede both LTP and LTD. In contrast, there is no indication that D-serine enhances LTD. These fundamental differences in altered receptor signaling may explain the largely non-overlapping transcriptomic signatures underlying chronic D-serine and CPP rearing and the lack of appreciable gene anti-regulation.

Also worth considering is that D-serine and CPP rearing may be promoting the development of synaptic NMDARs with drastically different compositional make-ups. During development, GluN2A is trafficked to the postsynaptic density and incorporated into synaptic NMDARs in an activity-dependent manner (Barria & Malinow, 2002). Moreover, the relative concentrations of D-serine and glycine at the synaptic cleft governs the rate at which GluN2B is trafficked and stabilized at the postsynaptic density (Ferreira et al., 2017). Specifically, at synapses where D-serine concentrations exceed that of glycine, GluN2B is actively retained at extrasynaptic sites. Because CPP prevents NMDAR signaling and thus NMDAR-mediated synaptic activation and maturation, it is plausible that GluN2A is hindered from being incorporated into synaptic NMDARs in the brains of CPP reared animals due to lack of activity. Therefore, synaptic NMDARs in D-serine and CPP reared animals may be predominantly composed of GluN1/N2A and GluN1/N2B, respectively. Such differences in molecular make-up could propel synapses in either experimental condition along drastically different time-courses of developmental plasticity and may potentially aid in explaining the marked divergence in, and lack of opposing gene expression patterns. To refine our model, it will be important to resolve how chronic D-serine and CPP treatment impact the molecular make-up of synaptic and extrasynaptic NMDARs at retinotectal synapses.

Coregulation constitutes a novel mechanism by which NMDAR co-agonism and blockade may converge to mediate gene expression. Although D-serine and CPP rearing induced many unique, non-overlapping patterns of gene expression, nearly one-third of D-serine- or CPP-regulated genes were also coregulated in the same direction—and to comparable fold-change magnitudes—by both rearing conditions. This was perhaps the most striking and perplexing finding that surfaced from the RNA-seq experiment. We anticipated that many genes would be anti-regulated based on the opposing effects of D-serine and CPP on NMDARs, but instead, D-serine and CPP appear to converge onto a subset of genes and promote their differential expression according to what are presumably analogous or overlapping mechanisms. A plausible explanation is that supraphysiological D-serine may have facilitated the internalization of NMDARs. Primary evidence that co-agonists can have this effect on the surface expression of NMDARs came from Nong et al. (2003), who demonstrated that glycine and D-serine prime NMDARs for internalization in a use-dependent manner—that is, only when the receptor is also bound by NMDA at the glutamate site. Blocking the glutamate binding site with APV prevented internalization, suggesting that receptor activation is necessary for receptor internalization due to co-agonist priming. It is possible that the functional outcomes of D-serine rearing are dynamic over time, differing over the short-, intermediate-, and long-terms. It is possible that, at some point within the first 24 h of rearing, supraphysiological levels of D-serine in the brain transiently manifest effects on glutamatergic transmission that contrast with what was demonstrated by Van Horn et al. (2017): namely, decreased NMDAR-mediated ionotropic or metabotropic signaling, much like what has been demonstrated in response to NMDAR blockade by CPP treatment. Any overlap such as this may result in a convergence of signaling pathways downstream of NMDARs that ultimately yield the coregulation of a subset of genes whose transcripts become poised for a transient homeostatic

response to synaptic non-activation. It is important to note that Nong et al. (2003) performed their studies on the effects of co-agonist-mediated NMDAR internalization on cultured hippocampal neurons. It has yet to be demonstrated that the same process occurs in the *Xenopus* brain. However, given the amenability of *Xenopus* to *in vivo* imaging and fluorescent labeling assays, this mystery may be feasibly elucidated by co-labeling GluN1-XFP in tectal neurons sparsely labeled with membrane-bound EGFP in animals reared in D-serine. A reduction in XFP-EGFP co-localization along a time-course of D-serine incubation would suggest a reduction in the surface expression of NMDARs. Moreover, it will be important to utilize more advanced analytical tools to comprehensively characterize gene expression in our RNA-seq dataset according to gene ontology and pathway analysis to identify possible upstream physiological bases, causes, and potential phenotypic outcomes of coregulation.

A plethora of genes revealed by transcriptomic analyses have implicated roles in plasticity and activity-dependent gene expression. The overarching purpose of this study was to provide unbiased characterizations of the transcriptomic landscapes in response to NMDAR augmentation and blockade. Indeed, many of the genes revealed in RNA-seq datasets have established roles in neural function, development, and plasticity. **Supplementary Figure 2** provides comprehensive lists of all D-serine-, CPP-, and co-regulated genes. Although there are many of interest, two D-serine-regulated genes are worth noting: the IEG NPAS4 (Neuronal PAS Domain Protein 4) and PRKCH (Protein Kinase C eta). Npas4 was upregulated by chronic D-serine treatment and has well-established roles in synaptic-nuclear signaling that contributes to the regulated development of glutamatergic and GABAergic synapses and the maintenance of neuronal excitatory/inhibitory balance (Spiegel et al., 2014). Indeed, regulation of intrinsic excitability is an important aspect of long-term maintenance of plasticity and the integration of

neurons into robust circuits. Prkch, which was upregulated by chronic D-serine treatment, is an isoform of protein kinase C (PKC). PKC has been heavily implicated in driving postsynaptic mechanisms of LTP at hippocampal synapses (Wang & Feng, 1992). Additionally, three intriguing genes regulated by chronic CPP treatment worth highlighting are NFAT3 (Nuclear Factor of Activated T Cells 3), GRIK5-like.1 (Glutamate Receptor KA2), and SEMA3A. Nfat, whose c3 isoform was up-regulated by chronic CPP rearing, is a transcription factor that contributes to synaptic and dendritic development in the *Xenopus* retinotectal circuit (Schwartz et al., 2009). Grik5-like.1 is a kainate receptor subunit. Kainate receptors are ionotropic glutamate receptors that are emerging as important mediators of neuronal excitability and synaptic plasticity (Lerma, 2005). Finally, Sema3a is an important molecular signal that has been implicated in regulating both axonal guidance and dendritic elaboration (Nakamura et al., 2000; Schlomann et al., 2009). Of the ten putative NMDAR-dependent D-serine-regulated genes, three are worth noting: TMEM163, SLC6A17, and LOC108709985. TMEM163, also known as synaptic vesicle protein 31 (SV31), has various roles in the regulation of glutamatergic and GABAergic synaptic vesicle lifecycles (Burré et al., 2007). SLC6A17, or synaptic vesicle protein NTT4/XT1, is an Na⁺-dependent transporter implicated in the presynaptic reuptake of neurotransmitters at glutamatergic and GABAergic synapses (Zaia & Reimer, 2009). Finally, LOC108709985 is “glutamate receptor 4” according to NCBI database, but little else exists regarding its functional annotation. Together, these genes suggest an important role of D-serine in modulating various pre- and postsynaptic mechanisms underlying synaptic transmission. Indeed, these RNA-seq datasets will undoubtedly serve an extraordinary basis from which new hypotheses can be explored, referenced, and tested.

Of particular interest for the lab’s ongoing investigations of developmental plasticity in the retinotectal system are the Ras- and Rab (Ras-related protein in brain)-family GTPases and their

regulatory proteins (e.g., guanine nucleotide exchange factors [GEFs] and GTPase activating proteins [GAPs]), and downstream MAPK effectors (e.g., ERK, JNK, and p39MAPK; Gu & Stornetta, 2007; Stornetta & Zhu, 2011; Volk et al., 2015; Zhang et al., 2018). Interestingly, Kim et al. (2005) demonstrated that bidirectional regulation of Ras-ERK activity contributes to AMPAR membrane insertion or removal, highlighting the importance of this signaling pathway in synaptic potentiation and maturation. Indeed, numerous genes related to Ras signaling are differentially expressed in response to D-serine, including Rasgrp3.S, Diras2.L, Rasl11b.S, Rab3a.L, Rab27a.S, Rab35.L, Rab2a.L, Rab30.S, Rem2.L, and Mapkapk5.L. The same is true with CPP: Diras3.L, Rabac1.S, Rab3a.S, and Mapk14.S. When the most stringent filters aimed at elucidating potential NMDAR-dependencies of D-serine-regulated genes are implemented (**fig. 12B**), none of these genes show up, but this does not necessarily negate their importance in D-serine-mediated signaling and plasticity. It is very likely that the observed effects of D-serine on retinotectal synapse maturation and structural refinement are being mediated, at least in part, by NMDAR-independent Ras-MAPK signaling. *Rem2* specifically, whose L homolog is downregulated by chronic D-serine rearing (**Supplementary fig. 2**), has been extensively implicated in structural remodeling in many organisms, including *Xenopus laevis* (Ghiretti & Paradis, 2014). Ghiretti et al. (2014) demonstrated that *Rem2*, whose transcription is induced by Ca²⁺ influx through L-VSCCs, actively inhibits dendritic arbor elaboration in the *Xenopus* optic tectum *in vivo*. This is inconsistent with our observations, which include that D-serine rearing promotes structural stabilization of arbors and *Rem2* down-regulation, but it could be the case that *Rem2* has differing roles in regulating axonal versus dendritic arbor structure. Alternatively, because D-serine augments NMDAR activation (Van Horn et al., 2017) with no established effect on L-VSCCs, perhaps the functional role of *Rem2* is dependent on which source of Ca²⁺ facilitates

its expression. This would be reminiscent of the many demonstrations that the source of Ca^{2+} is the primary determinant of which genes and gene programs are engaged (Lerea & McNamara, 1993; Bading et al., 1993; Deisseroth et al., 1996; Bito et al., 1996; Dolmetch et al., 2001; Hardingham et al., 2001; Hardingham et al., 2002; Karpova et al., 2013). It could be the case that the function of Rem2 in structural plasticity is interactive, dependent on what other genes are up- or down-regulated as determined by the source of synaptic or nuclear Ca^{2+} . In any case, this study corroborates our finding that the expression of Rem2, several other Ras-family proteins, are inducible by synaptic activation, but begs the questions: how does chronic D-serine rearing impact synaptic Ca^{2+} and L-VSCC signaling in the *Xenopus* retinotectal system? The answers to these questions will, in my opinion, be central in the pursuit to develop a more sophisticated model wherein D-serine is applied to interrogate the synaptic activity-dependencies of structural plasticity and gene expression. Nevertheless, given the overwhelming presence of Ras and Ras-like genes in our dataset, it stands to reason that Ras signaling pathways may be fundamentally important mechanisms by which D-serine contributes to activity-dependent gene expression and structural refinement in the *Xenopus* brain.

Conclusion

D-serine has proven to be an incredibly insightful tool for interrogating activity- and NMDAR-dependent neuronal processes such as circuit refinement, and now gene expression. Indeed, lingering questions remain—as they often do—such as whether additional NMDAR-independent pathways D-serine could be functioning to mediate axonal remodeling. Here, I have used D-serine rearing to show that its application is sufficient to drive distinct genomic programs, and that many

of the genes contained within these programs—only a few of which I could reasonably discuss here—are intimately tied to brain development, plasticity, and downstream NMDAR signaling.

References Cited

- Ackman JB, Burbridge TJ, Crair MC. Retinal waves coordinate patterned activity throughout the developing visual system. *Nature*. 2012 Oct 11;490(7419):219-25. doi: 10.1038/nature11529
- Ahn S, Riccio A, Ginty DD. Spatial considerations for stimulus-dependent transcription in neurons. *Annu Rev Physiol*. 2000;62:803-23. doi: 10.1146/annurev.physiol.62.1.803
- Aizenman CD, Cline HT. Enhanced visual activity in vivo forms nascent synapses in the developing retinotectal projection. *J Neurophysiol*. 2007 Apr;97(4):2949-57. doi: 10.1152/jn.00452.2006
- Akerman CJ, Cline HT. Depolarizing GABAergic conductances regulate the balance of excitation to inhibition in the developing retinotectal circuit in vivo. *J Neurosci*. 2006 May 10;26(19):5117-30. doi: 10.1523/JNEUROSCI.0319-06.2006
- Akerman CJ, Cline HT. Refining the roles of GABAergic signaling during neural circuit formation. *Trends Neurosci*. 2007 Aug;30(8):382-9. doi: 10.1016/j.tins.2007.06.002
- Albright TD, Jessell TM, Kandel ER, Posner MI. Neural science: a century of progress and the mysteries that remain. *Cell*. 2000 Feb 18;100 Suppl:S1-55
- Andreescu CE, Prestori F, Brandalise F, D'Errico A, De Jeu MT, Rossi P, Botta L, Kohr G, Perin P, D'Angelo E, De Zeeuw CI. NR2A subunit of the N-methyl D-aspartate receptors are required for potentiation at the mossy fiber to granule cell synapse and vestibulo-cerebellar motor learning. *Neuroscience*. 2011 Mar 10;176:274-83. doi: 10.1016/j.neuroscience.2010.12.024
- Andersen P, Sundberg SH, Sveen O, Wigström H. Specific long-lasting potentiation of synaptic transmission in hippocampal slices. *Nature*. 1977 Apr 21;266(5604):736-7. doi: 10.1038/266736a0
- Bading H, Ginty DD, Greenberg ME. Regulation of gene expression in hippocampal neurons by distinct calcium signaling pathways. *Science*. 1993 Apr 9;260(5105):181-6. doi: 10.1126/science.8097060
- Bading H, Greenberg ME. Stimulation of protein tyrosine phosphorylation by NMDA receptor activation. *Science*. 1991 Aug 23;253(5022):912-4. doi: 10.1126/science.1715095
- Bading H, Segal MM, Sucher NJ, Dudek H, Lipton SA, Greenberg ME. N-methyl-D-aspartate receptors are critical for mediating the effects of glutamate on intracellular calcium concentration and immediate early gene expression in cultured hippocampal neurons. *Neuroscience*. 1995 Feb;64(3):653-64. doi: 10.1016/0306-4522(94)00462-e

- Barria A, Malinow R. Subunit-specific NMDA receptor trafficking to synapses. *Neuron*. 2002 Jul 18;35(2):345-53. doi: 10.1016/s0896-6273(02)00776-6
- Barria A, Malinow R. NMDA receptor subunit composition controls synaptic plasticity by regulating binding to CaMKII. *Neuron*. 2005 Oct 20;48(2):289-301. doi: 10.1016/j.neuron.2005.08.034
- Barrionuevo G, Schottler F, Lynch G. The effects of repetitive low frequency stimulation on control and "potentiated" synaptic responses in the hippocampus. *Life Sci*. 1980 Dec 15;27(24):2385-91. doi: 10.1016/0024-3205(80)90509-3
- Barth AL, Malenka RC. NMDAR EPSC kinetics do not regulate the critical period for LTP at thalamocortical synapses. *Nat Neurosci*. 2001 Mar;4(3):235-6. doi: 10.1038/85070
- Bayer KU, De Koninck P, Leonard AS, Hell JW, Schulman H. Interaction with the NMDA receptor locks CaMKII in an active conformation. *Nature*. 2001 Jun 14;411(6839):801-5. doi: 10.1038/35081080
- Ben-Ari Y, Khazipov R, Leinekugel X, Caillard O, Gaiarsa JL. GABAA, NMDA and AMPA receptors: a developmentally regulated 'ménage à trois'. *Trends Neurosci*. 1997 Nov;20(11):523-9. doi: 10.1016/s0166-2236(97)01147-8
- Berberich S, Jensen V, Hvalby Ø, Seeburg PH, Köhr G. The role of NMDAR subtypes and charge transfer during hippocampal LTP induction. *Neuropharmacology*. 2007 Jan;52(1):77-86. doi: 10.1016/j.neuropharm.2006.07.016
- Bito H, Deisseroth K, Tsien RW. CREB phosphorylation and dephosphorylation: a Ca(2+)- and stimulus duration-dependent switch for hippocampal gene expression. *Cell*. 1996 Dec 27;87(7):1203-14. doi: 10.1016/s0092-8674(00)81816-4
- Bliss TV, Collingridge GL. A synaptic model of memory: long-term potentiation in the hippocampus. *Nature*. 1993 Jan 7;361(6407):31-9. doi: 10.1038/361031a0
- Bliss TV, Collingridge GL, Morris RG. Synaptic plasticity in health and disease: introduction and overview. *Philos Trans R Soc Lond B Biol Sci*. 2013 Dec 2;369(1633):20130129. doi: 10.1098/rstb.2013.0129
- Bliss TV, Lomo T. Long-lasting potentiation of synaptic transmission in the dentate area of the anaesthetized rabbit following stimulation of the perforant path. *J Physiol*. 1973 Jul;232(2):331-56. doi: 10.1113/jphysiol.1973.sp010273
- Bordji K, Becerril-Ortega J, Nicole O, Buisson A. Activation of extrasynaptic, but not synaptic, NMDA receptors modifies amyloid precursor protein expression pattern and increases amyloid- β production. *J Neurosci*. 2010 Nov 24;30(47):15927-42. doi: 10.1523/JNEUROSCI.3021-10.2010

- Bonhoeffer F, Huf J. Recognition of cell types by axonal growth cones in vitro. *Nature*. 1980 Nov 13;288(5787):162-4. doi: 10.1038/288162a0
- Bonni A, Brunet A, West AE, Datta SR, Takasu MA, Greenberg ME. Cell survival promoted by the Ras-MAPK signaling pathway by transcription-dependent and -independent mechanisms. *Science*. 1999 Nov 12;286(5443):1358-62. doi: 10.1126/science.286.5443.1358
- Brennan C, Monschau B, Lindberg R, Guthrie B, Drescher U, Bonhoeffer F, Holder N. Two Eph receptor tyrosine kinase ligands control axon growth and may be involved in the creation of the retinotectal map in the zebrafish. *Development*. 1997 Feb;124(3):655-64
- Bristow DR, Bowery NG, Woodruff GN. Light microscopic autoradiographic localisation of [3H]glycine and [3H]strychnine binding sites in rat brain. *Eur J Pharmacol*. 1986 Jul 31;126(3):303-7. doi: 10.1016/0014-2999(86)90062-2
- Brown A, Yates PA, Burrola P, Ortuño D, Vaidya A, Jessell TM, Pfaff SL, O'Leary DD, Lemke G. Topographic mapping from the retina to the midbrain is controlled by relative but not absolute levels of EphA receptor signaling. *Cell*. 2000 Jul 7;102(1):77-88. doi: 10.1016/s0092-8674(00)00012-x
- Burré J, Zimmermann H, Volkhardt W. Identification and characterization of SV31, a novel synaptic vesicle membrane protein and potential transporter. *J Neurochem*. 2007 Oct;103(1):276-87. doi: 10.1111/j.1471-4159.2007.04758.x
- Burzomato V, Frugier G, Pérez-Otaño I, Kittler JT, Attwell D. The receptor subunits generating NMDA receptor mediated currents in oligodendrocytes. *J Physiol*. 2010 Sep 15;588(Pt 18):3403-14. doi: 10.1113/jphysiol.2010.195503
- Cabelli RJ, Hohn A, Shatz CJ. Inhibition of ocular dominance column formation by infusion of NT-4/5 or BDNF. *Science*. 1995 Mar 17;267(5204):1662-6. doi: 10.1126/science.7886458
- Cang, J., and Feldheim, D. (2013). Developmental mechanisms of topographic map formation. *Annual Reviews Neuroscience*, 51-77
- Cantalops I, Haas K, Cline HT. Postsynaptic CPG15 promotes synaptic maturation and presynaptic axon arbor elaboration in vivo. *Nat Neurosci*. 2000 Oct;3(10):1004-11. doi: 10.1038/79823
- Carroll RC, Beattie EC, von Zastrow M, Malenka RC. Role of AMPA receptor endocytosis in synaptic plasticity. *Nat Rev Neurosci*. 2001 May;2(5):315-24. doi: 10.1038/35072500
- Castrén E, Pitkänen M, Sirviö J, Parsadanian A, Lindholm D, Thoenen H, Riekkinen PJ. The induction of LTP increases BDNF and NGF mRNA but decreases NT-3 mRNA in the

- dentate gyrus. *Neuroreport*. 1993 Jul;4(7):895-8. doi: 10.1097/00001756-199307000-00014
- Chawla S, Hardingham GE, Quinn DR, Bading H. CBP: a signal-regulated transcriptional coactivator controlled by nuclear calcium and CaM kinase IV. *Science*. 1998 Sep 4;281(5382):1505-9. doi: 10.1126/science.281.5382.1505
- Cline HT, Debski EA, Constantine-Paton M. N-methyl-D-aspartate receptor antagonist desegregates eye-specific stripes. *Proc Natl Acad Sci U S A*. 1987 Jun;84(12):4342-5. doi: 10.1073/pnas.84.12.4342
- Cline HT, Constantine-Paton M. NMDA receptor antagonists disrupt the retinotectal topographic map. *Neuron*. 1989 Oct;3(4):413-26. doi: 10.1016/0896-6273(89)90201-8
- Cline HT, Wu GY, Malinow R. In vivo development of neuronal structure and function. *Cold Spring Harb Symp Quant Biol*. 1996;61:95-104
- Coan EJ, Collingridge GL. Magnesium ions block an N-methyl-D-aspartate receptor-mediated component of synaptic transmission in rat hippocampus. *Neurosci Lett*. 1985 Jan 7;53(1):21-6. doi: 10.1016/0304-3940(85)90091-6
- Cohen-Cory S. BDNF modulates, but does not mediate, activity-dependent branching and remodeling of optic axon arbors in vivo. *J Neurosci*. 1999 Nov 15;19(22):9996-10003. doi: 10.1523/JNEUROSCI.19-22-09996.1999
- Cohen-Cory S, Fraser SE. Effects of brain-derived neurotrophic factor on optic axon branching and remodelling in vivo. *Nature*. 1995 Nov 9;378(6553):192-6. doi: 10.1038/378192a0.
- Cohan CS, Kater SB. Suppression of neurite elongation and growth cone motility by electrical activity. *Science*. 1986 Jun 27;232(4758):1638-40. doi: 10.1126/science.3715470
- Cole AJ, Saffen DW, Baraban JM, Worley PF. Rapid increase of an immediate early gene messenger RNA in hippocampal neurons by synaptic NMDA receptor activation. *Nature*. 1989 Aug 10;340(6233):474-6. doi: 10.1038/340474a0
- Collingridge GL, Kehl SJ, Loo R, McLennan H. Effects of kainic and other amino acids on synaptic excitation in rat hippocampal slices: 1. Extracellular analysis. *Exp Brain Res*. 1983a;52(2):170-8. doi: 10.1007/BF00236625
- Collingridge GL, Kehl SJ, McLennan H. Excitatory amino acids in synaptic transmission in the Schaffer collateral-commissural pathway of the rat hippocampus. *J Physiol*. 1983b Jan;334:33-46. doi: 10.1113/jphysiol.1983.sp014478
- Constantine-Paton M, Law MI. Eye-specific termination bands in tecta of three-eyed frogs. *Science*. 1978 Nov 10;202(4368):639-41. doi: 10.1126/science.309179

- Coupé P, Munz M, Manjón JV, Ruthazer ES, Collins DL. A CANDLE for a deeper in vivo insight. *Med Image Anal.* 2012 May;16(4):849-64. doi: 10.1016/j.media.2012.01.002
- Cramer KS, Gabriele ML. Axon guidance in the auditory system: multiple functions of Eph receptors. *Neuroscience.* 2014 Sep 26;277:152-62. doi: 10.1016/j.neuroscience.2014.06.068
- Dalton GL, Wu DC, Wang YT, Floresco SB, Phillips AG. NMDA GluN2A and GluN2B receptors play separate roles in the induction of LTP and LTD in the amygdala and in the acquisition and extinction of conditioned fear. *Neuropharmacology.* 2012 Feb;62(2):797-806. doi: 10.1016/j.neuropharm.2011.09.001
- Davies J, Francis AA, Jones AW, Watkins JC. 2-Amino-5-phosphonovalerate (2APV), a potent and selective antagonist of amino acid-induced and synaptic excitation. *Neurosci Lett.* 1981 Jan 1;21(1):77-81. doi: 10.1016/0304-3940(81)90061-6
- de Koning TJ, Snell K, Duran M, Berger R, Poll-The BT, Surtees R. L-serine in disease and development. *Biochem J.* 2003 May 1;371(Pt 3):653-61. doi: 10.1042/BJ20021785
- Deisseroth K, Bito H, Tsien RW. Signaling from synapse to nucleus: postsynaptic CREB phosphorylation during multiple forms of hippocampal synaptic plasticity. *Neuron.* 1996 Jan;16(1):89-101. doi: 10.1016/s0896-6273(00)80026-4
- Dent EW, Gertler FB. Cytoskeletal dynamics and transport in growth cone motility and axon guidance. *Neuron.* 2003 Oct 9;40(2):209-27. doi: 10.1016/s0896-6273(03)00633-0
- Dent EW, Gupton SL, Gertler FB. The growth cone cytoskeleton in axon outgrowth and guidance. *Cold Spring Harb Perspect Biol.* 2011 Mar 1;3(3):a001800. doi: 10.1101/cshperspect.a001800
- Dieterich DC, Karpova A, Mikhaylova M, Zdobnova I, König I, Landwehr M, Kreutz M, Smalla KH, Richter K, Landgraf P, Reissner C, Boeckers TM, Zuschratter W, Spilker C, Seidenbecher CI, Garner CC, Gundelfinger ED, Kreutz MR. Caldendrin-Jacob: a protein liaison that couples NMDA receptor signalling to the nucleus. *PLoS Biol.* 2008 Feb;6(2):e34. doi: 10.1371/journal.pbio.0060034
- Dragunow M, Beilharz E, Mason B, Lawlor P, Abraham W, Gluckman P. Brain-derived neurotrophic factor expression after long-term potentiation. *Neurosci Lett.* 1993 Oct 1;160(2):232-6. doi: 10.1016/0304-3940(93)90420-p
- Dragunow M, Robertson HA. Kindling stimulation induces c-fos protein(s) in granule cells of the rat dentate gyrus. *Nature.* 1987 Oct 1-7;329(6138):441-2. doi: 10.1038/329441a0
- Drescher, U., Kremoser, C., Handwerker, C., Löschinger, J., Noda, M., and Bonhoeffer, F. (1995). In vitro guidance of retinal ganglion cell axons by RAGS, a 25 kDa tectal protein related

- to ligands for Eph receptor tyrosine kinases. *Cell* 82, 359–370. doi: 10.1016/0092-8674(95)90425-5
- Dobin A, Davis CA, Schlesinger F, Drenkow J, Zaleski C, Jha S, Batut P, Chaisson M, Gingeras TR. STAR: ultrafast universal RNA-seq aligner. *Bioinformatics*. 2013 Jan 1;29(1):15-21. doi: 10.1093/bioinformatics/bts635
- Dolmetsch RE, Pajvani U, Fife K, Spotts JM, Greenberg ME. Signaling to the nucleus by an L-type calcium channel-calmodulin complex through the MAP kinase pathway. *Science*. 2001 Oct 12;294(5541):333-9. doi: 10.1126/science.1063395
- Douglas RM, Dragunow M, Robertson HA. High-frequency discharge of dentate granule cells, but not long-term potentiation, induces c-fos protein. *Brain Res*. 1988 Nov;464(3):259-62. doi: 10.1016/0169-328x(88)90033-2
- Douglas RM, Goddard GV. Long-term potentiation of the perforant path-granule cell synapse in the rat hippocampus. *Brain Res*. 1975 Mar 21;86(2):205-15. doi: 10.1016/0006-8993(75)90697-6
- Du JL, Wei HP, Wang ZR, Wong ST, Poo MM. Long-range retrograde spread of LTP and LTD from optic tectum to retina. *Proc Natl Acad Sci U S A*. 2009 Nov 10;106(45):18890-6. doi: 10.1073/pnas.0910659106
- Dudek SM, Bear MF. Homosynaptic long-term depression in area CA1 of hippocampus and effects of N-methyl-D-aspartate receptor blockade. *Proc Natl Acad Sci U S A*. 1992 May 15;89(10):4363-7. doi: 10.1073/pnas.89.10.4363
- Erreger K, Dravid SM, Banke TG, Wyllie DJ, Traynelis SF. Subunit-specific gating controls rat NR1/NR2A and NR1/NR2B NMDA channel kinetics and synaptic signalling profiles. *J Physiol*. 2005 Mar 1;563(Pt 2):345-58. doi: 10.1113/jphysiol.2004.080028
- Ewald RC, Van Keuren-Jensen KR, Aizenman CD, Cline HT. Roles of NR2A and NR2B in the development of dendritic arbor morphology in vivo. *J Neurosci*. 2008 Jan 23;28(4):850-61. doi: 10.1523/JNEUROSCI.5078-07.2008.
- Feldheim DA, Kim YI, Bergemann AD, Frisén J, Barbacid M, Flanagan JG. Genetic analysis of ephrin-A2 and ephrin-A5 shows their requirement in multiple aspects of retinocollicular mapping. *Neuron*. 2000 Mar;25(3):563-74. doi: 10.1016/s0896-6273(00)81060-0
- Feldheim DA, O'Leary DD. Visual map development: bidirectional signaling, bifunctional guidance molecules, and competition. *Cold Spring Harb Perspect Biol*. 2010 Nov;2(11):a001768. doi: 10.1101/cshperspect.a001768
- Feldman DE, Brainard MS, Knudsen EI. Newly learned auditory responses mediated by NMDA receptors in the owl inferior colliculus. *Science*. 1996 Jan 26;271(5248):525-8. doi: 10.1126/science.271.5248.525

- Fellin T, Pascual O, Gobbo S, Pozzan T, Haydon PG, Carmignoto G. Neuronal synchrony mediated by astrocytic glutamate through activation of extrasynaptic NMDA receptors. *Neuron*. 2004 Sep 2;43(5):729-43. doi: 10.1016/j.neuron.2004.08.011
- Feng B, Morley RM, Jane DE, Monaghan DT. The effect of competitive antagonist chain length on NMDA receptor subunit selectivity. *Neuropharmacology*. 2005 Mar;48(3):354-9. doi: 10.1016/j.neuropharm.2004.11.004
- Furuya S, Tabata T, Mitoma J, Yamada K, Yamasaki M, Makino A, Yamamoto T, Watanabe M, Kano M, Hirabayashi Y. L-serine and glycine serve as major astroglia-derived trophic factors for cerebellar Purkinje neurons. *Proc Natl Acad Sci U S A*. 2000 Oct 10;97(21):11528-33. doi: 10.1073/pnas.200364497
- Gandolfi D, Cerri S, Mapelli J, Polimeni M, Tritto S, Fuzzati-Armentero MT, Bigiani A, Blandini F, Mapelli L, D'Angelo E. Activation of the CREB/c-Fos Pathway during Long-Term Synaptic Plasticity in the Cerebellum Granular Layer. *Front Cell Neurosci*. 2017 Jun 28;11:184. doi: 10.3389/fncel.2017.00184
- García-Rodríguez C, Rao A. Nuclear factor of activated T cells (NFAT)-dependent transactivation regulated by the coactivators p300/CREB-binding protein (CBP). *J Exp Med*. 1998 Jun 15;187(12):2031-6. doi: 10.1084/jem.187.12.2031
- Gaze RM. The representation of the retina on the optic lobe of the frog. *Q J Exp Physiol Cogn Med Sci*. 1958 Apr;43(2):209-14. doi: 10.1113/expphysiol.1958.sp001318
- Ghiretti AE, Paradis S. Molecular mechanisms of activity-dependent changes in dendritic morphology: role of RGK proteins. *Trends Neurosci*. 2014 Jul;37(7):399-407. doi: 10.1016/j.tins.2014.05.003
- Ghiretti AE, Moore AR, Brenner RG, Chen LF, West AE, Lau NC, Van Hooser SD, Paradis S. Rem2 is an activity-dependent negative regulator of dendritic complexity in vivo. *J Neurosci*. 2014 Jan 8;34(2):392-407. doi: 10.1523/JNEUROSCI.1328-13.2014
- Ghosh A, Carnahan J, Greenberg ME. Requirement for BDNF in activity-dependent survival of cortical neurons. *Science*. 1994 Mar 18;263(5153):1618-23. doi: 10.1126/science.7907431
- Ghosh A, Greenberg ME. Calcium signaling in neurons: molecular mechanisms and cellular consequences. *Science*. 1995 Apr 14;268(5208):239-47. doi: 10.1126/science.7716515
- Ginty DD, Bonni A, Greenberg ME. Nerve growth factor activates a Ras-dependent protein kinase that stimulates c-fos transcription via phosphorylation of CREB. *Cell*. 1994 Jun 3;77(5):713-25. doi: 10.1016/0092-8674(94)90055-8
- Gnuegge L, Schmid S, Neuhauss SC. Analysis of the activity-deprived zebrafish mutant macho reveals an essential requirement of neuronal activity for the development of a fine-grained

- visuotopic map. *J Neurosci*. 2001 May 15;21(10):3542-8. doi: 10.1523/JNEUROSCI.21-10-03542.2001
- Gobert D, Schohl A, Kutsarova E, Ruthazer ES. TORC1 selectively regulates synaptic maturation and input convergence in the developing visual system. *Dev Neurobiol*. 2020 Sep;80(9-10):332-350. doi: 10.1002/dneu.22782
- Godement P, Bonhoeffer F. Cross-species recognition of tectal cues by retinal fibers in vitro. *Development*. 1989 Jun;106(2):313-20
- Gonda S, Giesen J, Sieberath A, West F, Buchholz R, Klatt O, Ziebarth T, Räk A, Kleinhubbert S, Riedel C, Hollmann M, Hamad MIK, Reiner A, Wahle P. GluN2B but Not GluN2A for Basal Dendritic Growth of Cortical Pyramidal Neurons. *Front Neuroanat*. 2020 Nov 13;14:571351. doi: 10.3389/fnana.2020.571351
- Graef IA, Mermelstein PG, Stankunas K, Neilson JR, Deisseroth K, Tsien RW, Crabtree GR. L-type calcium channels and GSK-3 regulate the activity of NF-ATc4 in hippocampal neurons. *Nature*. 1999 Oct 14;401(6754):703-8. doi: 10.1038/44378
- Graef IA, Wang F, Charron F, Chen L, Neilson J, Tessier-Lavigne M, Crabtree GR. Neurotrophins and netrins require calcineurin/NFAT signaling to stimulate outgrowth of embryonic axons. *Cell*. 2003 May 30;113(5):657-70. doi: 10.1016/s0092-8674(03)00390-8
- Greenberg ME, Ziff EB. Stimulation of 3T3 cells induces transcription of the c-fos proto-oncogene. *Nature*. 1984 Oct 4-10;311(5985):433-8. doi: 10.1038/311433a0
- Greenberg ME, Greene LA, Ziff EB. Nerve growth factor and epidermal growth factor induce rapid transient changes in proto-oncogene transcription in PC12 cells. *J Biol Chem*. 1985 Nov 15;260(26):14101-10
- Greenberg ME, Ziff EB, Greene LA. Stimulation of neuronal acetylcholine receptors induces rapid gene transcription. *Science*. 1986 Oct 3;234(4772):80-3. doi: 10.1126/science.3749894
- Groc L, Heine M, Cousins SL, Stephenson FA, Lounis B, Cognet L, Choquet D. NMDA receptor surface mobility depends on NR2A-2B subunits. *Proc Natl Acad Sci U S A*. 2006 Dec 5;103(49):18769-74. doi: 10.1073/pnas.0605238103
- Groth RD, Mermelstein PG. Brain-derived neurotrophic factor activation of NFAT (nuclear factor of activated T-cells)-dependent transcription: a role for the transcription factor NFATc4 in neurotrophin-mediated gene expression. *J Neurosci*. 2003 Sep 3;23(22):8125-34. doi: 10.1523/JNEUROSCI.23-22-08125.2003
- Gu Y, Stornetta RL. Synaptic plasticity, AMPA-R trafficking, and Ras-MAPK signaling. *Acta Pharmacol Sin*. 2007 Jul;28(7):928-36. doi: 10.1111/j.1745-7254.2007.00609.x

- Hardingham GE, Arnold FJ, Bading H. A calcium microdomain near NMDA receptors: on switch for ERK-dependent synapse-to-nucleus communication. *Nat Neurosci.* 2001 Jun;4(6):565-6. doi: 10.1038/88380
- Hardingham GE, Arnold FJ, Bading H. Nuclear calcium signaling controls CREB-mediated gene expression triggered by synaptic activity. *Nat Neurosci.* 2001 Mar;4(3):261-7. doi: 10.1038/85109
- Hardingham GE, Bading H. Coupling of extrasynaptic NMDA receptors to a CREB shut-off pathway is developmentally regulated. *Biochim Biophys Acta.* 2002 Nov 4;1600(1-2):148-53. doi: 10.1016/s1570-9639(02)00455-7
- Hardingham GE, Bading H. Synaptic versus extrasynaptic NMDA receptor signalling: implications for neurodegenerative disorders. *Nat Rev Neurosci.* 2010 Oct;11(10):682-96. doi: 10.1038/nrn2911
- Hardingham GE, Fukunaga Y, Bading H. Extrasynaptic NMDARs oppose synaptic NMDARs by triggering CREB shut-off and cell death pathways. *Nat Neurosci.* 2002 May;5(5):405-14. doi: 10.1038/nn835
- Hashimoto A, Nishikawa T, Oka T, Takahashi K. Endogenous D-serine in rat brain: N-methyl-D-aspartate receptor-related distribution and aging. *J Neurochem.* 1993 Feb;60(2):783-6. doi: 10.1111/j.1471-4159.1993.tb03219.x
- Hata Y, Stryker MP. Control of thalamocortical afferent rearrangement by postsynaptic activity in developing visual cortex. *Science.* 1994 Sep 16;265(5179):1732-5. doi: 10.1126/science.8085163
- Hatton CJ, Paoletti P. Modulation of triheteromeric NMDA receptors by N-terminal domain ligands. *Neuron.* 2005 Apr 21;46(2):261-74. doi: 10.1016/j.neuron.2005.03.005
- Hay N, Sonenberg N. Upstream and downstream of mTOR. *Genes Dev.* 2004 Aug 15;18(16):1926-45. doi: 10.1101/gad.1212704
- Hayakawa K, Hirosawa M, Tabei Y, Arai D, Tanaka S, Murakami N, Yagi S, Shiota K. Epigenetic switching by the metabolism-sensing factors in the generation of orexin neurons from mouse embryonic stem cells. *J Biol Chem.* 2013 Jun 14;288(24):17099-110. doi: 10.1074/jbc.M113.455899
- Hayashi Y, Shi SH, Esteban JA, Piccini A, Poncer JC, Malinow R. Driving AMPA receptors into synapses by LTP and CaMKII: requirement for GluR1 and PDZ domain interaction. *Science.* 2000 Mar 24;287(5461):2262-7. doi: 10.1126/science.287.5461.2262
- Hebb, D.O. *The organization of behavior: A neuropsychological theory.* 1949 John Wiley & Sons, New York

- Hensch TK. Critical period plasticity in local cortical circuits. *Nat Rev Neurosci*. 2005 Nov;6(11):877-88. doi: 10.1038/nrn1787
- Herring BE, Nicoll RA. Long-Term Potentiation: From CaMKII to AMPA Receptor Trafficking. *Annu Rev Physiol*. 2016;78:351-65. doi: 10.1146/annurev-physiol-021014-071753
- Herron CE, Lester RA, Coan EJ, Collingridge GL. Frequency-dependent involvement of NMDA receptors in the hippocampus: a novel synaptic mechanism. *Nature*. 1986 Jul 17-23;322(6076):265-8. doi: 10.1038/322265a0
- Hestrin S. Developmental regulation of NMDA receptor-mediated synaptic currents at a central synapse. *Nature*. 1992 Jun 25;357(6380):686-9. doi: 10.1038/357686a0
- Higenell V, Han SM, Feldheim DA, Scalia F, Ruthazer ES. Expression patterns of Ephs and ephrins throughout retinotectal development in *Xenopus laevis*. *Dev Neurobiol*. 2012 Apr;72(4):547-63. doi: 10.1002/dneu.20930
- Hindges R, McLaughlin T, Genoud N, Henkemeyer M, O'Leary D. EphB forward signaling controls directional branch extension and arborization required for dorsal-ventral retinotopic mapping. *Neuron*. 2002 Aug 1;35(3):475-87. doi: 10.1016/s0896-6273(02)00799-7
- Hirabayashi Y, Furuya S. Roles of l-serine and sphingolipid synthesis in brain development and neuronal survival. *Prog Lipid Res*. 2008 May;47(3):188-203. doi: 10.1016/j.plipres.2008.01.003
- Holt CE. The topography of the initial retinotectal projection. *Prog Brain Res*. 1983;58:339-45. doi: 10.1016/S0079-6123(08)60035-7
- Holt CE, Harris WA. Order in the initial retinotectal map in *Xenopus*: a new technique for labelling growing nerve fibres. *Nature*. 1983 Jan 13;301(5896):150-2. doi: 10.1038/301150a0
- Holthoff K, Kovalchuk Y, Konnerth A. Dendritic spikes and activity-dependent synaptic plasticity. *Cell Tissue Res*. 2006 Nov;326(2):369-77. doi: 10.1007/s00441-006-0263-8
- Hornberger MR, Dütting D, Ciossek T, Yamada T, Handwerker C, Lang S, Weth F, Huf J, Wessel R, Logan C, Tanaka H, Drescher U. Modulation of EphA receptor function by coexpressed ephrinA ligands on retinal ganglion cell axons. *Neuron*. 1999 Apr;22(4):731-42. doi: 10.1016/s0896-6273(00)80732-1
- Hu SC, Chrivia J, Ghosh A. Regulation of CBP-mediated transcription by neuronal calcium signaling. *Neuron*. 1999 Apr;22(4):799-808. doi: 10.1016/s0896-6273(00)80738-2
- Hubel DH. Exploration of the primary visual cortex, 1955-78. *Nature*. 1982 Oct 7;299(5883):515-24. doi: 10.1038/299515a0

- Hubel DH, Wiesel TN. The period of susceptibility to the physiological effects of unilateral eye closure in kittens. *J Physiol.* 1970 Feb;206(2):419-36. doi: 10.1113/jphysiol.1970.sp009022
- Hunt SP, Pini A, Evan G. Induction of c-fos-like protein in spinal cord neurons following sensory stimulation. *Nature.* 1987 Aug 13-19;328(6131):632-4. doi: 10.1038/328632a0
- Impey S, Fong AL, Wang Y, Cardinaux JR, Fass DM, Obrietan K, Wayman GA, Storm DR, Soderling TR, Goodman RH. Phosphorylation of CBP mediates transcriptional activation by neural activity and CaM kinase IV. *Neuron.* 2002 Apr 11;34(2):235-44. doi: 10.1016/s0896-6273(02)00654-2
- Ivanov A, Pellegrino C, Rama S, Dumalska I, Salyha Y, Ben-Ari Y, Medina I. Opposing role of synaptic and extrasynaptic NMDA receptors in regulation of the extracellular signal-regulated kinases (ERK) activity in cultured rat hippocampal neurons. *J Physiol.* 2006 May 1;572(Pt 3):789-98. doi: 10.1113/jphysiol.2006.105510
- Jalili V, Afgan E, Gu Q, Clements D, Blankenberg D, Goecks J, Taylor J, Nekrutenko A. The Galaxy platform for accessible, reproducible and collaborative biomedical analyses: 2020 update. *Nucleic Acids Res.* 2020 Jul 2;48(W1):W395-W402. doi: 10.1093/nar/gkaa434. Erratum in: *Nucleic Acids Res.* 2020 Aug 20;48(14):8205-8207
- Jin SX, Feig LA. Long-term potentiation in the CA1 hippocampus induced by NR2A subunit-containing NMDA glutamate receptors is mediated by Ras-GRF2/Erk map kinase signaling. *PLoS One.* 2010 Jul 22;5(7):e11732. doi: 10.1371/journal.pone.0011732
- Johnson JW, Ascher P. Glycine potentiates the NMDA response in cultured mouse brain neurons. *Nature.* 1987 Feb 5-11;325(6104):529-31. doi: 10.1038/325529a0
- Kalil K, Dent EW. Touch and go: guidance cues signal to the growth cone cytoskeleton. *Curr Opin Neurobiol.* 2005 Oct;15(5):521-6. doi: 10.1016/j.conb.2005.08.005
- Kamenetz F, Tomita T, Hsieh H, Seabrook G, Borchelt D, Iwatsubo T, Sisodia S, Malinow R. APP processing and synaptic function. *Neuron.* 2003 Mar 27;37(6):925-37. doi: 10.1016/s0896-6273(03)00124-7
- Kao TJ, Law C, Kania A. Eph and ephrin signaling: lessons learned from spinal motor neurons. *Semin Cell Dev Biol.* 2012 Feb;23(1):83-91. doi: 10.1016/j.semcdb.2011.10.016
- Karpova A, Mikhaylova M, Bera S, Bär J, Reddy PP, Behnisch T, Rankovic V, Spilker C, Bethge P, Sahin J, Kaushik R, Zuschratter W, Kähne T, Naumann M, Gundelfinger ED, Kreutz MR. Encoding and transducing the synaptic or extrasynaptic origin of NMDA receptor signals to the nucleus. *Cell.* 2013 Feb 28;152(5):1119-33. doi: 10.1016/j.cell.2013.02.002
- Keith RE, Azcarate JM, Keith MJ, Hung CW, Badakhsh MF, Dumas TC. Direct Intracellular Signaling by the Carboxy terminus of NMDA Receptor GluN2 Subunits Regulates

- Dendritic Morphology in Hippocampal CA1 Pyramidal Neurons. *Neuroscience*. 2019 Jan 1;396:138-153. doi: 10.1016/j.neuroscience.2018.11.021
- Kesner P, Schohl A, Warren EC, Ma F, Ruthazer ES. Postsynaptic and Presynaptic NMDARs Have Distinct Roles in Visual Circuit Development. *Cell Rep*. 2020 Jul 28;32(4):107955. doi: 10.1016/j.celrep.2020.107955
- Kessels HW, Nabavi S, Malinow R. Metabotropic NMDA receptor function is required for β -amyloid-induced synaptic depression. *Proc Natl Acad Sci U S A*. 2013 Mar 5;110(10):4033-8. doi: 10.1073/pnas.1219605110
- Kim MJ, Dunah AW, Wang YT, Sheng M. Differential roles of NR2A- and NR2B-containing NMDA receptors in Ras-ERK signaling and AMPA receptor trafficking. *Neuron*. 2005 Jun 2;46(5):745-60. doi: 10.1016/j.neuron.2005.04.031
- Kirkwood A, Bear MF. Homosynaptic long-term depression in the visual cortex. *J Neurosci*. 1994 May;14(5 Pt 2):3404-12. doi: 10.1523/JNEUROSCI.14-05-03404.1994
- Kleckner NW, Dingledine R. Requirement for glycine in activation of NMDA-receptors expressed in *Xenopus* oocytes. *Science*. 1988 Aug 12;241(4867):835-7. doi: 10.1126/science.2841759
- Koester HJ, Sakmann B. Calcium dynamics in single spines during coincident pre- and postsynaptic activity depend on relative timing of back-propagating action potentials and subthreshold excitatory postsynaptic potentials. *Proc Natl Acad Sci U S A*. 1998 Aug 4;95(16):9596-601. doi: 10.1073/pnas.95.16.9596
- Korte M, Carroll P, Wolf E, Brem G, Thoenen H, Bonhoeffer T. Hippocampal long-term potentiation is impaired in mice lacking brain-derived neurotrophic factor. *Proc Natl Acad Sci U S A*. 1995 Sep 12;92(19):8856-60. doi: 10.1073/pnas.92.19.8856
- Kutsarova E, Munz M, Ruthazer ES. Rules for Shaping Neural Connections in the Developing Brain. *Front Neural Circuits*. 2017 Jan 10;10:111. doi: 10.3389/fncir.2016.00111. PMID: 28119574; PMCID: PMC5223306
- Lanahan A, Worley P. Immediate-early genes and synaptic function. *Neurobiol Learn Mem*. 1998 Jul-Sep;70(1-2):37-43. doi: 10.1006/nlme.1998.3836
- Larson J, Lynch G. Induction of synaptic potentiation in hippocampus by patterned stimulation involves two events. *Science*. 1986 May 23;232(4753):985-8. doi: 10.1126/science.3704635
- Larson J, Wong D, Lynch G. Patterned stimulation at the theta frequency is optimal for the induction of hippocampal long-term potentiation. *Brain Res*. 1986 Mar 19;368(2):347-50. doi: 10.1016/0006-8993(86)90579-2

- Le Bail M, Martineau M, Sacchi S, Yatsenko N, Radzishevsky I, Conrod S, Ait Ouares K, Wolosker H, Pollegioni L, Billard JM, Mothet JP. Identity of the NMDA receptor coagonist is synapse specific and developmentally regulated in the hippocampus. *Proc Natl Acad Sci U S A*. 2015 Jan 13;112(2):E204-13. doi: 10.1073/pnas.1416668112
- LeBlanc JJ, Fagiolini M. Autism: a "critical period" disorder? *Neural Plast*. 2011;2011:921680. doi: 10.1155/2011/921680
- Lehmann J, Schneider J, McPherson S, Murphy DE, Bernard P, Tsai C, Bennett DA, Pastor G, Steel DJ, Boehm C, et al. CPP, a selective N-methyl-D-aspartate (NMDA)-type receptor antagonist: characterization in vitro and in vivo. *J Pharmacol Exp Ther*. 1987 Mar;240(3):737-46
- Leinekugel X, Medina I, Khalilov I, Ben-Ari Y, Khazipov R. Ca²⁺ oscillations mediated by the synergistic excitatory actions of GABA(A) and NMDA receptors in the neonatal hippocampus. *Neuron*. 1997 Feb;18(2):243-55. doi: 10.1016/s0896-6273(00)80265-2
- Lemke G, Reber M. Retinotectal mapping: new insights from molecular genetics. *Annu Rev Cell Dev Biol*. 2005;21:551-80. doi: 10.1146/annurev.cellbio.20.022403.093702
- Leonard AS, Lim IA, Hemsworth DE, Horne MC, Hell JW. Calcium/calmodulin-dependent protein kinase II is associated with the N-methyl-D-aspartate receptor. *Proc Natl Acad Sci U S A*. 1999 Mar 16;96(6):3239-44. doi: 10.1073/pnas.96.6.3239
- Lerea LS, McNamara JO. Ionotropic glutamate receptor subtypes activate c-fos transcription by distinct calcium-requiring intracellular signaling pathways. *Neuron*. 1993 Jan;10(1):31-41. doi: 10.1016/0896-6273(93)90239-n
- Lerma J. Kainate receptor physiology. *Curr Opin Pharmacol*. 2006 Feb;6(1):89-97. doi: 10.1016/j.coph.2005.08.004
- Lessmann V, Gottmann K, Heumann R. BDNF and NT-4/5 enhance glutamatergic synaptic transmission in cultured hippocampal neurones. *Neuroreport*. 1994 Dec 30;6(1):21-5. doi: 10.1097/00001756-199412300-00007
- Levine ES, Dreyfus CF, Black IB, Plummer MR. Brain-derived neurotrophic factor rapidly enhances synaptic transmission in hippocampal neurons via postsynaptic tyrosine kinase receptors. *Proc Natl Acad Sci U S A*. 1995 Aug 15;92(17):8074-7. doi: 10.1073/pnas.92.17.8074
- Levy WB, Steward O. Synapses as associative memory elements in the hippocampal formation. *Brain Res*. 1979 Oct 19;175(2):233-45. doi: 10.1016/0006-8993(79)91003-5
- Li S, Tian X, Hartley DM, Feig LA. Distinct roles for Ras-guanine nucleotide-releasing factor 1 (Ras-GRF1) and Ras-GRF2 in the induction of long-term potentiation and long-term

- depression. *J Neurosci*. 2006 Feb 8;26(6):1721-9. doi: 10.1523/JNEUROSCI.3990-05.2006
- Li Y, Sacchi S, Pollegioni L, Basu AC, Coyle JT, Bolshakov VY. Identity of endogenous NMDAR glycine site agonist in amygdala is determined by synaptic activity level. *Nat Commun*. 2013;4:1760. doi: 10.1038/ncomms2779
- Liao Y, Smyth GK, Shi W. featureCounts: an efficient general purpose program for assigning sequence reads to genomic features. *Bioinformatics*. 2014 Apr 1;30(7):923-30. doi: 10.1093/bioinformatics/btt656
- Lisman J, Schulman H, Cline H. The molecular basis of CaMKII function in synaptic and behavioural memory. *Nat Rev Neurosci*. 2002 Mar;3(3):175-90. doi: 10.1038/nrn753
- Liu Z, Hamodi AS, Pratt KG. Early development and function of the *Xenopus* tadpole retinotectal circuit. *Curr Opin Neurobiol*. 2016 Dec;41:17-23. doi: 10.1016/j.conb.2016.07.002
- Liu L, Wong TP, Pozza MF, Lingenhoehl K, Wang Y, Sheng M, Auberson YP, Wang YT. Role of NMDA receptor subtypes in governing the direction of hippocampal synaptic plasticity. *Science*. 2004 May 14;304(5673):1021-4. doi: 10.1126/science.1096615
- Liu Y, Wong TP, Aarts M, Rooyackers A, Liu L, Lai TW, Wu DC, Lu J, Tymianski M, Craig AM, Wang YT. NMDA receptor subunits have differential roles in mediating excitotoxic neuronal death both in vitro and in vivo. *J Neurosci*. 2007 Mar 14;27(11):2846-57. doi: 10.1523/JNEUROSCI.0116-07.2007
- Livak KJ, Schmittgen TD. Analysis of relative gene expression data using real-time quantitative PCR and the 2(-Delta Delta C(T)) Method. *Methods*. 2001 Dec;25(4):402-8. doi: 10.1006/meth.2001.1262
- Lonze BE, Riccio A, Cohen S, Ginty DD. Apoptosis, axonal growth defects, and degeneration of peripheral neurons in mice lacking CREB. *Neuron*. 2002 Apr 25;34(3):371-85. doi: 10.1016/s0896-6273(02)00686-4
- Love MI, Huber W, Anders S. Moderated estimation of fold change and dispersion for RNA-seq data with DESeq2. *Genome Biol*. 2014;15(12):550. doi: 10.1186/s13059-014-0550-8
- Lüscher C, Malenka RC. NMDA receptor-dependent long-term potentiation and long-term depression (LTP/LTD). *Cold Spring Harb Perspect Biol*. 2012 Jun 1;4(6):a005710. doi: 10.1101/cshperspect.a005710
- Lynch GS, Dunwiddie T, Gribkoff V. Heterosynaptic depression: a postsynaptic correlate of long-term potentiation. *Nature*. 1977 Apr 21;266(5604):737-9. doi: 10.1038/266737a0

- Lynch G, Larson J, Kelso S, Barrionuevo G, Schottler F. Intracellular injections of EGTA block induction of hippocampal long-term potentiation. *Nature*. 1983 Oct 20-26;305(5936):719-21. doi: 10.1038/305719a0
- MacDermott AB, Mayer ML, Westbrook GL, Smith SJ, Barker JL. NMDA-receptor activation increases cytoplasmic calcium concentration in cultured spinal cord neurones. *Nature*. 1986 May 29-Jun 4;321(6069):519-22. doi: 10.1038/321519a0
- MacKay MB, Kravtseyuk M, Thomas R, Mitchell ND, Dursun SM, Baker GB. D-Serine: Potential Therapeutic Agent and/or Biomarker in Schizophrenia and Depression? *Front Psychiatry*. 2019 Feb 6;10:25. doi: 10.3389/fpsy.2019.00025
- Madeira C, Lourenco MV, Vargas-Lopes C, Suemoto CK, Brandão CO, Reis T, Leite RE, Laks J, Jacob-Filho W, Pasqualucci CA, Grinberg LT, Ferreira ST, Panizzutti R. d-serine levels in Alzheimer's disease: implications for novel biomarker development. *Transl Psychiatry*. 2015 May 5;5(5):e561. doi: 10.1038/tp.2015.52
- Malinow R, Malenka RC. AMPA receptor trafficking and synaptic plasticity. *Annu Rev Neurosci*. 2002;25:103-26. doi: 10.1146/annurev.neuro.25.112701.142758
- Malinow R, Schulman H, Tsien RW. Inhibition of postsynaptic PKC or CaMKII blocks induction but not expression of LTP. *Science*. 1989 Aug 25;245(4920):862-6. doi: 10.1126/science.2549638
- Mann F, Ray S, Harris W, Holt C. Topographic mapping in dorsoventral axis of the *Xenopus* retinotectal system depends on signaling through ephrin-B ligands. *Neuron*. 2002 Aug 1;35(3):461-73. doi: 10.1016/s0896-6273(02)00786-9
- Mantamadiotis T, Lemberger T, Bleckmann SC, Kern H, Kretz O, Martin Villalba A, Tronche F, Kellendonk C, Gau D, Kapfhammer J, Otto C, Schmid W, Schütz G. Disruption of CREB function in brain leads to neurodegeneration. *Nat Genet*. 2002 May;31(1):47-54. doi: 10.1038/ng882
- Martel MA, Wyllie DJ, Hardingham GE. In developing hippocampal neurons, NR2B-containing N-methyl-D-aspartate receptors (NMDARs) can mediate signaling to neuronal survival and synaptic potentiation, as well as neuronal death. *Neuroscience*. 2009 Jan 12;158(1):334-43. doi: 10.1016/j.neuroscience.2008.01.080
- Martin SJ, Grimwood PD, Morris RG. Synaptic plasticity and memory: an evaluation of the hypothesis. *Annu Rev Neurosci*. 2000;23:649-711. doi: 10.1146/annurev.neuro.23.1.649
- Massey PV, Bashir ZI. Long-term depression: multiple forms and implications for brain function. *Trends Neurosci*. 2007 Apr;30(4):176-84. doi: 10.1016/j.tins.2007.02.005
- Massey PV, Johnson BE, Moulton PR, Auberson YP, Brown MW, Molnar E, Collingridge GL, Bashir ZI. Differential roles of NR2A and NR2B-containing NMDA receptors in cortical

- long-term potentiation and long-term depression. *J Neurosci*. 2004 Sep 8;24(36):7821-8. doi: 10.1523/JNEUROSCI.1697-04.2004
- Mayer ML, Westbrook GL, Guthrie PB. Voltage-dependent block by Mg²⁺ of NMDA responses in spinal cord neurones. *Nature*. 1984 May 17-23;309(5965):261-3. doi: 10.1038/309261a0
- Mayr B, Montminy M. Transcriptional regulation by the phosphorylation-dependent factor CREB. *Nat Rev Mol Cell Biol*. 2001 Aug;2(8):599-609. doi: 10.1038/35085068
- McAllister AK, Lo DC, Katz LC. Neurotrophins regulate dendritic growth in developing visual cortex. *Neuron*. 1995 Oct;15(4):791-803. doi: 10.1016/0896-6273(95)90171-x
- McAllister AK, Katz LC, Lo DC. Neurotrophin regulation of cortical dendritic growth requires activity. *Neuron*. 1996 Dec;17(6):1057-64. doi: 10.1016/s0896-6273(00)80239-1
- McLaughlin T, Hindges R, Yates PA, O'Leary DD. Bifunctional action of ephrin-B1 as a repellent and attractant to control bidirectional branch extension in dorsal-ventral retinotopic mapping. *Development*. 2003a Jun;130(11):2407-18. doi: 10.1242/dev.00467
- McLaughlin T, Torborg CL, Feller MB, O'Leary DD. Retinotopic map refinement requires spontaneous retinal waves during a brief critical period of development. *Neuron*. 2003b Dec 18;40(6):1147-60. doi: 10.1016/s0896-6273(03)00790-6
- McLennan H, Lodge D. The antagonism of amino acid-induced excitation of spinal neurones in the cat. *Brain Res*. 1979 Jun 15;169(1):83-90. doi: 10.1016/0006-8993(79)90375-5
- Meister M, Wong RO, Baylor DA, Shatz CJ. Synchronous bursts of action potentials in ganglion cells of the developing mammalian retina. *Science*. 1991 May 17;252(5008):939-43. doi: 10.1126/science.2035024
- Meyer, R. L., and Wolcott, L. L. (1987). Compression and expansion without impulse activity in the retinotectal projection of goldfish. *J. Neurobiol.* 18, 549–567. doi: 10.1002/neu.480180606
- Miller KD, Chapman B, Stryker MP. Visual responses in adult cat visual cortex depend on N-methyl-D-aspartate receptors. *Proc Natl Acad Sci U S A*. 1989 Jul;86(13):5183-7. doi: 10.1073/pnas.86.13.5183
- Milnerwood AJ, Gladding CM, Pouladi MA, Kaufman AM, Hines RM, Boyd JD, Ko RW, Vasuta OC, Graham RK, Hayden MR, Murphy TH, Raymond LA. Early increase in extrasynaptic NMDA receptor signaling and expression contributes to phenotype onset in Huntington's disease mice. *Neuron*. 2010 Jan 28;65(2):178-90. doi: 10.1016/j.neuron.2010.01.008
- Morgan JI, Cohen DR, Hempstead JL, Curran T. Mapping patterns of c-fos expression in the central nervous system after seizure. *Science*. 1987 Jul 10;237(4811):192-7. doi: 10.1126/science.3037702

- Morgan JI, Curran T. Role of ion flux in the control of c-fos expression. *Nature*. 1986 Aug 7-13;322(6079):552-5. doi: 10.1038/322552a0
- Monschau B, Kremoser C, Ohta K, Tanaka H, Kaneko T, Yamada T, Handwerker C, Hornberger MR, Löschinger J, Pasquale EB, Siever DA, Verderame MF, Müller BK, Bonhoeffer F, Drescher U. Shared and distinct functions of RAGS and ELF-1 in guiding retinal axons. *EMBO J*. 1997 Mar 17;16(6):1258-67. doi: 10.1093/emboj/16.6.1258
- Monyer H, Burnashev N, Laurie DJ, Sakmann B, Seeburg PH. Developmental and regional expression in the rat brain and functional properties of four NMDA receptors. *Neuron*. 1994 Mar;12(3):529-40. doi: 10.1016/0896-6273(94)90210-0
- Mu Y, Poo MM. Spike timing-dependent LTP/LTD mediates visual experience-dependent plasticity in a developing retinotectal system. *Neuron*. 2006 Apr 6;50(1):115-25. doi: 10.1016/j.neuron.2006.03.009
- Mulkey RM, Herron CE, Malenka RC. An essential role for protein phosphatases in hippocampal long-term depression. *Science*. 1993 Aug 20;261(5124):1051-5. doi: 10.1126/science.8394601
- Mulkey RM, Endo S, Shenolikar S, Malenka RC. Involvement of a calcineurin/inhibitor-1 phosphatase cascade in hippocampal long-term depression. *Nature*. 1994 Jun 9;369(6480):486-8. doi: 10.1038/369486a0
- Mulkey RM, Malenka RC. Mechanisms underlying induction of homosynaptic long-term depression in area CA1 of the hippocampus. *Neuron*. 1992 Nov;9(5):967-75. doi: 10.1016/0896-6273(92)90248-c
- Munz, M., Gobert, D., Schohl, A., Poquérusse, J., Podgorski, K., Spratt, P., et al. (2014). Rapid Hebbian axonal remodeling mediated by visual stimulation. *Science* 344, 904–909. doi: 10.1126/science.1251593
- Nabavi S, Kessels HW, Alfonso S, Aow J, Fox R, Malinow R. Metabotropic NMDA receptor function is required for NMDA receptor-dependent long-term depression. *Proc Natl Acad Sci U S A*. 2013 Mar 5;110(10):4027-32. doi: 10.1073/pnas.1219454110
- Nakamura F, Kalb RG, Strittmatter SM. Molecular basis of semaphorin-mediated axon guidance. *J Neurobiol*. 2000 Aug;44(2):219-29. doi: 10.1002/1097-4695(200008)44:2<219::aid-neu11>3.0.co;2-w
- Nedivi E, Hevroni D, Naot D, Israeli D, Citri Y. Numerous candidate plasticity-related genes revealed by differential cDNA cloning. *Nature*. 1993 Jun 24;363(6431):718-22. doi: 10.1038/363718a0

- Nedivi E, Fieldust S, Theill LE, Hevron D. A set of genes expressed in response to light in the adult cerebral cortex and regulated during development. *Proc Natl Acad Sci U S A*. 1996 Mar 5;93(5):2048-53. doi: 10.1073/pnas.93.5.2048
- Nedivi E, Wu GY, Cline HT. Promotion of dendritic growth by CPG15, an activity-induced signaling molecule. *Science*. 1998 Sep 18;281(5384):1863-6. doi: 10.1126/science.281.5384.1863
- Neveian T, Sakmann B. Single spine Ca²⁺ signals evoked by coincident EPSPs and backpropagating action potentials in spiny stellate cells of layer 4 in the juvenile rat somatosensory barrel cortex. *J Neurosci*. 2004 Feb 18;24(7):1689-99. doi: 10.1523/JNEUROSCI.3332-03.2004
- Nong Y, Huang YQ, Ju W, Kalia LV, Ahmadian G, Wang YT, Salter MW. Glycine binding primes NMDA receptor internalization. *Nature*. 2003 Mar 20;422(6929):302-7. doi: 10.1038/nature01497
- Nowak, L., Bregestovski, P., Ascher, P., and Herbet, A. (1984). Magnesium gates glutamate-activated channels in mouse central neurones. *Nature* 307, 462–465. doi: 10.1038/307462a0
- O'Rourke NA, Fraser SE. Dynamic changes in optic fiber terminal arbors lead to retinotopic map formation: an in vivo confocal microscopic study. *Neuron*. 1990 Aug;5(2):159-71. doi: 10.1016/0896-6273(90)90306-z
- Paoletti P, Bellone C, Zhou Q. NMDA receptor subunit diversity: impact on receptor properties, synaptic plasticity and disease. *Nat Rev Neurosci*. 2013 Jun;14(6):383-400. doi: 10.1038/nrn3504
- Papadia S, Soriano FX, Léveillé F, Martel MA, Dakin KA, Hansen HH, Kaindl A, Sifringer M, Fowler J, Stefovská V, McKenzie G, Craigon M, Corriveau R, Ghazal P, Horsburgh K, Yankner BA, Wyllie DJ, Ikonomidou C, Hardingham GE. Synaptic NMDA receptor activity boosts intrinsic antioxidant defenses. *Nat Neurosci*. 2008 Apr;11(4):476-87. doi: 10.1038/nn2071
- Papouin T, Ladépêche L, Ruel J, Sacchi S, Labasque M, Hanini M, Groc L, Pollegioni L, Mothet JP, Oliet SH. Synaptic and extrasynaptic NMDA receptors are gated by different endogenous coagonists. *Cell*. 2012 Aug 3;150(3):633-46. doi: 10.1016/j.cell.2012.06.029
- Patterson SL, Abel T, Deuel TA, Martin KC, Rose JC, Kandel ER. Recombinant BDNF rescues deficits in basal synaptic transmission and hippocampal LTP in BDNF knockout mice. *Neuron*. 1996 Jun;16(6):1137-45. doi: 10.1016/s0896-6273(00)80140-3
- Patterson SL, Grover LM, Schwartzkroin PA, Bothwell M. Neurotrophin expression in rat hippocampal slices: a stimulus paradigm inducing LTP in CA1 evokes increases in BDNF and NT-3 mRNAs. *Neuron*. 1992 Dec;9(6):1081-8. doi: 10.1016/0896-6273(92)90067-n

- Qian Z, Gilbert ME, Colicos MA, Kandel ER, Kuhl D. Tissue-plasminogen activator is induced as an immediate-early gene during seizure, kindling and long-term potentiation. *Nature*. 1993 Feb 4;361(6411):453-7. doi: 10.1038/361453a0
- Rahman TN, Munz M, Kutsarova E, Bilash OM, Ruthazer ES. Stentian structural plasticity in the developing visual system. *Proc Natl Acad Sci U S A*. 2020 May 19;117(20):10636-10638. doi: 10.1073/pnas.2001107117
- Ramoas AS, Mower AF, Liao D, Jafri SI. Suppression of cortical NMDA receptor function prevents development of orientation selectivity in the primary visual cortex. *J Neurosci*. 2001 Jun 15;21(12):4299-309. doi: 10.1523/JNEUROSCI.21-12-04299.2001
- Rashid T, Upton AL, Blentic A, Ciossek T, Knöll B, Thompson ID, Drescher U. Opposing gradients of ephrin-As and EphA7 in the superior colliculus are essential for topographic mapping in the mammalian visual system. *Neuron*. 2005 Jul 7;47(1):57-69. doi: 10.1016/j.neuron.2005.05.030
- Reber, M., Burrola, P., and Lemke, G. (2004). A relative signalling model for the formation of a topographic neural map. *Nature* 431, 847–853. doi: 10.1038/nature02957
- Reh TA, Constantine-Paton M. Eye-specific segregation requires neural activity in three-eyed *Rana pipiens*. *J Neurosci*. 1985 May;5(5):1132-43. doi: 10.1523/JNEUROSCI.05-05-01132.1985
- Roche KW, Standley S, McCallum J, Dune Ly C, Ehlers MD, Wenthold RJ. Molecular determinants of NMDA receptor internalization. *Nat Neurosci*. 2001 Aug;4(8):794-802. doi: 10.1038/90498
- Ruthazer ES, Akerman CJ, Cline HT. Control of axon branch dynamics by correlated activity in vivo. *Science*. 2003 Jul 4;301(5629):66-70. doi: 10.1126/science.1082545
- Saffen DW, Cole AJ, Worley PF, Christy BA, Ryder K, Baraban JM. Convulsant-induced increase in transcription factor messenger RNAs in rat brain. *Proc Natl Acad Sci U S A*. 1988 Oct;85(20):7795-9. doi: 10.1073/pnas.85.20.7795
- Sagar SM, Sharp FR, Curran T. Expression of c-fos protein in brain: metabolic mapping at the cellular level. *Science*. 1988 Jun 3;240(4857):1328-31. doi: 10.1126/science.3131879
- Sakaguchi DS, Murphey RK. Map formation in the developing *Xenopus* retinotectal system: an examination of ganglion cell terminal arborizations. *J Neurosci*. 1985 Dec;5(12):3228-45. doi: 10.1523/JNEUROSCI.05-12-03228.1985
- Sasabe J, Chiba T, Yamada M, Okamoto K, Nishimoto I, Matsuoka M, Aiso S. D-serine is a key determinant of glutamate toxicity in amyotrophic lateral sclerosis. *EMBO J*. 2007 Sep 19;26(18):4149-59. doi: 10.1038/sj.emboj.7601840

- Saxton RA, Sabatini DM. mTOR Signaling in Growth, Metabolism, and Disease. *Cell*. 2017 Apr 6;169(2):361-371. doi: 10.1016/j.cell.2017.03.035
- Schell MJ, Molliver ME, Snyder SH. D-serine, an endogenous synaptic modulator: localization to astrocytes and glutamate-stimulated release. *Proc Natl Acad Sci U S A*. 1995 Apr 25;92(9):3948-52. doi: 10.1073/pnas.92.9.3948
- Schlomann U, Schwamborn JC, Müller M, Fässler R, Püschel AW. The stimulation of dendrite growth by Sema3A requires integrin engagement and focal adhesion kinase. *J Cell Sci*. 2009 Jun 15;122(Pt 12):2034-42. doi: 10.1242/jcs.038232
- Schmidt, J. T., and Easter, S. S. (1978). Independent biaxial reorganization of the retinotectal projection: a reassessment. *Exp. Brain Res*. 31, 155–162. doi: 10.1007/bf00237596
- Schmidt JT, Edwards DL. Activity sharpens the map during the regeneration of the retinotectal projection in goldfish. *Brain Res*. 1983 Jun 13;269(1):29-39. doi: 10.1016/0006-8993(83)90959-9
- Schwartz N, Schohl A, Ruthazer ES. Neural activity regulates synaptic properties and dendritic structure in vivo through calcineurin/NFAT signaling. *Neuron*. 2009 Jun 11;62(5):655-69. doi: 10.1016/j.neuron.2009.05.007
- Shamah SM, Lin MZ, Goldberg JL, Estrach S, Sahin M, Hu L, Bazalakova M, Neve RL, Corfas G, Debant A, Greenberg ME. EphA receptors regulate growth cone dynamics through the novel guanine nucleotide exchange factor ephexin. *Cell*. 2001 Apr 20;105(2):233-44. doi: 10.1016/s0092-8674(01)00314-2
- Sheng M, Greenberg ME. The regulation and function of c-fos and other immediate early genes in the nervous system. *Neuron*. 1990 Apr;4(4):477-85. doi: 10.1016/0896-6273(90)90106-p
- Shi SH, Hayashi Y, Petralia RS, Zaman SH, Wenthold RJ, Svoboda K, Malinow R. Rapid spine delivery and redistribution of AMPA receptors after synaptic NMDA receptor activation. *Science*. 1999 Jun 11;284(5421):1811-6. doi: 10.1126/science.284.5421.1811
- Shipton OA, Paulsen O. GluN2A and GluN2B subunit-containing NMDA receptors in hippocampal plasticity. *Philos Trans R Soc Lond B Biol Sci*. 2013 Dec 2;369(1633):20130163. doi: 10.1098/rstb.2013.0163
- Sild M, Van Horn MR. Astrocytes use a novel transporter to fill gliotransmitter vesicles with D-serine: evidence for vesicular synergy. *J Neurosci*. 2013 Jun 19;33(25):10193-4. doi: 10.1523/JNEUROSCI.1665-13.2013
- Silva AJ, Kogan JH, Frankland PW, Kida S. CREB and memory. *Annu Rev Neurosci*. 1998;21:127-48. doi: 10.1146/annurev.neuro.21.1.127

- Sperry, R. W. (1943). Effect of 180 degree rotation of the retinal field on visuomotor coordination. *J. Exp. Zool.* 92, 263–279. doi: 10.1002/jez.1400920303
- Sperry, R. W. (1963). Chemoaffinity in the orderly growth of nerve fiber patterns and connections. *Proc. Natl. Acad. Sci. U S A* 50, 703–710. doi: 10.1073/pnas.50.4.703
- Spiegel I, Mardinly AR, Gabel HW, Bazinet JE, Couch CH, Tzeng CP, Harmin DA, Greenberg ME. Npas4 regulates excitatory-inhibitory balance within neural circuits through cell-type-specific gene programs. *Cell.* 2014 May 22;157(5):1216-29. doi: 10.1016/j.cell.2014.03.058
- Steigerwald F, Schulz TW, Schenker LT, Kennedy MB, Seeburg PH, Köhr G. C-Terminal truncation of NR2A subunits impairs synaptic but not extrasynaptic localization of NMDA receptors. *J Neurosci.* 2000 Jun 15;20(12):4573-81. doi: 10.1523/JNEUROSCI.20-12-04573.2000
- Stornetta RL, Zhu JJ. Ras and Rap signaling in synaptic plasticity and mental disorders. *Neuroscientist.* 2011 Feb;17(1):54-78. doi: 10.1177/1073858410365562
- Suetterlin P, Drescher U. Target-independent ephrina/EphA-mediated axon-axon repulsion as a novel element in retinocollicular mapping. *Neuron.* 2014 Nov 19;84(4):740-52. doi: 10.1016/j.neuron.2014.09.023
- Tabuchi A. Synaptic plasticity-regulated gene expression: a key event in the long-lasting changes of neuronal function. *Biol Pharm Bull.* 2008 Mar;31(3):327-35. doi: 10.1248/bpb.31.327
- Tao X, Finkbeiner S, Arnold DB, Shaywitz AJ, Greenberg ME. Ca²⁺ influx regulates BDNF transcription by a CREB family transcription factor-dependent mechanism. *Neuron.* 1998 Apr;20(4):709-26. doi: 10.1016/s0896-6273(00)81010-7
- Uziel D, Garcez P, Lent R, Peuckert C, Niehage R, Weth F, Bolz J. Connecting thalamus and cortex: the role of ephrins. *Anat Rec A Discov Mol Cell Evol Biol.* 2006 Feb;288(2):135-42. doi: 10.1002/ar.a.20286
- Van Dongen AM, editor. *Biology of the NMDA Receptor.* Boca Raton (FL): CRC Press/Taylor & Francis; 2009.
- Van Horn MR, Sild M, Ruthazer ES. D-serine as a gliotransmitter and its roles in brain development and disease. *Front Cell Neurosci.* 2013 Apr 23;7:39. doi: 10.3389/fncel.2013.00039
- Van Horn MR, Strasser A, Miraucourt LS, Pollegioni L, Ruthazer ES. The Gliotransmitter d-Serine Promotes Synapse Maturation and Axonal Stabilization In Vivo. *J Neurosci.* 2017 Jun 28;37(26):6277-6288. doi: 10.1523/JNEUROSCI.3158-16.2017

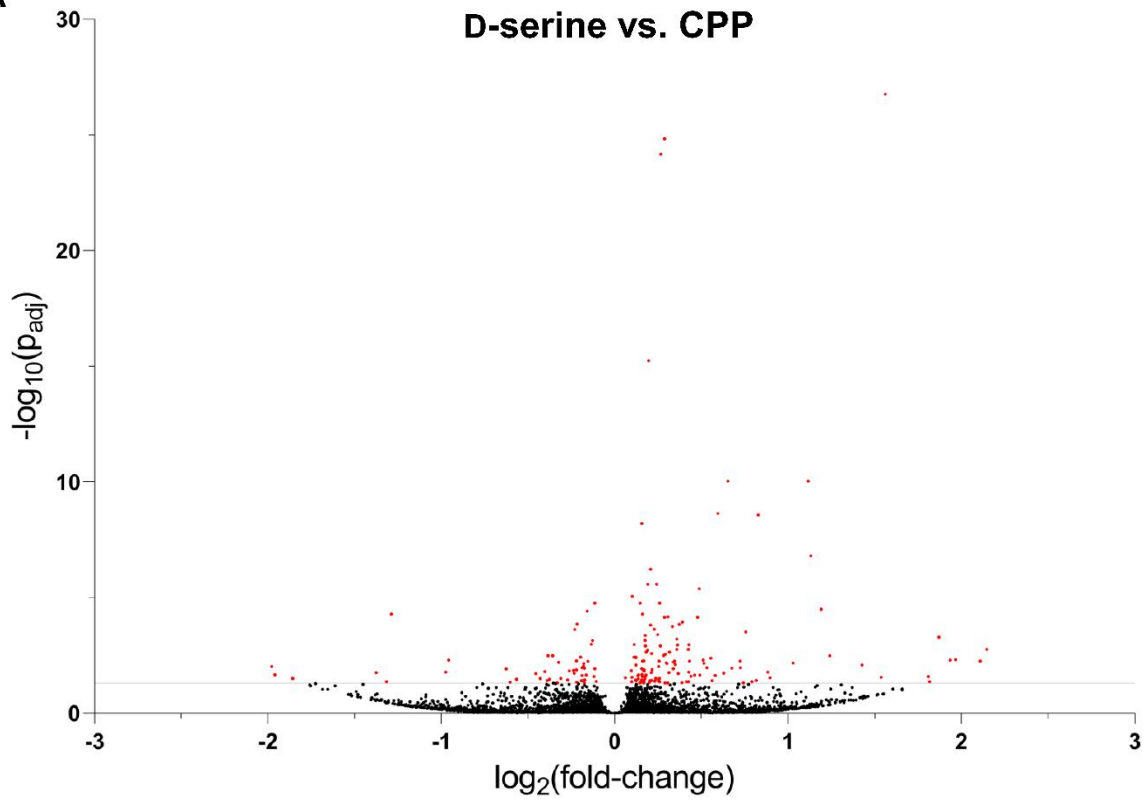
- Volianskis A, France G, Jensen MS, Bortolotto ZA, Jane DE, Collingridge GL. Long-term potentiation and the role of N-methyl-D-aspartate receptors. *Brain Res.* 2015 Sep 24;1621:5-16. doi: 10.1016/j.brainres.2015.01.016
- Volk L, Chiu SL, Sharma K, Huganir RL. Glutamate synapses in human cognitive disorders. *Annu Rev Neurosci.* 2015 Jul 8;38:127-49. doi: 10.1146/annurev-neuro-071714-033821
- von Engelhardt J, Coserea I, Pawlak V, Fuchs EC, Köhr G, Seeburg PH, Monyer H. Excitotoxicity in vitro by NR2A- and NR2B-containing NMDA receptors. *Neuropharmacology.* 2007 Jul;53(1):10-7. doi: 10.1016/j.neuropharm.2007.04.015
- Walter J, Henke-Fahle S, Bonhoeffer F. Avoidance of posterior tectal membranes by temporal retinal axons. *Development.* 1987a Dec;101(4):909-13
- Walter J, Kern-Veits B, Huf J, Stolze B, Bonhoeffer F. Recognition of position-specific properties of tectal cell membranes by retinal axons in vitro. *Development.* 1987b Dec;101(4):685-96.
- Wang JH, Feng DP. Postsynaptic protein kinase C essential to induction and maintenance of long-term potentiation in the hippocampal CA1 region. *Proc Natl Acad Sci U S A.* 1992 Apr 1;89(7):2576-80. doi: 10.1073/pnas.89.7.2576
- Wang CC, Held RG, Chang SC, Yang L, Delpire E, Ghosh A, Hall BJ. A critical role for GluN2B-containing NMDA receptors in cortical development and function. *Neuron.* 2011 Dec 8;72(5):789-805. doi: 10.1016/j.neuron.2011.09.023
- West AE, Chen WG, Dalva MB, Dolmetsch RE, Kornhauser JM, Shaywitz AJ, Takasu MA, Tao X, Greenberg ME. Calcium regulation of neuronal gene expression. *Proc Natl Acad Sci U S A.* 2001 Sep 25;98(20):11024-31. doi: 10.1073/pnas.191352298
- Wiesel TN. Postnatal development of the visual cortex and the influence of environment. *Nature.* 1982 Oct 14;299(5884):583-91. doi: 10.1038/299583a0
- Wigström H, Gustafsson B. Postsynaptic control of hippocampal long-term potentiation. *J Physiol (Paris).* 1986;81(4):228-36
- Wolosker H. NMDA receptor regulation by D-serine: new findings and perspectives. *Mol Neurobiol.* 2007 Oct;36(2):152-64. doi: 10.1007/s12035-007-0038-6
- Wolosker H. Serine racemase and the serine shuttle between neurons and astrocytes. *Biochim Biophys Acta.* 2011 Nov;1814(11):1558-66. doi: 10.1016/j.bbapap.2011.01.001
- Wolosker H, Radzishevsky I. The serine shuttle between glia and neurons: implications for neurotransmission and neurodegeneration. *Biochem Soc Trans.* 2013 Dec;41(6):1546-50. doi: 10.1042/BST20130220

- Wolosker H, Balu DT, Coyle JT. The Rise and Fall of the d-Serine-Mediated Gliotransmission Hypothesis. *Trends Neurosci.* 2016 Nov;39(11):712-721. doi: 10.1016/j.tins.2016.09.007
- Wolosker H, Balu DT. D-Serine as the gatekeeper of NMDA receptor activity: implications for the pharmacologic management of anxiety disorders. *Transl Psychiatry.* 2020 Jun 9;10(1):184. doi: 10.1038/s41398-020-00870-x
- Wong RO, Meister M, Shatz CJ. Transient period of correlated bursting activity during development of the mammalian retina. *Neuron.* 1993 Nov;11(5):923-38. doi: 10.1016/0896-6273(93)90122-8
- Wu GY, Deisseroth K, Tsien RW. Activity-dependent CREB phosphorylation: convergence of a fast, sensitive calmodulin kinase pathway and a slow, less sensitive mitogen-activated protein kinase pathway. *Proc Natl Acad Sci U S A.* 2001 Feb 27;98(5):2808-13. doi: 10.1073/pnas.051634198
- Wu G, Malinow R, Cline HT. Maturation of a central glutamatergic synapse. *Science.* 1996 Nov 8;274(5289):972-6. doi: 10.1126/science.274.5289.972
- Xing J, Ginty DD, Greenberg ME. Coupling of the RAS-MAPK pathway to gene activation by RSK2, a growth factor-regulated CREB kinase. *Science.* 1996 Aug 16;273(5277):959-63. doi: 10.1126/science.273.5277.959
- Yap EL, Greenberg ME. Activity-Regulated Transcription: Bridging the Gap between Neural Activity and Behavior. *Neuron.* 2018 Oct 24;100(2):330-348. doi: 10.1016/j.neuron.2018.10.013
- Yang T, Davis RJ, Chow CW. Requirement of two NFATc4 transactivation domains for CBP potentiation. *J Biol Chem.* 2001 Oct 26;276(43):39569-76. doi: 10.1074/jbc.M102961200
- Yang Y, Ge W, Chen Y, Zhang Z, Shen W, Wu C, Poo M, Duan S. Contribution of astrocytes to hippocampal long-term potentiation through release of D-serine. *Proc Natl Acad Sci U S A.* 2003 Dec 9;100(25):15194-9. doi: 10.1073/pnas.2431073100
- Zafra F, Hengerer B, Leibrock J, Thoenen H, Lindholm D. Activity dependent regulation of BDNF and NGF mRNAs in the rat hippocampus is mediated by non-NMDA glutamate receptors. *EMBO J.* 1990 Nov;9(11):3545-50
- Zafra F, Castrén E, Thoenen H, Lindholm D. Interplay between glutamate and gamma-aminobutyric acid transmitter systems in the physiological regulation of brain-derived neurotrophic factor and nerve growth factor synthesis in hippocampal neurons. *Proc Natl Acad Sci U S A.* 1991 Nov 15;88(22):10037-41. doi: 10.1073/pnas.88.22.10037
- Zaia KA, Reimer RJ. Synaptic Vesicle Protein NTT4/XT1 (SLC6A17) Catalyzes Na⁺-coupled Neutral Amino Acid Transport. *J Biol Chem.* 2009 Mar 27;284(13):8439-48. doi: 10.1074/jbc.M806407200

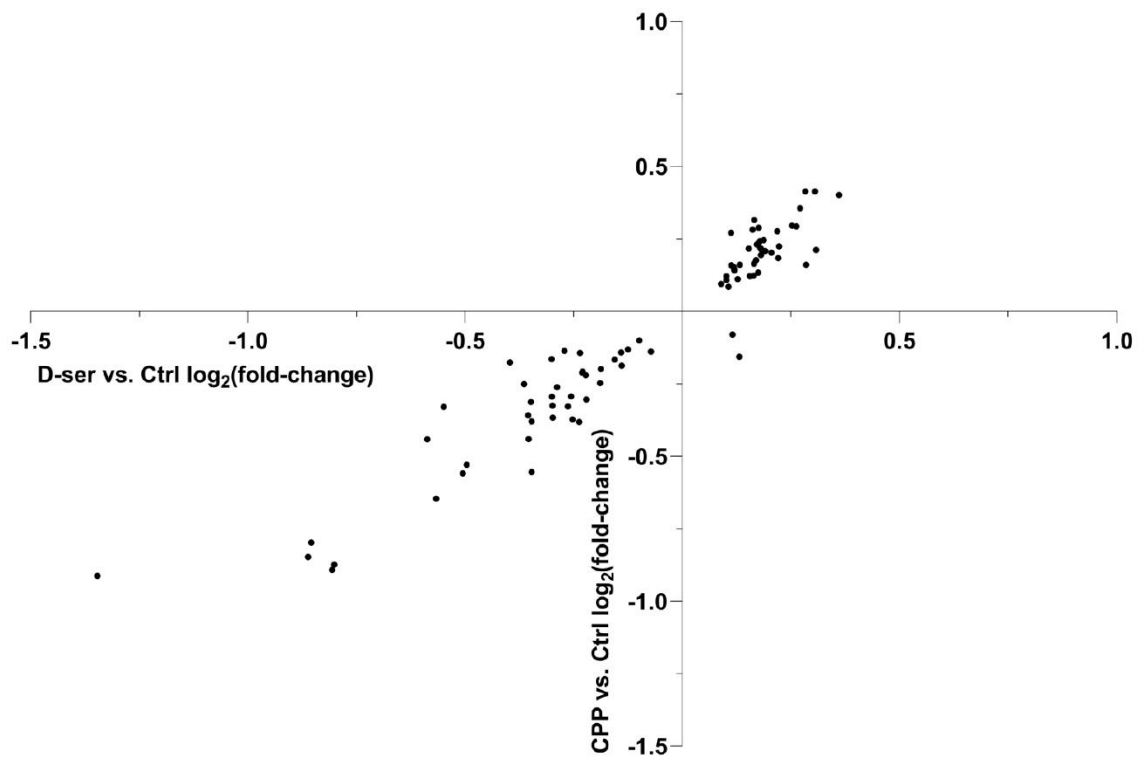
- Zhang SJ, Steijaert MN, Lau D, Schütz G, Delucinge-Vivier C, Descombes P, Bading H. Decoding NMDA receptor signaling: identification of genomic programs specifying neuronal survival and death. *Neuron*. 2007 Feb 15;53(4):549-62. doi: 10.1016/j.neuron.2007.01.025
- Zhang L, Zhang P, Wang G, Zhang H, Zhang Y, Yu Y, Zhang M, Xiao J, Crespo P, Hell JW, Lin L, Haganir RL, Zhu JJ. Ras and Rap Signal Bidirectional Synaptic Plasticity via Distinct Subcellular Microdomains. *Neuron*. 2018 May 16;98(4):783-800.e4. doi: 10.1016/j.neuron.2018.03.049
- Zhao JP, Constantine-Paton M. NR2A^{-/-} mice lack long-term potentiation but retain NMDA receptor and L-type Ca²⁺ channel-dependent long-term depression in the juvenile superior colliculus. *J Neurosci*. 2007 Dec 12;27(50):13649-54. doi: 10.1523/JNEUROSCI.3153-07.2007
- Zhou Y, Takahashi E, Li W, Halt A, Wiltgen B, Ehninger D, Li GD, Hell JW, Kennedy MB, Silva AJ. Interactions between the NR2B receptor and CaMKII modulate synaptic plasticity and spatial learning. *J Neurosci*. 2007 Dec 12;27(50):13843-53. doi: 10.1523/JNEUROSCI.4486-07.2007
- Zhu JJ, Qin Y, Zhao M, Van Aelst L, Malinow R. Ras and Rap control AMPA receptor trafficking during synaptic plasticity. *Cell*. 2002 Aug 23;110(4):443-55. doi: 10.1016/s0092-8674(02)00897-8
- Zou DJ, Cline HT. Expression of constitutively active CaMKII in target tissue modifies presynaptic axon arbor growth. *Neuron*. 1996 Mar;16(3):529-39. doi: 10.1016/s0896-6273(00)80072-0

Appendix

A



B



↑ **Supplementary Figure 1. Relationships between treatment-induced gene expression in primary dataset.** (A) DGE analysis of D-serine vs. CPP rearing conditions. Each point corresponds to a gene. 183 genes in red were significantly more or less abundant in one treatment condition compared to the other and were thus differentially expressed. For example, genes with a positive \log_2 fold-change reflect a transcript that was more abundant in the D-serine condition than in the CPP condition. (B) Genes that were coregulated in response to D-serine and CPP treatment ($n = 83$ genes) displayed a striking positive linear relationship when plotted according to their corresponding \log_2 fold-changes ($R^2 = 0.91$). Genes residing in quadrants 1 or 3 were coregulated by D-serine and CPP, and genes positioned in quadrant 2 were anti-regulated by D-serine and CPP. These data reveal an unexpected degree of coregulation of gene products downstream of both putative NMDAR augmentation and blockade and suggest the convergence onto a subset of effectors, whether in signaling pathways or directly in the nucleus, that control the expression of one or multiple gene programs. Notably, however, coregulated genes did not constitute majorities of the genes that were regulated in response to either rearing condition on their own, but the percentages are nonetheless striking: 23.8% and 29.3% of D-serine regulated genes and CPP-regulated genes, respectively, were coregulated by both treatments.

↓ **Supplementary Figure 2. Comprehensive list of differentially expressed genes from batch-effects-removed RNA-seq dataset.** (A) D-serine-regulated genes ($n = 698$), e.g., DGE analysis of D-serine reared samples vs. Control reared samples. (B) CPP-regulated genes ($n = 558$), e.g., DGE analysis of CPP reared samples vs. Control reared samples. (C) Genes coregulated by D-serine and CPP rearing ($n = 182$). Rearing occurred for 24 hours prior to brain mRNA extraction and RNA-sequencing. DGE analysis was performed using DESeq2 software (Love et al., 2014) via Galaxy Project (Jalili et al., 2020). DGE evaluated based on \log_2 fold-change and adjusted p-value. The number of genes in A, B, and C more than double the number of genes identified in corresponding lists from the primary dataset.

A

D-serine vs. Control		
GeneID	log2fc	p-adj
abat.S	-0.27	3.30E-22
LOC108714009	1.20	7.27E-20
rasgrp3.S	1.01	1.13E-17
mgea5.S	-0.40	2.54E-15
MGC68458	-0.23	1.50E-14
coch.L	-0.55	2.14E-12
LOC108717474	0.58	5.96E-12
znf207.S	0.29	1.83E-11
Xelaev18009926m	-1.66	4.22E-11
slc43a2.S	-0.36	1.06E-10
atp1b1.L	-0.35	1.07E-10
ctc4.L	0.31	3.24E-10
slc43a2.L	-0.30	4.41E-10
tcp1.L	0.17	4.41E-10
LOC108716042	-1.37	1.23E-09
theg-like.S	-1.40	1.23E-09
elovf1.L	-2.44	5.15E-09
shmt2.L	0.18	1.14E-08
azin1.L	-0.27	2.56E-08
them6.L	0.31	2.63E-08
angptl4.L	-0.30	2.64E-08
fam198a.L	-0.36	6.93E-08
glul-like.1.S	-0.25	7.84E-08
slc38a4.L	-0.45	1.27E-07
LOC108714210	0.11	1.39E-07
raif	0.12	1.82E-07
eif2b3.L	0.19	1.95E-07
slc16a6.L	-0.58	2.13E-07
ca2.S	-0.81	2.37E-07
nfe2l2.L	-0.29	2.83E-07
prkch.L	0.79	3.48E-07
diras2.L	0.25	3.84E-07
saib.S	0.14	4.15E-07
tmem163.L	0.13	6.11E-07
LOC108719218	-0.35	6.44E-07
colec12.L	-0.31	6.49E-07
nop2.L	0.31	7.67E-07
steap3.L	0.49	9.55E-07
dhx15.L	0.18	1.08E-06
znf326.S	0.13	1.21E-06
gpcpd1.L	-0.25	1.21E-06
srsf3.S	0.09	1.38E-06
LOC108705068	-1.33	1.40E-06
slc26a9.S	-1.32	1.60E-06
LOC108703254	0.45	1.83E-06
slc6a13.L	-0.33	2.43E-06
ccdc63.S	-0.47	2.43E-06
ache.S	-0.22	2.73E-06
LOC108718338	-0.68	3.22E-06
bud31.L	0.22	3.63E-06
fbxw9.S	0.21	3.91E-06
snu13.L	0.29	6.13E-06
olmf4.L	-1.07	6.17E-06
slc26a9.L	-1.13	6.71E-06
LOC108701401	0.39	9.31E-06
Xelaev18016982m	-0.19	1.15E-05
mtdh.L	0.08	1.18E-05
rprm.S	0.33	1.25E-05
tgfb3.S	-0.40	1.35E-05
LOC108700399	0.16	1.53E-05
serinc1.S	-0.15	1.57E-05
osr1.L	-0.59	1.81E-05
gpr153.L	0.16	1.81E-05
papss1.L	-0.26	2.08E-05
btf34.S	0.14	2.14E-05
psma5.S	0.16	2.17E-05
eif5.L	0.21	2.29E-05
canx.S	0.12	2.46E-05
cnbp.S	0.16	2.53E-05
aurka.S	0.22	2.96E-05
mgea5.L	-0.14	3.25E-05
tfcp2l1.S	-0.59	3.50E-05
pamr1.S	-0.87	3.75E-05
hspa8.S	0.15	4.44E-05
mf34.L	0.20	5.46E-05
p2ry1.L	0.24	5.77E-05
nde1.S	0.12	5.77E-05
pthid1.L	0.24	5.81E-05
glul-like.1.L	-0.29	7.05E-05
olmf2a.L	-0.25	7.35E-05
sec11c.L	0.16	7.85E-05
kcnk3.S	-0.39	8.06E-05
stip1.L	0.21	8.30E-05
ctc2.S	0.15	9.50E-05
snu13.S	0.26	9.50E-05
mf2.S	0.12	9.73E-05
psmb4.S	0.19	0.0001016

B

CPP vs. Control		
GeneID	log2fc	p-adj
rrp12.S	0.27	4.81E-19
shmt2.L	0.24	5.60E-13
slc6a17.S	-0.19	7.10E-13
grik5-like.1.L	-0.17	3.97E-12
LOC108718126	-0.41	2.59E-11
snu13.L	0.42	3.32E-10
nop2.L	0.42	3.72E-10
LOC108709985	-0.14	8.45E-09
glul-like.1.S	-0.29	3.22E-08
utp4.L	0.32	6.86E-08
nup155.L	0.16	1.73E-07
prmt1.S	0.22	2.56E-07
tmem163.L	-0.16	2.72E-07
ca2.S	-0.90	3.93E-07
atp1b1.L	-0.31	1.12E-06
aurka.S	0.28	1.12E-06
mhp.S	-0.43	1.19E-06
aimf3.L	-0.56	1.27E-06
mt4.L	-1.00	1.52E-06
gpx3.S	-0.34	1.95E-06
nolc1.L	0.28	2.26E-06
angptl4.L	-0.29	2.48E-06
LOC108707066	-0.40	2.69E-06
mife8.L	-0.38	4.56E-06
apoc1-like.L	-0.43	5.17E-06
nde1.S	0.15	6.22E-06
lhb.S	-0.23	6.42E-06
fa2h.L	-0.97	7.73E-06
srsf3.S	0.10	8.58E-06
nip7.L	0.29	8.98E-06
nfatc3.S	0.23	8.98E-06
npdc1.2.S	-0.46	8.98E-06
grik5-like.1.S	-0.15	9.85E-06
LOC108719218	-0.36	1.25E-05
gart.L	0.25	2.01E-05
LOC108698872	-0.37	2.01E-05
cdc14a.L	0.25	2.54E-05
prelp.S	-0.30	3.25E-05
syt13-like.S	-0.31	3.59E-05
snu13.S	0.30	3.84E-05
serinc1.S	-0.16	5.30E-05
apbb3.L	-0.20	6.66E-05
farsb.L	0.25	6.66E-05
mhp.L	-0.36	6.66E-05
ache.S	-0.22	7.20E-05
kpna2.S	0.18	7.20E-05
srsf10.S	0.16	8.91E-05
proca1.L	-0.37	0.0001192
ddx39	0.16	0.0001296
ncl.S	0.14	0.0001706
sst.S	-0.25	0.0001846
tcp1.L	0.12	0.0001938
ankrd9.L	-0.42	0.0002352
snap25.S	-0.18	0.0002397
LOC108704964	-0.26	0.0002409
camk2d.L	-0.15	0.0002513
tmpo.L	0.14	0.0002513
fyxd7.L	-0.34	0.0003024
abat.S	-0.13	0.0003101
trmt6.L	0.35	0.0003505
Xelaev18033745m	-0.20	0.0003505
dio2.L	0.15	0.0003505
wipf3-like.L	-0.36	0.0003653
plp1.L	-0.60	0.0003742
MGC68458	-0.14	0.0003808
vcam1.S	-0.19	0.0003882
chgb.L	-0.17	0.0003889
tac1.S	-0.31	0.0003889
rexo4.S	0.21	0.0003889
polr1a.L	0.30	0.0003923
mtfhd1.L	0.23	0.0003923
LOC108713013	-0.12	0.0004122
nat10.L	0.20	0.00042
aqp1.L	-0.30	0.00042
aqp1.S	-0.40	0.0004295
clic6.S	-0.58	0.0004387
ccb2.L	-0.59	0.0004844
slc43a2.S	-0.25	0.0004938
LOC108710196	0.24	0.0005252
sorbs3.S	0.62	0.0005252
pamr1.S	-0.86	0.0005252
ruvb1.S	0.22	0.0005355
sdha.S	-0.21	0.0005472
LOC108715402	-0.41	0.0005691
snap25.L	-0.12	0.0006044
tsr1.L	0.23	0.0006271
npdc1.2.L	-0.41	0.0006523

C

Coregulated Genes				
GeneID	D-serine vs. Ctrl		CPP vs. Ctrl	
	log2fc	p-adj	log2fc	p-adj
abat.S	-0.27	3.296E-22	-0.13	0.0003101
ache.L	-0.14	0.0205505	-0.18	0.0037041
ache.S	-0.22	2.726E-06	-0.22	7.202E-05
acta2.S	-0.28	0.026787	-0.37	0.0059918
ahcy.L	0.13	0.0173946	0.17	0.0038929
aifm3.L	-0.35	0.0025901	-0.56	1.269E-06
angptl4.L	-0.30	2.64E-08	-0.29	2.476E-06
ankrd13a.S	0.11	0.0384082	0.14	0.020217
ankrd9.L	0.24	0.0407662	-0.42	0.0002352
aqp1.L	-0.22	0.0081778	-0.30	0.00042
aqp1.S	-0.25	0.0287663	-0.40	0.0004295
atp1b1.L	-0.35	1.069E-10	-0.31	1.124E-06
atp1b1.S	-0.18	0.0222958	-0.20	0.0238913
aurka.S	0.22	2.959E-05	0.28	1.124E-06
bmp3.L	-0.28	0.0004416	-0.21	0.0454195
btg1.L	-0.09	0.0393313	-0.13	0.0014709
bud31.L	0.22	3.625E-06	0.19	0.0018896
ca2.S	-0.81	2.372E-07	-0.90	3.933E-07
caacna1f.L	0.43	0.0160395	0.54	0.0033227
cacybp.S	0.16	0.0175199	0.22	0.0017055
ctc4.L	0.31	3.236E-10	0.21	0.0007755
cct6a.L	0.10	0.0237507	0.11	0.0359606
cdk11b.S	0.17	0.0020364	0.16	0.0180283
cmpk1.S	0.14	0.0088672	0.13	0.0377424
cnbp.S	0.16	2.525E-05	0.12	0.0088065
coch.L	-0.55	2.145E-12	-0.33	0.0011232
cpt1b.L	-0.50	0.0130017	-0.53	0.0183493
crnk1.S	0.14	0.015364	0.14	0.0345881
csnk2a2.S	0.10	0.0028475	0.11	0.0054249
cwc15.S	0.13	0.0178244	0.13	0.0400238
ddx39	0.12	0.0046543	0.16	0.0001296
ddx47.L	0.19	0.0009188	0.21	0.0012366
dennd6b.L	-0.10	0.0004416	-0.10	0.0019603
dhx15.L	0.18	1.084E-06	0.14	0.0032602
dmrt2.L	0.18	0.0071902	0.17	0.0285239
dnttp2.L	0.15	0.0108521	0.15	0.0219818
ecm1.L	-1.05	0.0219439	-1.06	0.0428686
eif3a.L	0.08	0.0463438	0.12	0.0059242
eif6.L	0.16	0.0410005	0.19	0.0183493
epm2a.L	-0.50	0.0005876	-0.45	0.009531
fam102b.S	-0.31	0.0010334	-0.26	0.0249046
fam110b.S	-0.13	0.0387226	-0.20	0.0011749
fam163b.L	0.10	0.0232415	-0.11	0.0180283
fam198a.L	-0.36	6.927E-08	-0.21	0.0248064
farsa.S	0.18	0.0272499	0.22	0.0092347
fbx9.L	-0.11	0.0163802	-0.11	0.0372786
fcn1.S	-0.81	0.0011478	-0.89	0.0015102
fkbp2.S	0.17	0.013817	0.22	0.0018192
fstl5.S	-0.12	0.0004628	-0.13	0.0011749
gart.S	0.23	0.0217134	0.29	0.0054315
gart.L	0.19	0.0006076	0.25	2.006E-05
gdpd5.S	-0.14	0.0407906	-0.18	0.0115367
glul-like.1.L	-0.29	7.045E-05	-0.26	0.0028745
glul-like.1.S	-0.25	7.841E-08	-0.29	3.217E-08
gpn1.L	0.13	0.0288917	0.14	0.0349452
grp.L	-0.33	0.0238471	-0.50	0.0007296
gltf2.S	0.14	0.0308938	0.19	0.0032042
gucy1b3.S	-0.08	0.0454542	-0.10	0.0209001
haha1.L	0.15	0.0131966	0.14	0.0489087
hnmpab.L	0.14	0.0121514	0.14	0.0256637
hnmpk.L	0.06	0.0075424	0.06	0.0363232
hsp11.S	0.21	0.0001056	0.16	0.0234234
kcnk3.S	-0.39	8.056E-05	-0.27	0.0465099
kons2.L	-0.20	0.0216135	-0.29	0.0016049
kif11.S	0.15	0.0245667	0.19	0.0060069
krt8.S	-0.21	0.0068029	-0.20	0.0265291
LOC108698540	-0.34	0.0117142	-0.33	0.0404407
LOC108698597	-0.30	0.0037762	-0.27	0.0306768
LOC108698872	-0.25	0.0033722	-0.37	2.006E-05
LOC108699803	0.11	0.0414512	0.13	0.0377424
LOC108700399	0.16	1.527E-05	0.12	0.0078945
LOC108701106	-0.66	0.0023742	-0.60	0.0205634
LOC108702925	0.14	0.0045057	0.13	0.0337264
LOC108704340	-0.44	0.0355467	-0.54	0.0179088
LOC108707047	0.14	0.0013945	0.11	0.0408583
LOC108709207	-0.19	0.0022599	-0.20	0.0039762
LOC108709985	-0.07	0.0054058	-0.14	8.448E-09
LOC108710196	0.18	0.0073557	0.24	0.0005252
LOC108711485	0.27	0.0012641	0.30	0.0011749
LOC108714204	0.38	0.0286619	0.53	0.0021334
LOC108714210	0.11	1.385E-07	0.09	0.000664
LOC108714307	-0.68	0.039998	-0.77	0.0391506
LOC108715624	-0.11	0.0298885	-0.14	0.0080385
LOC108716040	0.76	0.0019886	0.62	0.0402158
LOC108716042	-1.37	1.228E-09	-0.93	0.0012366
LOC108716057	0.13	0.0244148	0.14	0.03283
LOC108717444	-0.23	0.0004473	-0.21	0.0080366

plaa.L	0.14	0.0001056	LOC108714210	0.09	0.000664	LOC108718667	0.30	0.0130017	0.30	0.0285239
hsp11.S	0.21	0.0001056	grp.L	-0.50	0.0007296	LOC108719218	-0.35	6.439E-07	-0.36	1.249E-05
prmt1.S	0.15	0.0001062	ctc4.L	0.21	0.0007755	lsm12.L	0.13	0.0161327	0.13	0.0381604
tial1.L	0.13	0.0001081	LOC100137691	-0.35	0.0007755	lsm3.L	0.17	0.0141823	0.20	0.008227
prpf40a.S	0.13	0.0001309	tcn2.L	-0.37	0.0008689	mak16.L	0.23	0.0412518	0.30	0.0093612
gnb3.L	-0.59	0.0001592	vsn11.S	-0.16	0.0009467	mtge8.L	-0.24	0.0049617	-0.38	4.565E-06
LOC108711534	0.34	0.0001773	stip1.L	0.20	0.0009761	MGC68458	-0.23	1.502E-14	-0.14	0.0003808
tdrd5.L	-0.55	0.0001773	sh3gl2.L	-0.09	0.0010749	MGC84433	0.11	0.0205332	0.14	0.0048768
lman1.L	-0.28	0.0001844	rtc.b.L	0.15	0.0011232	mgea5.S	-0.40	2.536E-15	-0.17	0.0158031
atp1a1.L	-0.27	0.0001844	wdr36.L	0.26	0.0011232	mpnk2.L	-0.24	0.0326091	-0.26	0.0409317
LOC108706907	-0.18	0.0001821	coc.h.L	-0.33	0.0011232	mpdu1.L	0.13	0.0085353	0.16	0.0028745
prmt5.S	0.23	0.0002399	ranpb1.L	0.16	0.0011321	msx2.L	-0.35	0.0050233	-0.38	0.0059155
sic35b1.L	0.21	0.0003146	Xelaev18000855m	-0.65	0.0011363	mthfd1.L	0.17	0.005757	0.23	0.0003923
azin1.S	-0.29	0.0003564	nudt1.S	0.36	0.0011374	nat10.L	0.12	0.0342224	0.20	0.00042
LOC108702599	0.31	0.0003667	prmt5.L	0.20	0.0011691	ncl.S	0.12	0.0003857	0.14	0.0001706
ncl.S	0.12	0.0003857	fstf5.S	-0.13	0.0011749	nde1.S	0.12	5.767E-05	0.15	6.224E-06
src.S	0.15	0.0003857	LOC108711485	0.30	0.0011749	nelfe.S	0.10	0.0226657	0.11	0.0309556
LOC108697009	-0.34	0.0004257	fam110b.S	-0.20	0.0011749	neurod4.S	0.18	0.0064028	0.21	0.0030257
bmp3.L	-0.28	0.0004416	frmd7.L	0.50	0.0012004	nfe2l2.L	-0.29	2.827E-07	-0.18	0.0244926
dennd6b.L	-0.10	0.0004416	suc1g2.L	0.12	0.0012271	nip7.L	0.18	0.0094857	0.29	8.983E-06
LOC108717444	-0.23	0.0004473	LOC108716042	-0.93	0.0012366	nipsnap3a.S	-0.30	0.0094891	-0.32	0.0115367
fstf5.S	-0.12	0.0004628	ror.a.S	-0.39	0.0012366	nln.L	-0.10	0.0148474	-0.10	0.0347621
MGC146850.L	0.62	0.0004628	ddx47.L	0.21	0.0012366	nolc1.L	0.16	0.0090317	0.28	2.265E-06
ccdc50.L	0.29	0.0004661	pycr1.L	0.23	0.0012438	nop2.L	0.31	7.665E-07	0.42	3.724E-10
rprd1b.L	-0.14	0.0004661	vip.L	-0.33	0.001259	nudt1.S	0.27	0.0100359	0.36	0.0011374
tsc22d1.L	-0.10	0.0004714	ell3.L	-0.38	0.0012646	ola1.L	0.11	0.0464692	0.12	0.0465099
mfsd14b.S	0.12	0.0004823	prmt5.S	0.23	0.0013782	olml2a.L	-0.25	7.352E-05	-0.17	0.0382556
brd7.L	0.11	0.0004823	LOC108703389	-0.18	0.0014709	pam1.S	-0.87	3.749E-05	-0.86	0.0005252
psmb7.S	0.22	0.0005213	btg1.L	-0.13	0.0014709	pi4ka.L	-0.14	0.00201	-0.14	0.0065035
fam177a1.L	0.24	0.0005348	fcn1.S	-0.89	0.0015102	pir.L	-0.43	0.0355834	-0.60	0.0044153
slc2a12.L	-0.87	0.0005369	kcnk2.L	-0.29	0.0016049	pkn3.S	0.36	0.0049617	0.41	0.0042038
LOC108719043	-0.59	0.0005537	cacybp.S	0.22	0.0017055	polr1a.L	0.19	0.0249889	0.30	0.0003923
LOC108716135	-0.86	0.0005623	tlf2.L	0.24	0.00172	polr2e.S	0.23	0.0215902	0.25	0.0127261
epm2a.L	-0.50	0.0005876	gja7.S	0.24	0.0017395	polr3e.L	0.17	0.0050263	0.18	0.0104486
gart.L	0.19	0.0006076	LOC108698140	-0.44	0.0017694	ppan.L	0.22	0.039998	0.30	0.0054315
negr1.L	0.11	0.0006168	psap.S	-0.13	0.0017946	ppid.S	0.19	0.0309447	0.20	0.0475343
LOC108717958	0.47	0.0006168	fkbp2.S	0.22	0.0018192	prelp.S	-0.16	0.0299382	-0.30	3.254E-05
proca1.L	-0.30	0.0006607	bud31.L	0.19	0.0018896	prmt1.S	0.15	0.0001062	0.22	2.559E-07
rrp12.S	0.11	0.0006607	uimc1.L	0.25	0.0018998	prmt5.L	0.14	0.0255593	0.20	0.0011691
ddx47.L	0.19	0.0009188	wdr43.L	0.26	0.0018998	prmt5.S	0.23	0.0002399	0.23	0.0013782
LOC108702537	-0.50	0.0009563	rax.S	0.57	0.0019129	proca1.L	-0.30	0.0006607	-0.37	0.0001192
MGC86492.S	0.09	0.0009678	dennd6b.L	-0.10	0.0019603	psma3.L	0.17	0.0101516	0.15	0.0479608
scnn1a.L	-0.58	0.0009978	phyh.S	-0.20	0.0019992	psma5.S	0.16	2.167E-05	0.11	0.036781
psmb3.L	0.17	0.0009978	lhx3.L	-0.42	0.0020632	psma7.L	0.18	0.0012649	0.20	0.0022843
fam102b.S	-0.31	0.0010334	Xelaev18022528m	-0.87	0.0021059	psmd3.S	0.16	0.002411	0.13	0.0441492
pdgfra.L	-0.31	0.0010552	blmh.S	0.15	0.0021188	ralb	0.12	1.819E-07	-0.08	0.009531
Xetrov90018014m.L	0.66	0.0010997	cdc25a.L	0.24	0.0021188	rbp4.S	-0.23	0.0013741	-0.21	0.0140813
srsf2.L	0.17	0.0010997	LOC108714204	0.53	0.0021334	rrp12.S	0.11	0.0006607	0.27	4.808E-19
lipg.L	-0.52	0.0011019	ctps1.L	0.23	0.0021495	rrs1.S	0.26	0.0475005	0.36	0.0090028
LOC108712469	0.89	0.0011168	psma7.L	0.20	0.0022843	rtcb.L	0.12	0.0081383	0.15	0.0011232
fcn1.S	-0.81	0.0011478	asf1b.L	0.14	0.0023895	ruvb11.S	0.18	0.0020664	0.22	0.0005355
tat.S	-0.60	0.0012521	mcm6.2.L	0.20	0.0028534	ruvb12.L	0.19	0.0328933	0.22	0.0234234
xbp1.S	-0.32	0.0012641	mpdu1.L	0.16	0.0028745	serinc1.S	-0.15	1.572E-05	-0.16	5.303E-05
LOC108711485	0.27	0.0012641	rflb.S	-1.20	0.0028745	sh3gl2.L	-0.06	0.0274751	-0.09	0.0010749
psma7.L	0.18	0.0012649	cta.L	-0.07	0.0028745	shmt2.L	0.18	1.141E-08	0.24	5.599E-13
gm2a.L	-0.34	0.0013419	glul-like.1.L	-0.26	0.0028745	slc25a12.L	-0.21	0.0049394	-0.21	0.0183493
sh3kbp1.S	0.22	0.0013462	diexf.S	0.22	0.0028745	slc2a12.L	-0.87	0.0005369	-0.81	0.0059155
LOC108709791	-0.12	0.0013741	maseh2c.L	0.28	0.0029128	slc38a4.L	-0.45	1.273E-07	-0.25	0.0349452
cdc5l.L	-0.07	0.0013741	neurod4.S	0.21	0.0030257	slc41a1.S	-0.35	0.0125227	-0.44	0.0032586
rbp4.S	-0.23	0.0013741	npb.L	-0.35	0.0030257	slc43a2.L	-0.30	4.406E-10	-0.16	0.0153683
LOC108707047	0.14	0.0013945	gtf2h1.L	0.15	0.0030357	slc43a2.S	-0.36	1.056E-10	-0.25	0.0004938
stf6gal2.L	-0.12	0.0014415	npm3.L	0.46	0.0030718	slc4a4.S	-0.57	0.0054058	-0.65	0.0037919
rimkib-like.L	-0.07	0.0015357	LOC108713945	0.18	0.0032026	slc6a17.S	0.08	0.0117961	-0.19	7.097E-13
LOC108699172	-0.29	0.0015902	gtf2f2.S	0.19	0.0032042	slco2b1.L	-0.63	0.0160395	-0.70	0.0157467
snmp40.S	0.18	0.001598	vfg.L	-0.52	0.0032285	snmp40.S	0.18	0.001598	0.16	0.0129876
fam117b.L	-0.11	0.0017442	ehd1.S	0.25	0.0032285	snrpc.S	0.12	0.0474001	0.15	0.0259776
faf2.L	0.16	0.001772	slc41a1.S	-0.44	0.0032586	snu13.L	0.29	6.128E-06	0.42	3.316E-10
slc38a5.S	0.20	0.0018115	dhx15.L	0.14	0.0032602	snu13.S	0.26	9.497E-05	0.30	3.844E-05
fads1.S	-0.18	0.0018943	cacna1f.L	0.54	0.0033227	srsf2.L	0.17	0.0010997	0.17	0.0050789
kans11.L	0.09	0.0019287	got2.S	-0.10	0.0035134	srsf3.S	0.09	1.382E-06	0.10	8.578E-06
LOC108708885	-0.73	0.0019311	g3bp1.L	0.15	0.0036144	sst.S	-0.19	0.0025337	-0.25	0.0001846
LOC108716040	0.76	0.0019886	fen1.L	0.27	0.0036403	stip1.L	0.21	8.3E-05	0.20	0.0009761
smurf1.S	-0.28	0.0019886	kif20a.S	0.29	0.0036502	suc1g2.L	0.10	0.0032138	0.12	0.0012271
pi4ka.L	-0.14	0.00201	ache.L	-0.18	0.0037041	suox.L	-0.26	0.0135557	-0.33	0.003835
cdk11b.S	0.17	0.0020364	nefm.L	-0.23	0.0037101	tac1.S	-0.19	0.0292659	-0.31	0.0003889
ruvb11.S	0.18	0.0020664	Xelaev18042670m	0.36	0.0037669	tcp1.L	0.17	4.406E-10	0.12	0.0001938
pex19.S	0.11	0.0022003	sic4a4.S	-0.65	0.0037919	tfcp2h1.S	-0.59	3.504E-05	-0.44	0.0157467
Xelaev18012648m	0.71	0.0022599	tsr3.L	0.16	0.0038145	tgfb11.L	-0.16	0.0137455	-0.17	0.0161964
LOC108709207	-0.19	0.0022599	suox.L	-0.33	0.003835	tial1.L	0.13	0.0001081	0.11	0.0054153
LOC108716523	-0.30	0.0022599	nol12.S	0.23	0.003835	tinagl1.L	-0.51	0.0131641	-0.56	0.0132904
LOC108701106	-0.66	0.0023742	Xelaev18038532m	-0.82	0.0038365	tma16.L	0.23	0.0205481	0.26	0.0171633
fitm2.L	-0.21	0.0023836	ahcy.L	0.17	0.0038929	tmem163.L	0.13	6.109E-07	-0.16	2.716E-07
psmc1.S	0.14	0.002411	neff.L	-0.31	0.0039334	tmem206.L	0.29	0.0035399	0.28	0.0161964
psmd3.S	0.16	0.002411	cdk1.L	0.18	0.003945	tmpo.L	0.09	0.022958	0.14	0.0002513
LOC108695405	0.98	0.002423	LOC108709207	-0.20	0.0039762	tsr1.L	0.16	0.0167966	0.23	0.0006271
sst.S	-0.19	0.0025337	nrg2.L	0.43	0.0040564	txnl1.S	0.12	0.0273029	0.15	0.0104486
LOC108696503	0.79	0.002574	dimt1.L	0.29	0.0040875	utp4.L	0.17	0.0081778	0.32	6.855E-08
aifm3.L	-0.35	0.0025901	slitkr1.L	-0.10	0.0041163	vars.S	0.18	0.0328933	0.22	0.0127932
ppp2r2d.S	0.15	0.0026346	orc1.L	0.25	0.0041642	vcam1.S	-0.14	0.0058016	-0.19	0.0003882
LOC108698753	0.18	0.0026346	pkn3.S	0.41	0.0042038	vip.L	-0.23	0.0244148	-0.33	0.001259
atp8a1.S	-0.26	0.0026857	pir.L	-0.60	0.0044153	wdr4.S	0.21	0.0205481	0.27	0.0054063
fbx4.L	-0.67	0.002746	xpc4.L	0.22	0.0044153	Xelaev18033745m	-0.13	0.0216135	-0.20	0.0003505
chac1.L	-0.41	0.0027598	rbp7.L	0.17	0.0044716	Xelaev18043812m	-0.32	0.0326091	-0.36	0.0359606
LOC108701216	0.20	0.0027598	stx1b.L	-0.10	0.0047099	zfn207.S	0.29	1.827E-11	0.16	0.0051585
LOC108697600	-0.90	0.0028046	bsg.L	-0.12	0.0047099	zfn326.S	0.13	1.206E-06	0.08	0.0257551

adams15.L	-0.56	0.0028469	LOC108713946	0.36	0.0047099
csnk2a2.S	0.10	0.0028475	smarcd1.S	0.12	0.0048698
LOC108702234	0.14	0.0029776	MGC84433	0.14	0.0048768
ifrd1.L	0.15	0.0030539	ipo4.L	0.36	0.0049898
ttbk1.L	0.11	0.0030539	thg1.L	0.20	0.005014
shprh.S	-0.16	0.0030539	srsf2.L	0.17	0.0050789
LOC108713207	-0.50	0.0031564	znf207.S	0.16	0.0051585
slc1g2.L	0.10	0.0032138	meis1.L	-0.25	0.0052762
LOC108698872	-0.25	0.0033722	polr2f.S	0.24	0.005365
LOC108713395	0.24	0.0035399	LOC108708478	0.07	0.0054063
mark2	0.12	0.0035399	wdr4.S	0.27	0.0054063
tmem206.L	0.29	0.0035399	tial1.L	0.11	0.0054153
gmps.S	0.13	0.0035399	tmem255a.L	-0.17	0.0054153
exosc4.S	0.20	0.0036454	LOC108715314	0.38	0.0054188
flad1.L	0.17	0.0036454	LOC108717058	0.15	0.0054249
mdm1.L	-0.25	0.0037278	csnk2a2.S	0.11	0.0054249
rilp1.S	0.23	0.003758	gar1.S	0.29	0.0054315
LOC108698597	-0.30	0.0037762	ppan.L	0.30	0.0054315
slc22a16.L	-0.74	0.0038189	ccnb1.2.L	0.18	0.0057288
cbr4.L	-0.27	0.0039577	kl.S	-0.36	0.0057501
eif1ax.L	0.15	0.0039577	msx2.L	-0.38	0.0059155
cngb1.L	0.24	0.0039835	slc2a12.L	-0.81	0.0059155
cir1.L	0.11	0.0042675	eif3a.L	0.12	0.0059242
LOC108702925	0.14	0.0045057	acta2.S	-0.37	0.0059918
adgra3.L	-0.14	0.0045476	kif11.S	0.19	0.0060069
LOC108700150	-0.17	0.0045476	LOC108715931	-0.12	0.0061163
cct4.S	0.11	0.0045699	meis1.S	-0.30	0.0063899
fen1.S	0.22	0.0045934	noc3l.S	0.19	0.0064901
ddx39	0.12	0.0046543	pi4ka.L	-0.14	0.0065035
cpsf3.L	0.15	0.0046543	camk2d.S	-0.14	0.006652
rasi11b.S	0.42	0.0047404	penk.L	-0.19	0.0068897
zmat5.S	0.22	0.0047404	paqr9.L	-0.19	0.006968
strn3.S	0.09	0.0049281	LOC108718747	0.16	0.0071234
LOC108704083	-0.80	0.0049388	sord.L	-0.83	0.0072886
esf1.L	0.14	0.0049394	LOC108697293	-0.46	0.0074803
slc25a12.L	-0.21	0.0049394	MGC69089	-0.10	0.007513
mige8.L	-0.24	0.0049617	adcyap1.L	-0.18	0.0075918
pkn3.S	0.36	0.0049617	ppp3ca.S	-0.10	0.0076932
rf139.L	0.15	0.0050076	LOC108708303	-0.27	0.0076932
specc1.L	0.12	0.0050085	LOC108700399	0.12	0.0078945
kif1c.S	0.19	0.0050233	LOC108717444	-0.21	0.0080366
fam160a1.L	-0.45	0.0050233	LOC108715624	-0.14	0.0080385
msx2.L	-0.35	0.0050233	lsm3.L	0.20	0.008227
sh3y1.L	-0.36	0.0050233	fgf12.S	-0.16	0.0082967
spock2.L	-0.06	0.0050233	atad5.L	0.15	0.0086608
cers1.S	-0.28	0.0050263	fzd5.S	0.15	0.0086608
polr3e.L	0.17	0.0050263	cnbp.S	0.12	0.0088065
psmb3.S	0.15	0.0051694	LOC108710170	0.46	0.0089895
elavl3.L	-0.09	0.0053864	rrs1.S	0.36	0.0090028
aoah.L	-0.66	0.0053864	cbfa2t3.L	0.15	0.0092032
cwc25.L	0.12	0.0053864	farsa.S	0.22	0.0092347
slc4a4.S	-0.57	0.0054058	LOC108713072	0.18	0.0092516
LOC108709985	-0.07	0.0054058	mak16.L	0.30	0.0093612
iqub.L	-0.41	0.0055782	bcl6.L	-0.43	0.0093674
mthfd1.L	0.17	0.005757	mapk14.S	0.20	0.009531
vcam1.S	-0.14	0.0058016	ralb	-0.08	0.009531
LOC108717752	-0.43	0.0059464	epm2a.L	-0.45	0.009531
onecut1.2.S	-0.18	0.0060737	lamp5.S	-0.35	0.009531
neurod4.S	0.18	0.0064028	ddit4.S	-0.31	0.009531
krt8.S	-0.21	0.0068029	frzb-1	-0.53	0.009531
LOC108715327	0.12	0.0069317	pdyn.S	-0.40	0.0097125
ubxn6.L	-0.19	0.0069813	lbh.L	-0.16	0.0099611
psmc3.S	0.15	0.0070551	pes1.L	0.21	0.0104486
dmrta2.L	0.18	0.0071902	txn1.S	0.15	0.0104486
lin28a.L	0.93	0.0072861	LOC108697903	-0.30	0.0104486
LOC108704274	-0.32	0.0073283	polr3e.L	0.18	0.0104486
ydjc.L	0.24	0.0073304	LOC100653495	0.18	0.0104987
LOC108710196	0.18	0.0073557	LOC108710922	-0.20	0.0106746
zfp91.S	0.14	0.0073589	sema3a.L	-0.16	0.0109596
LOC108704343	-0.24	0.0073694	tttl5.L	0.27	0.0113193
rf170.L	-0.31	0.0073735	nipsnap3a.S	-0.32	0.0115367
slc7a5.L	-0.16	0.007404	gdpd5.S	-0.18	0.0115367
LOC108716766	-0.43	0.007404	cln5.L	0.79	0.0116499
mettl3.L	0.21	0.0074604	c11orf87.L	-0.14	0.0116639
nrf1.L	0.14	0.0074604	rexo2.L	0.28	0.0116639
oaf.S	-0.39	0.0074727	slitr4.L	-0.15	0.0116639
hnmpk.L	0.06	0.0075424	chtf18.L	0.22	0.0118171
LOC108700270	-0.47	0.0075424	nol9.L	0.23	0.0120094
Xelaev18029465m	0.53	0.0079387	Xelaev18022529m	-0.82	0.0121959
rtcb.L	0.12	0.0081383	pdck4.L	-0.27	0.0121959
tmem38a.S	0.60	0.0081383	spry4.S	-0.27	0.0127932
Xelaev18045516m	-0.55	0.0081383	pmp2.S	-0.39	0.0127932
utp4.L	0.17	0.0081778	vars.S	0.22	0.0127932
slc16a14.S	-0.26	0.0081778	sub1.L	0.14	0.0129876
aqp1.L	-0.22	0.0081778	snmp40.S	0.16	0.0129876
zc4h2.L	0.12	0.0081778	LOC108719665	-0.50	0.0129876
mpdu1.L	0.13	0.0085353	tinagl1.L	-0.56	0.0132904
LOC108718108	-0.33	0.0086278	ckb.L	-0.17	0.0132904
slc38a1.L	-0.33	0.0087765	e2f4.S	0.20	0.0134683
cmpk1.S	0.14	0.0088672	ruvb2	0.18	0.0135506
p2ry1.S	0.19	0.0089854	pip4k2c.L	-0.24	0.0135854
nolc1.L	0.16	0.0090317	mettl1.L	0.25	0.0136789
rsph3.L	-0.27	0.0091693	eno1.S	-0.13	0.0137861
nip7.L	0.18	0.0094857	tars.L	0.16	0.0139998
phb.L	0.16	0.0094857	plekha1.L	0.22	0.0140415
nipsnap3a.S	-0.30	0.0094891	rbp4.S	-0.21	0.0140813

wdr77.S	0.14	0.0094891	c18orf25.S	0.17	0.014258
gja5.S	-0.34	0.010015	uba2.L	0.09	0.0145159
samhd1.L	-0.15	0.010015	mpepl1.L	0.15	0.0146494
LOC108702162	-0.10	0.010015	LOC108715046	-0.20	0.0151454
nudr1.S	0.27	0.0100359	slc43a2.L	-0.16	0.0153683
bcorf1.L	-0.18	0.0100634	diras3.L	-0.30	0.0153683
psma3.L	0.17	0.0101516	slc38a5.L	0.23	0.0156728
nup107.S	0.11	0.0103012	slco2b1.L	-0.70	0.0157467
raver2.L	0.13	0.0104252	atp2b1.S	-0.12	0.0157467
gsta1.L	0.23	0.0104252	paxip1.S	0.15	0.0157467
cdkn1a.L	-0.35	0.0106411	tfcp2l1.S	-0.44	0.0157467
zbtb43.L	-0.19	0.0106828	mgea5.S	-0.17	0.0158031
Xelaev18030365m	0.84	0.0107372	LOC108717147	-0.09	0.0159749
tlk2.L	0.10	0.0108174	tmem206.L	0.28	0.0161964
drd4.L	0.73	0.0108521	igfb1i1.L	-0.17	0.0161964
LOC108715419	0.11	0.0108521	pola2.L	0.25	0.0168327
dnrtip2.L	0.15	0.0108521	LOC108709796	-0.38	0.0170639
Xelaev18027151m	-0.19	0.010873	tma16.L	0.26	0.0171633
psmd12.L	0.16	0.0109214	LOC108696824	-0.12	0.0172158
LOC108714054	-0.53	0.0110092	pld6.S	0.47	0.0172158
psmc2.S	0.13	0.0110246	otx1.S	0.28	0.0173756
metap2.L	0.13	0.0111708	LOC108704340	-0.54	0.0179088
loc100497154.S	0.78	0.0113723	cdk11b.S	0.16	0.0180283
LOC108698540	-0.34	0.0117142	fam163b.L	-0.11	0.0180283
scarb1.S	-0.37	0.0117142	cdca7L.L	0.22	0.0180629
lmo2.S	0.21	0.0117142	hibadh.S	-0.15	0.0180629
slc6a17.S	0.08	0.0117961	cryl1.L	-0.23	0.0180985
Xelaev18024038m	-0.22	0.0119714	coro2b.L	-0.20	0.0180985
mybl2.S	0.19	0.0119714	LOC108704043	0.21	0.0183173
hnmpab.L	0.14	0.0121514	patz1.S	0.13	0.0183493
selm.L	0.17	0.0124138	gsap.L	0.62	0.0183493
psmd8.L	0.14	0.0124138	cpt1b.L	-0.53	0.0183493
slc41a1.S	-0.35	0.0125227	LOC108715578	0.20	0.0183493
dbi.L	0.16	0.0126155	meis3.L	-0.20	0.0183493
bhlhe40.S	0.37	0.0127122	elf6.L	0.19	0.0183493
LOC108696863	-0.13	0.0130005	slc25a12.L	-0.21	0.0183493
cpt1b.L	-0.50	0.0130017	pms2.L	0.38	0.0183493
rbfox2.S	-0.10	0.0130017	LOC108703510	-0.51	0.0185858
LOC108718667	0.30	0.0130017	exosc6.L	0.20	0.0189914
tinagl1.L	-0.51	0.0131641	chrhp.L	-0.26	0.019356
hmha1.L	0.15	0.0131966	fyd6.L	-0.09	0.019356
c5orf24.S	-0.16	0.0133257	Xelaev18046186m	-0.20	0.0196679
rab3a.L	0.12	0.0134045	rad51.L	0.18	0.0200716
cxorf40a.S	0.37	0.0134257	fancd.L	0.57	0.0200716
phkb.S	-0.12	0.0134572	LOC108699518	-0.90	0.0200716
Xelaev18035913m	-0.34	0.0134572	tram1.L	0.15	0.0201749
sgk1.L	-0.31	0.0135401	ankrd13a.S	0.14	0.020217
suox.L	-0.26	0.0135557	crabp1.S	-0.36	0.0202655
cntrl.L	0.11	0.0135557	aco1.L	-0.15	0.0202971
bean1.L	0.09	0.0136922	lmbn1.S	0.13	0.0202971
tgfb1i1.L	-0.16	0.0137455	rmtl1.L	0.50	0.0205634
fkbp2.S	0.17	0.013817	LOC108713890	0.60	0.0205634
LOC108696111	0.12	0.013817	LOC108701106	-0.60	0.0205634
klf9.L	-0.48	0.0139153	LOC108697991	-0.58	0.0208419
map3k7.L	0.10	0.0139153	gucy1b3.S	-0.10	0.0209001
srrm3.L	0.10	0.0139689	slc45a1.S	-0.15	0.021525
arl2.L	0.16	0.0140069	osbp13.S	-0.31	0.0217181
lsm3.L	0.17	0.0141823	cse11.L	0.19	0.0217181
kdm3a.S	0.10	0.0143457	polr2e.S	0.25	0.0217261
ubxn1.S	0.12	0.0143825	mcm4.L	0.14	0.0217261
Xelaev18030603m	-0.44	0.0143825	n6amt1.L	0.21	0.0218437
LOC108699116	-0.51	0.0144014	osbp2.S	-0.24	0.021921
nln.L	-0.10	0.0148474	eed.S	0.17	0.021921
enc1.L	-0.12	0.0148922	dnrtip2.L	0.15	0.0219818
gpr182.L	0.43	0.0149757	cdca7.S	0.16	0.0219818
ptpn9.L	0.12	0.0150955	pth1r.L	-0.35	0.0224232
LOC108695772	-1.07	0.0150961	mtr.L	0.29	0.0226982
isoc1.L	-0.11	0.0151742	gcnt7.L	0.53	0.0227725
chac2.S	0.22	0.0151742	lyrm2.L	-0.37	0.0234234
znf235.L	-0.31	0.0153156	hsph1.S	0.16	0.0234234
crnk1.S	0.14	0.015364	ruvl2.L	0.22	0.0234234
wdr44.L	0.08	0.0155737	LOC108705377	-0.68	0.0234801
basp1.L	0.11	0.015688	slc40a1.S	-0.19	0.0234801
slco2b1.L	-0.63	0.0160395	slc16a3.L	-0.15	0.0238913
cacna1f.L	0.43	0.0160395	atp1b1.S	-0.20	0.0238913
efhd2.L	0.14	0.0160395	LOC108698172	0.23	0.0238913
LOC108696336	-0.73	0.0161164	stmn3.S	-0.09	0.0238913
psmb5.L	0.19	0.0161327	Xelaev18028825m	-0.39	0.0241532
LOC108715638	-0.49	0.0161327	knj12.S	-0.55	0.0241532
lsm12.L	0.13	0.0161327	iah1.L	0.24	0.0242287
ppie.L	0.15	0.0162318	LOC108715136	0.55	0.0243203
LOC108706917	0.19	0.016358	LOC108699392	-0.12	0.0243203
LOC108697713	-0.19	0.016358	nfe2l2.L	-0.18	0.0244926
LOC398702	0.08	0.016358	rd3.S	-0.62	0.0245379
LOC108710179	-0.15	0.0163802	LOC108710996	-0.23	0.0247712
fbxo9.L	-0.11	0.0163802	fam198a.L	-0.21	0.0248064
sos2.L	0.09	0.0163802	rabac1.S	-0.96	0.0248907
LOC108701408	0.11	0.016382	LOC108713304	-0.10	0.0249046
akap11.L	-0.09	0.0165396	fam102b.S	-0.26	0.0249046
tsr1.L	0.16	0.0167966	lace1.L	-0.20	0.0249046
c1qtnf2.L	-0.95	0.0167966	cadm3.L	-0.07	0.0249046
lrp4.S	-0.11	0.0167966	gad1.1.L	-0.15	0.0249586
plekhf1.S	-0.70	0.0167966	MGC145330.L	-0.18	0.0250172
adck5.L	0.21	0.0167966	knj13.S	-0.29	0.0251924
cchcr1.L	-0.14	0.0168317	hnmpab.L	0.14	0.0256637
LOC108714433	-0.11	0.016865	LOC733321	-0.33	0.0256637

aes.S	0.13	0.0169549	bcl6.S	-0.25	0.0256637
Xelaev18001208m	-0.24	0.0169549	znf326.S	0.08	0.0257551
fis1.S	0.10	0.0170563	kiaa1614.L	0.10	0.025881
ptbp2.S	0.14	0.0170563	snrpc.S	0.15	0.0259776
LOC108709441	0.64	0.0172649	kpna2.L	0.15	0.0260444
ahcy.L	0.13	0.0173946	Xelaev18031102m	-0.71	0.0260848
cacybp.S	0.16	0.0175199	prf18.S	-0.26	0.0261937
rad23b.S	0.08	0.0177202	spc24.L	0.20	0.0264283
cwc15.S	0.13	0.0178244	Xelaev18020816m	-0.35	0.0264283
mf20.L	0.09	0.0185809	krt8.S	-0.20	0.0265291
smpd3.S	-0.20	0.0185841	ifrd2.L	0.22	0.026635
Xelaev18030685m	-0.10	0.0185841	naa50.L	0.14	0.0270687
por.S	-0.13	0.0186215	wdhd1.L	0.26	0.0272237
ednra.S	-0.27	0.0187663	fam213a.S	-0.51	0.0279385
slc25a24.S	0.23	0.0191686	mob3a.L	0.17	0.0283533
LOC108696337	-0.54	0.0195217	LOC108701705	-0.27	0.0283533
wdr60.L	0.16	0.0195474	dmrta2.L	0.17	0.0285239
dars.S	0.14	0.0195662	LOC108718667	0.30	0.0285239
LOC108708029	-0.23	0.0197307	MGC115598	0.35	0.0287141
smg7.S	0.11	0.0197307	c18orf25.L	0.24	0.0294252
ppp4r3b.S	0.11	0.0197307	gpi.L	-0.19	0.0302217
sntb1.L	-0.30	0.0197307	mis18a.S	0.27	0.0304421
LOC108695922	-1.15	0.0197307	Xelaev18041239m	-0.19	0.0304421
rab27a.S	0.69	0.020037	LOC108698597	-0.27	0.0306768
hgsnat.L	-0.13	0.0200585	nelfe.S	0.11	0.0309556
LOC108696787	-0.13	0.0202539	ppp3ca.L	-0.11	0.0310755
rfc3.L	0.12	0.0202971	abhd12.S	-0.11	0.0310755
LOC445843	-0.75	0.0202971	pip5k1b.L	-0.15	0.0310886
LOC108699256	0.66	0.0204791	snrpa1.S	0.19	0.0310886
epha4.L	-0.10	0.0205332	e2f4.L	0.20	0.0310886
MGC84433	0.11	0.0205332	rb1.L	0.18	0.0311248
tma16.L	0.23	0.0205481	ezh2.L	0.12	0.0312817
Xelaev18004834m	0.68	0.0205481	aldh18a1.L	0.23	0.0312817
wdr4.S	0.21	0.0205481	gabara1.S	-0.12	0.0312817
chmp2a.S	0.22	0.0205481	ifl3.S	0.06	0.0313896
c9orf172.L	-0.15	0.0205481	ston2.L	0.13	0.0321696
ache.L	-0.14	0.0205505	hoxd3.L	-1.11	0.0322374
Xelaev18013256m	-0.76	0.0205527	LOC108709689	-0.34	0.0324412
LOC108713238	-0.52	0.0206007	cenpi.L	0.21	0.0324412
LOC108715124	-0.20	0.0208694	gphn.L	-0.09	0.0324412
el13.S	-0.61	0.0208806	ddx56.S	0.24	0.0327071
tor1a.L	-0.89	0.0208948	eif2a.S	0.12	0.0327071
Xelaev18005107m	-0.13	0.0209996	LOC108707265	-0.36	0.0328074
gtf2a1.S	0.14	0.0210012	LOC108716057	0.14	0.03283
rem2.L	-0.31	0.0211206	sox21.S	0.21	0.03283
smn2.L	0.12	0.021245	LOC108701567	0.54	0.0329286
tmem63c.L	-0.11	0.021245	lcat.L	-0.27	0.0331823
npr3.L	-0.24	0.0215212	smarcd1.L	0.10	0.0337264
polr2e.S	0.23	0.0215902	LOC108710089	-0.56	0.0337264
psma5.L	0.16	0.0216135	LOC108702925	0.13	0.0337264
LOC108705299	-0.71	0.0216135	ahcyl1.S	-0.14	0.0338057
LOC108705784	0.20	0.0216135	btf3l4.L	0.12	0.0338057
kons2.L	-0.20	0.0216135	bsg.S	-0.13	0.0343258
Xelaev18033745m	-0.13	0.0216135	LOC108718911	-0.21	0.0343258
cdhr1.L	0.23	0.0216135	LOC108699846	0.12	0.0343258
Xelaev18047071m	0.40	0.0216135	ebpl.S	0.20	0.0345532
gar1.S	0.23	0.0217134	rad54l2.L	0.14	0.0345881
tmem129.L	-0.19	0.0217188	cmkl1.S	0.14	0.0345881
fosl2.L	0.57	0.0217795	nln.L	-0.10	0.0347621
ergic2.S	0.14	0.0218148	slc30a1.L	-0.22	0.0347621
mapkapk5.L	-0.14	0.0219439	LOC108702939	0.14	0.0347621
Xelaev18033924m	-0.48	0.0219439	slc38a4.L	-0.25	0.0349452
ecm1.L	-1.05	0.0219439	gpn1.L	0.14	0.0349452
map2k3	0.12	0.0220895	socs2.S	0.38	0.0349774
efcab14.S	0.09	0.0221377	itm2b.L	-0.12	0.0350228
lrp8.S	-0.14	0.0221377	ndufs1.S	-0.19	0.0353613
paip1.L	0.12	0.0221895	adipor2.L	-0.14	0.035404
fubp3.S	0.10	0.0221895	pth2.L	-0.68	0.0359121
abhd6.L	0.15	0.0222958	LOC108703741	0.17	0.0359606
arhgef40.L	-0.17	0.0222958	hells.S	0.19	0.0359606
atp1b1.S	-0.18	0.0222958	rcf1.L	0.26	0.0359606
tmpo.L	0.09	0.0222958	emb.S	-0.36	0.0359606
Xelaev18044113m	-0.17	0.0222958	cct6a.L	0.11	0.0359606
fn1.S	-0.28	0.0222958	shpk.S	-0.31	0.0359606
nfyf.L	0.09	0.0225632	asns.L	0.17	0.0359606
Xelaev18013255m	0.75	0.0225943	Xelaev18043812m	-0.36	0.0359606
cebpb.L	-0.42	0.0226635	ndufa10.S	-0.12	0.0359606
nelfe.S	0.10	0.0226657	hnmpl.L	0.06	0.0363232
dnajc12.S	-0.47	0.022896	fam189a1.S	-0.18	0.0366399
kif2a.S	0.09	0.0228971	dusp6.L	-0.19	0.0366562
LOC108712545	-0.14	0.0232415	atg4d.L	-0.26	0.0367547
fam163b.L	0.10	0.0232415	ift81.L	-0.23	0.036781
susd6.L	0.10	0.0232415	psma5.S	0.11	0.036781
hey1.S	0.21	0.0237494	LOC108710859	0.15	0.036781
LOC108714852	0.11	0.0237507	dnmt1.S	0.14	0.036781
cct6a.L	0.10	0.0237507	h2afj.S	-0.09	0.036781
grp.L	-0.33	0.0238471	ccdc129.L	-0.29	0.036781
rsr2.S	-0.19	0.0238471	ap5s1.L	-0.24	0.036781
prps1.L	0.10	0.0238471	LOC108697493	-0.43	0.036781
kiaa0556.L	-0.22	0.0238471	kptn.L	-0.23	0.036781
r3hdm4.S	-0.12	0.0239499	lhfp12.S	0.20	0.0369147
msmo1.S	-0.27	0.0240439	clk3.L	0.30	0.0369147
acad11.L	-0.33	0.024394	stag1.L	0.13	0.0369352
pisd.L	0.13	0.0244148	LOC108716284	-0.12	0.0372786
LOC108716057	0.13	0.0244148	fbxo9.L	-0.11	0.0372786
ddx17.L	-0.19	0.0244148	erbb3.L	-0.36	0.0374246

vip.L	-0.23	0.0244148	cmpk1.S	0.13	0.0377424
rimk1a.L	-0.21	0.0244148	LOC108699803	0.13	0.0377424
ubqln1.L	-0.16	0.024444	reg.L	-0.17	0.0380173
lmod2.S	-0.72	0.024444	trmt1.L	0.31	0.0390968
Xelaev18031338m	-0.87	0.024444	MGC84141	-0.20	0.0381604
kff11.S	0.15	0.0245667	ism12.L	0.13	0.0381604
tpv23b.L	0.17	0.0247171	LOC108718782	-0.37	0.0382556
LOC108702748	-0.63	0.0249235	olfm12a.L	-0.17	0.0382556
polr1a.L	0.19	0.0249889	snx30.S	0.15	0.0382745
LOC108711604	-1.16	0.0249889	LOC108699950	0.15	0.0382745
LOC108703993	-0.13	0.0250129	LOC108702993	0.18	0.0383712
myo1f.L	-0.40	0.0250129	slc16a12.S	-0.48	0.0384799
cyp27a1	-0.30	0.0250129	LOC108698773	-0.29	0.0386521
cldn1.S	-0.28	0.0250867	LOC108714307	-0.77	0.0391506
LOC108697883	0.49	0.0252293	pgam5.S	0.19	0.0393713
tmed10.L	0.11	0.025286	exo1.S	0.24	0.0393713
znf518b.S	-0.30	0.0253514	aggf1.S	0.23	0.0395021
LOC108715692	-0.14	0.0253727	cwc15.S	0.13	0.0400238
prmt5.L	0.14	0.0255593	hoxa3.L	-0.91	0.0401089
ddx23.S	0.12	0.0257294	LOC108716040	0.62	0.0402158
mrp138.L	0.14	0.0258984	LOC108698540	-0.33	0.0404407
c16orf72.S	0.08	0.0258984	LOC108698243	-0.17	0.0404834
LOC108704795	-0.28	0.0264326	ca2.L	-0.30	0.0406284
vps33a.L	-0.12	0.0266874	usp4.S	0.14	0.0406398
wdr47.S	-0.12	0.0266874	ppp1r3c.1.L	-0.58	0.0406398
acta2.S	-0.28	0.026787	LOC108707047	0.11	0.0408583
farsa.S	0.18	0.0272499	lzts3.L	-0.13	0.0409183
txn1.S	0.12	0.0273029	mab21l2.S	-0.44	0.0409183
fez2.L	0.08	0.0273029	snob.L	-0.08	0.0409183
sh3gl2.L	-0.06	0.0274751	mknk2.L	-0.26	0.0409317
arf1.L	0.08	0.0274947	LOC108701634	-0.48	0.0418326
plat.L	-0.35	0.0277802	ddx21.L	-0.13	0.0418377
vopp1.L	-0.15	0.0279404	Xelaev18020729m	-0.42	0.0419954
pds5b.L	-0.10	0.0279779	apex1.L	0.08	0.0423836
LOC108711179	-0.20	0.0279779	LOC108714329	-0.28	0.0425638
rab35.L	0.14	0.028226	LOC108709941	0.38	0.0425638
LOC108698669	-0.30	0.0284659	MGC115585	0.25	0.0425638
LOC108714204	0.38	0.0286619	sybu.S	-0.14	0.0425638
bph.L	-0.40	0.0286619	mrp11.S	-0.17	0.0426177
sgms1.S	-0.29	0.0286619	c1ql4.L	-0.10	0.0426918
mmel1.S	-0.34	0.0286619	oxr1.S	-0.22	0.0426918
LOC108711102	-0.13	0.0287663	hoxb3.S	-0.91	0.0426918
LOC108711632	-0.35	0.0287663	ecm1.L	-1.06	0.0426866
aqp1.S	-0.25	0.0287663	rangap1.L	0.21	0.0428816
LOC108697729	-0.16	0.0287663	pgk1.L	-0.12	0.0434686
gpn1.L	0.13	0.0288917	amfr.L	-0.12	0.0438539
tac1.S	-0.19	0.0292659	c19orf25.L	0.20	0.0441492
c8orf33.L	0.22	0.0292659	nmd3.L	0.18	0.0441492
c3orf70.L	-0.12	0.029494	LOC108719276	-0.29	0.0441492
mfsd2a.S	0.20	0.0298194	psmd3.S	0.13	0.0441492
cct7.S	0.17	0.0298194	rpa1.L	0.14	0.0443514
znf385a.S	0.19	0.0298194	sdpr.L	-0.24	0.0443514
LOC108719681	-0.90	0.0298194	itga7.L	-0.17	0.0444359
kcng1.L	0.24	0.0298194	cd2ap.S	0.15	0.0447296
LOC108715624	-0.11	0.0298885	slc16a6.S	-0.37	0.0447893
LOC108697876	-0.14	0.0298885	bmp3.L	-0.21	0.0454195
prelp.S	-0.16	0.0299382	tbl3.L	0.28	0.0456099
Xelaev18023338m	-0.76	0.0299382	tead4.S	0.16	0.046077
LOC108708284	-0.42	0.0301871	LOC108718647	0.24	0.0463766
LOC108702627	-0.12	0.0304948	ola1.L	0.12	0.0465099
LOC108706826	0.14	0.0305743	rcc1.S	0.30	0.0465099
sept11.L	-0.16	0.0306245	MGC114939	0.28	0.0465099
gtf2f2.S	0.14	0.0308938	kenn3.S	-0.27	0.0465099
ppid.S	0.19	0.0309447	cdc6.S	0.28	0.0465099
gpbp1.L	-0.26	0.03114	atp2b4.L	-0.15	0.046561
wipi1.L	0.11	0.03114	hspa5.S	0.14	0.0469801
LOC108710795	-0.78	0.0316583	ppid.S	0.20	0.0475343
mcrs1.L	0.09	0.0316583	glud1.L	-0.26	0.0475343
ppig.L	0.11	0.0316607	glib.S	-0.12	0.0478568
pdia3.S	0.07	0.0322512	MGC84997	0.24	0.0479157
LOC108697732	-0.28	0.0322512	n6amt2.S	0.34	0.0479157
esm1.S	0.98	0.0325365	rrp15.S	0.28	0.0479157
LOC108708460	0.14	0.0325365	psma3.L	0.15	0.0479608
snrpe.S	0.14	0.0325365	elk1.L	0.22	0.0479996
mknk2.L	-0.24	0.0326091	rab3a.S	-0.13	0.0483514
Xelaev18043812m	-0.32	0.0326091	lhx1.L	-0.44	0.0483514
LOC108697267	-0.13	0.0326277	LOC108698591	-0.32	0.0483514
dapk3.L	0.13	0.032814	LOC108703029	-0.12	0.0483514
ngfr.S	-0.14	0.032814	LOC108696944	-0.40	0.0488886
slc6a1	-0.07	0.0328933	tfp.L	0.11	0.048899
dgkq.L	-0.20	0.0328933	hmha1.L	0.14	0.0489087
ruvb2.L	0.19	0.0328933	pex1.L	0.21	0.0489087
vars.S	0.18	0.0328933	pla2g15.S	-0.59	0.0492683
lrguk.L	-0.30	0.0330129	gpc3.L	-0.19	0.0494628
ajap1.L	0.12	0.0331506	nkain3.S	-0.24	0.0495253
Xelaev18013307m	-0.17	0.0332418	meis2.S	-0.18	0.0497027
desi1.L	-0.12	0.0332654	skiv2l2.S	0.16	0.0497382
pligrk.L	-0.21	0.0334435	scg5.S	-0.10	0.0499244
qrich1.1.S	0.10	0.0337143			
ndufv1.L	0.09	0.0337143			
LOC108699192	0.12	0.0337143			
znf581.L	-0.19	0.0337683			
nat10.L	0.12	0.0342224			
prpsap1.S	0.15	0.0343444			
Xelaev18030072m	-0.29	0.0343785			

MGC52759	0.14	0.0343785
socs3	0.54	0.0343785
rab2a.L	0.09	0.0344452
sh3gl2.S	0.09	0.0345728
pex5l.L	-0.32	0.0348554
LOC108715791	0.33	0.0349556
LOC108712576	-0.35	0.0351596
hnrnp1.L	0.12	0.0351596
LOC108704340	-0.44	0.0355467
tmed7.L	0.08	0.0355467
pir.L	-0.43	0.0355834
LOC108701707	0.25	0.0359552
cactin.L	0.11	0.0360278
zfyve28-like.1.S	0.24	0.0360278
slitrk5.L	-0.13	0.0360278
timp3.S	-0.36	0.0360278
ogfr1.S	0.32	0.0360278
mfn2.L	-0.10	0.0360278
LOC108697904	-0.18	0.0360278
spata4.L	-0.27	0.0363733
trove2.L	-0.35	0.0364407
mgc75753.S	0.12	0.0364407
ikzf1.L	-0.37	0.0364407
mtif3.L	-0.15	0.0364481
map3k10.L	0.08	0.0364481
casp2.L	0.10	0.0365599
LOC108711452	-0.48	0.0366385
mrps24.S	0.14	0.0368136
dnah12.L	-0.40	0.037736
comt.L	0.17	0.0379627
htatsf1.S	0.11	0.0379627
LOC108706601	0.24	0.0380299
nucb1.S	0.09	0.0380299
LOC108698377	-0.13	0.0382158
fbxo31.L	0.11	0.0383353
ankrd13a.S	0.11	0.0384082
stxbp3.L	0.20	0.0384834
fam110b.S	-0.13	0.0387226
LOC108710729	0.24	0.0388538
LOC108717099	-0.19	0.0388538
bin1.S	-0.10	0.0388538
stip1.S	0.14	0.0389564
paqr5.L	-0.96	0.0389661
LOC108718654	-0.26	0.0389704
LOC108710331	-0.20	0.0391416
LOC108708136	-0.75	0.039234
big1.L	-0.09	0.0393313
upf1.S	-0.08	0.0394964
gamt.L	0.27	0.039998
ppan.L	0.22	0.039998
LOC108714307	-0.68	0.039998
arsg.L	0.37	0.0401378
LOC108710088	0.89	0.0402438
cacna2d2.L	-0.13	0.0402543
sun1.S	-0.12	0.0402543
ankrd34b.L	-0.29	0.0402804
Xelaev18035461m	-0.30	0.0403599
pddc1.L	0.19	0.0405724
pkp3.L	0.20	0.0405785
sh3bp4.L	0.08	0.0407068
vps35.L	-0.09	0.0407198
tubb2b.S	0.12	0.0407198
ankrd9.L	0.24	0.0407662
gdpd5.S	-0.14	0.0407906
Xelaev18026345m	-0.22	0.0408696
LOC108712815	-0.52	0.0410005
lmcd1.S	-0.47	0.0410005
eif6.L	0.16	0.0410005
trip1.L	-0.22	0.0411766
LOC100485199-like.S	-0.45	0.0412015
ubxn4.L	0.10	0.0412015
mak16.L	0.23	0.0412518
LOC108699803	0.11	0.0414512
enc1.2.L	-0.11	0.0415147
hapln4.L	-0.86	0.0415147
cdc37.S	0.10	0.0415147
mettl7a.L	-0.29	0.0420842
urml.S	0.20	0.04219
ulk2.L	-0.11	0.042348
dock5.L	0.15	0.0423763
c1qbp.S	0.14	0.0427107
LOC108709757	-0.35	0.0428425
LOC108699177	-0.32	0.0428425
Xetrov90001896m.L	-0.45	0.0428709
LOC108709189	0.16	0.0428709
rab30.S	0.15	0.0428709
aqp3.S	-0.54	0.0431063
kcnq2.S	-0.17	0.0434449
mylip.S	0.47	0.0437421
LOC108703268	0.89	0.0442038
mrps31.S	0.11	0.0443393
LOC108711216	-0.29	0.0443393
LOC108696429	-0.24	0.0443393
LOC108718274	0.22	0.0444002
gxyt1.L	-0.11	0.0444131

mgc145260.L	0.16	0.0444131
patz1.L	-0.11	0.0446975
fth1.L	-0.14	0.0447704
LOC108701155	0.18	0.0448097
gucy1b3.S	-0.08	0.0454542
mf144a.S	0.13	0.0454632
mad2l1.L	-0.14	0.0454766
usb1.L	0.22	0.0454766
cldn1.L	-0.27	0.0454766
tmem47.L	-0.09	0.0454899
tor4a.S	0.40	0.0459007
wrb.L	-0.21	0.0459124
tuba4a.S	0.11	0.046197
ef3a.L	0.08	0.0463438
nob1.S	0.18	0.0464467
nmur1.S	0.20	0.0464467
eed.L	0.17	0.0464506
ola1.L	0.11	0.0464692
LOC108717031	-0.15	0.0464692
arf3.L	-0.07	0.0464692
h2afy2.L	0.08	0.0464692
ndnf.S	-0.23	0.0466999
tsc22d3.S	-0.16	0.0468452
LOC108697686	0.72	0.0469661
cnn2.S	0.80	0.0474001
mrps6.S	0.13	0.0474001
snrpc.S	0.12	0.0474001
rrs1.S	0.26	0.0475005
set.S	0.09	0.0478202
psmb2.L	0.16	0.0478202
tnfrsf12a.S	-0.43	0.0483191
glce.L	-0.14	0.0483465
prlr.S	-0.24	0.0484783
sipa1l3.L	-0.11	0.048652
npas4.S	0.63	0.0487957
LOC108696640	0.87	0.0487957
s1pr1.S	0.11	0.0492507
ndufs3.S	0.13	0.0496724